Laminar Radial Flow between Parallel Discs

and its Application to Viscometry

by

J. Ll. Moses, B.Sc.

Submitted for the degree of Ph.D.

The University of Glasgow

October 1967.

SUMMARY OF THESIS

This thesis forms a report of the work carried out by the author in the development of a radial flow viscometer. This was done to supplement existing measurements made by more conventional methods and to make use of certain advantages that the method has over other forms of flow viscometers.

The viscometer, which consists principally of two flat discs separated by a known distance, the fluid being forced to flow radially inward and leaving through a hole in the centre of one of the discs, has the disadvantage that there is a pressure loss due to inertia effects that cannot be expressed exactly. The author has been mainly concerned with investigating the various solutions available to determine which one agrees best with experiment. Within experimental error it was found that a solution obtained by expressing the pressure and velocities of the Navier Stokes equations by power series was satisfactory. The author has obtained an alternative solution which, although not exact, appears to agree well with the above solution.

A series of measurements of the viscosity of water in the range $0\,^{\circ}C$ to $90\,^{\circ}C$ are given which agree on average to within $\pm$ 1.5% to $\pm$ 2% with recognised values. These measurements were only of a preliminary nature and it is felt that with more development the accuracy could be improved.

A description of a high pressure viscometer designed by the author making use of the radial flow method is given which is capable of working 1000 atmospheres pressure and $500^{\circ}C$. This viscometer produces a steady flow through the plates by a pellet falling down a glass drop tube as is used in Rankine viscometers. An optical method of timing the fall of the mercu

ProQuest Number: 10646176

ProQuest 10646176

Published by ProQuest LLC (2017). Copyright of the Dissertation is held by the Author.

ProQuest LLC.
789 East Eisenhower Parkway
P.O. Box 1346
Ann Arbor, MI 48106 – 1346

pellet has been devised which is an improvement on the method using

platinum contact wires.

Thesis
3001
copy 2

CONTENTS

PREFACE

This thesis forms a report of the work carried out by the author in the development of a radial flow viscometer. This was done to supplement existing measurements made by more conventional methods and to make use of certain advantages that the method has over other forms of flow viscometers.

The viscometer, which consists principally of two flat discs separated by a known distance, the fluid being forced to flow radially inward and leaving through a hole in the centre of one of the discs, has the disadvantage that there is a pressure loss due to inertia effects that cannot be expressed exactly. The author has been mainly concerned with investigating the various solutions available to determine which one agrees best with experiment. Within experimental error it was found that a solution obtained by expressing the pressure and velocities of the Navier Stokes equations by power series was satisfactory. The author has obtained an alternative solution which, although not exact, appears to agree well with the above solution.

A series of measurements of the viscosity of water in the range 0 ^{o}C to 90 ^{o}C are given which agree on average to within $\pm$ 1.5% to $\pm$ 2% with recognised values. These measurements were only of a preliminary nature and it is felt that with more development the accuracy could be improved.

A description of a high pressure viscometer designed by the author making use of the radial flow method is given which is capable of working at 1000 atmospheres pressure and 500°C. This viscometer produces a steady flow through the plates by a pellet falling down a glass drop tube as is used in Rankine viscometers. An optical method of timing the fall of the mercury

pellet has been devised which is an improvement on the method using platinum contact wires.

LIST OF SYMBOLS

Unless otherwise defined in the text, the symbols used in this thesis have the following meaning:-

D   diameter of drop tube

$\mathcal{f}$ function of r

g   gravity

2h   plate separation

L   timed length of drop tube

M   mass flow rate

p   pressure

Q   volume flow rate

Re   Reynolds Number for a pipe of diameter d

r, Θ, z cylindrical coordinates

r_1, r_2 inner and outer radii at which pressure tappings are situated

R   outside radius of plates

ρ density

ρ_P density of fluid at plates

ρ_D density of fluid at drop tube

t   time

T   temperature $^{\circ}C$

u, v, w component of velocity in r, θ, and z directions

$\bar{u}$ mean velocity

U_0 velocity at centre of channel

μ viscosity

v kinematic viscosity

W   weight of pellet

LIST OF FIGURES

CHAPTER I

The work described in this thesis was undertaken to investigate the possibility of constructing a new type of viscometer which could produce measurements comparable in accuracy to that of other methods. It was felt that measurements made with a new type of viscometer were required to supplement measurements done by more conventional methods and, in addition, would help in making a wider choice of instruments available in the future.

Introduction

Below is given a brief resume of the recognised methods of viscometry available and discussion of their advantages and disadvantages. A more extensive survey can be obtained from references (1), (2), (3), and (4).

For the past sixty years or so the most common type of viscometer used has been the capillary viscometer. Essentially this entails passing the fluid through a capillary tube of known radius and measuring the pressure drop across its ends corresponding to a certain mass flow rate.

There are several good reasons why this method should appeal to experimenters investigating the viscosity of fluids:-

(a) The Navier Stokes equations for fully developed laminar flow in a pipe can be solved exactly and thus no dubiety exists as to how well the equation describes the flow regime.

(b) Much research has been conducted into the stability of flow through a tube which gives the experimenter precise knowledge of the limitations

to which measurements can be conducted. It is well known that although the roughness of the tube could have a possible effect, from the results of Reynolds (5) and Nikuradse (6), to name but two, laminar flow can be assumed to exist for a Reynolds Number less than 2000 where $Re = \dfrac{\bar{\rho}\bar{u}d}{\mu}$.

(c)   The precision with which it is possible to obtain capillaries of accurately uniform bore has been much improved especially of glass and quartz tubes.

(d)   The wealth of knowledge that exists concerning capillary visco-meters e.g. description of precision manometers, flowmeters and other ancillary measuring equipment and in addition, the experiences of numerous experimenters which give better understanding of the difficulties encountered and how best they can be avoided.

However certain difficulties have to be overcome before measurements can be regarded as reliable.

By far the greatest difficulty that has presented itself has been the development of a suitable correction to account for the additional pressure drop at the entry of the capillary arising from the velocity profile changing from an assumed uniform distribution at the entrance to the fully developed parabolic distribution further downstream. A further correction to the pressure drop must be made to allow for the viscous forces between the converging and diverging streamlines at the entrance and exit of the capillary. These corrections could be reduced to a negligible amount in comparison with the total pressure drop across the tube if the capillary were made long enough. However the manu-facturing difficulty of producing long capillaries with a bore of the necessary precision is great. In addition such capillaries would

necessitate the added difficulty of maintaining a uniform temperature over a long distance.

Swindells, Coe, and Godfrey (7) in their accurate determination of the viscosity of water at 20 $^{\circ}$C, which is now accepted as a primary reference point, rendered the end effects negligible by simultaneously treating data obtained with pairs of capillaries having the same inside diameter but different in length.

Another method of eliminating end effects is to use a viscometer with two capillaries in series as Latto(25) and Shifrin(26) did for their measurements on steam. This provides two simultaneous equations which can be solved assuming, of course, that the end effects are the same for both capillaries.

In any absolute measurement which must be regarded as more valuable than one found by secondary methods, the bore of the capillary must be known to a high accuracy since it appears to the fourth power in the working equation. A compromise has to be made on how large the diameter can be in relation to the length of the capillary since a tube of large diameter necessitates a long capillary to minimise end effects.

The bore of the tube can be measured by passing a bead of mercury of known mass along the tube in a series of steps and observing its change in length. This method, in addition to giving the size of the bore at various positions, gives information concerning the variation of diameter.

Another method of determining the diameter of the capillary is to fill it with mercury and measure the electrical resistance of the mercury and, from the resistivity of the mercury, the mean diameter of

the capillary can be deduced.

These methods only apply to transparent capillaries as at present metal capillaries cannot be measured with sufficient accuracy. Many workers have used capillary viscometers as secondary instruments, the usual calibrating fluids being water or nitrogen. This dispenses with the difficulty mentioned above of having a large enough bore to minimise inaccuracies in bore determinations and yet small enough to keep the length of the capillary tube reasonable.

Typical viscometers using calibrated capillaries are the Rankine viscometers of Kjelland-Fosterud (8), Whitelaw (9), Ray (10) and Timrot and Khlopkina (11) for measurements with steam at high pressures and temperatures. Although it is felt that the primary measurement is the more valuable, highly reproducible results can be obtained from secondary instruments and in some cases is the only practical choice depending on the nature of the test fluid.

Thus it would appear that if sufficient time and resources are available capillary viscometers can be made to give very accurate results e.g. Swindells, Coe and Godfrey (7) although errors can still be incurred in the measuring of the capillary bore, accounting for end effects and if the bore is conical or elliptical. These latter effects cannot be accounted for theoretically and no method is available for removing or improving them. Nevertheless it is felt that the measurements reported with capillary viscometers are sufficiently accurate and that in the light of these measurements it was necessary to produce a new form of viscometer by which their results could be compared.

It might be argued that the oscillating body viscometers offer a

suitable alternative to capillary viscometers. However oscillating body viscometers have been thoroughly investigated at Brown University by Kestin et al (references (12), (13), (14), (15) and (16)), and consequently to make a viscometer of this type would only lead to duplication of effort. Some of their theoretical and practical difficulties are discussed below.

At present three types of oscillating body viscometers are used:-

(a)   a disc oscillating between fixed plates;

(b)   a sphere oscillating in a fluid of infinite extent;

(c)   a sphere filled with a fluid oscillating in a vacuum.

As secondary instruments these methods can be used to give highly reproducible results but as instruments capable of producing absolute measurements of a high accuracy some doubts exist mainly due to incompleteness of the theory describing the motion. For example, an exact solution of the differential equation describing the motion of an oscillating disc can only be obtained for a disc of infinite radius where the end effects are negligible. However in practice this is not the case and consequently the end effects have to be accounted for by an approximate theory which only permits an evaluation to the necessary accuracy by calibration with a fluid of known viscosity.

The solution to the equation of motion for the oscillating sphere is exact for many applications, although for the case of a sphere oscillating in a fluid of infinite extent a correction of a semi-empirical nature has to be added to account for the drag on the suspension system which holds the mirror. This correction can be made negligible for the disc oscillating between fixed plates.

For the sphere oscillating in a vacuum an equation has been obtained numerically by Kearsley (17) and by Roscoe and Bainbridge (18) the latter using this method in their determination of water at 20 ^{o}C. From a manufacturing point of view the disc is much easier to make and hence less errors should occur due to small irregularities of shape.

Although mechanically simple several difficulties can arise. One of the main difficulties would appear to be in the alignment and especially its maintenance throughout the experiments. This problem appears to be more critical in the case of the disc oscillating between two fixed parallel plates since a constant gap needs to be maintained over the range of temperatures of the measurements. Care must also be taken as to how best to attach the wire to the suspended body so that it hangs properly. If, for example, a small chuck is used it should be ensured that the wire is not moving in the chuck.

Usually quite a large volume has to be maintained at a constant temperature so that care must be taken when designing a suitable furnace.

Several factors arise which throw some doubt on the accuracy to which the torsional constant of the wire is known. It is not known conclusively to what extent the change of tensile stress has on the torsional constant of the wire although it would appear to be small, or, for that matter, the effect of temperature cycling. It is also necessary to determine the internal friction of the wire throughout the range of temperatures at which the experiments are to be conducted. Thus from the work at Brown University it would appear that high reproducibility can be obtained for oscillating body viscometers although absolute measurements are not as accurate. In fact, various investigations

give values of viscosity slightly higher than for the same fluid using capillary methods, this effect tending to increase at higher temperatures. It would appear that comparison should thus be made with some other form of viscometer.

The author has not considered the possibility of constructing a rotating cylinder viscometer since this project has been undertaken by a colleague in this laboratory (ref. (19)).

It would appear that this form of viscometer has distinct possibilities of producing accurate measurements although some of the difficulties characteristic of the oscillating body viscometers have to be overcome.

The equations of motion for a rotating cylinder viscometer can be solved exactly and much work has been done, especially by Taylor (20) on the stability of the fluid between concentric cylinders whether it be the inner or outer cylinder that is rotating with the other cylinder stationary. He showed that for the outer cylinder rotating laminar flow existed up to a Reynolds number of at least 10^4, this being the limit of his apparatus, but for the inner cylinder rotating, above a Reynolds number of 5×10^4 he found that instability set in due to the centrifugal forces setting up a secondary flow in the annulus between the cylinders. However for viscometry it is customary to rotate the outer cylinder which is the more stable regime.

As stated above some of the difficulties encountered with oscillating body viscometers have to be overcome for a rotating cylinder viscometer. Some uncertainty arises in the value of the torsional constant of the suspension wire due to internal friction and the effect

of tensile stress. Thus the wire needs to be calibrated over the range of temperatures of the viscosity measurements.

As with oscillating body viscometers a relatively large volume has to be maintained at a constant temperature otherwise secondary flows can be set up due to convection. This can present quite a problem since a means must be devised to observe the mirror attached to the suspended cylinder. This is usually accomplished by some form of window which, unless care is taken, can give rise to a large heat loss. The temperature stability can also be affected by the heat generated from the rotating seal on the shaft which drives the outer cylinder, although this can be overcome by using a magnetic drive which removes the need for a rotating seal.

As found with oscillating disc viscometers great care must be taken to ensure that the inner cylinder hangs properly otherwise fouling of the cylinder with the guard cylinders can occur. It is also essential to maintain a constant gap between the inner and outer cylinders since any eccentricity can affect the accuracy of the viscometer.

The guard cylinders mentioned above are used to extend the flow pattern beyond the ends of the suspended cylinder and thus minimise the end effects. However secondary flows can be set up between the rotating cylinder and the ends of the pressure vessel which must be taken into consideration.

It is felt that the rotating cylinder viscometer although complicated in nature, is capable of rendering accurate absolute measurements over a wide range of conditions comparable with any

measurements made with capillary viscometers.

At first it was thought that an annulus type viscometer as used by Jackson (21), (22) offered an acceptable alternative to capillary viscometers. Since it is a flow through viscometer capable of giving absolute measurements the difficulties of measuring the flow rate and pressure drop are similar to the capillary viscometer. However several distinct advantages exist with annulus flow viscometers:-

(a) Since pressure tappings can be easily drilled in the wall of the cylinder without distorting the flow, the end effects which can only be estimated on a semi-empirical basis with capillary viscometers, can be eliminated by placing the pressure tappings far enough downstream.

(b) The size of the cylinders can be obtained with modern gauging equipment to a very high accuracy and probably equally important the cylinders can be easily inspected for out of roundness. One difficulty however would appear to be in aligning the inner cylinder to be concentric with the outer cylinder and maintaining the annular gap constant over the temperature range of the experiments.

Apart from this difficulty it was found that the results of Jackson for steam compared unfavourably with those obtained by capillary and oscillating body viscometers, the results being anything up to 10% lower. A more exact series of experiments was conducted in an attempt to discover the discrepancy but little improvement in the results was obtained. No explanation could be found for the consistently low values and on the suggestion of Jackson in his paper that another form of flow viscometer be developed to verify or disprove his results, the author was prompted to investigate the type of viscometer described below.

It was thus decided to make a radial flow viscometer as first outlined by Gumbel (23) in Barr's "Monograph of Viscometry".[*] This viscometer consists principally of two flat discs fixed a known distance apart, the test fluid being forced radially inward or outward and leaving or entering the viscometer through a hole in the centre of one of the discs. Being an open circuit viscometer, the same care must be taken with measuring pressure drops and mass flow rates as with capillary or annulus viscometers.

The same advantages as are present with the annulus viscometer over the capillary viscometer are possessed with a radial flow instrument:-

(a)   The plates can be made flat to a high accuracy and inspected readily.

(b)   Since pressure tappings are easily drilled in flat plates and blemishes etc readily detectable, the pressure tappings can be placed a sufficient distance downstream of the plate entrance to avoid end effects. This is not possible with capillary viscometers due to the fine bores used.

An added attraction over both capillary and annulus viscometers is the fact that the plate separation is raised in the working formula only to the third power as compared with the fourth power for the radius of a capillary or the outer and inner diameters of the cylinders of an annulus viscometer. Admittedly in the latter case the lengths to be measured are larger and readily gauged to a high precision with the modern methods available. Thus the accuracy to which the plate separation needs to be known is not as essential as for capillary viscometers. However in the author's experience this measurement accounted for the largest single error so that to obtain good absolute

[*]For further comment see Appendix (1).

measurement an accurate method of measuring the plate separation
needs to be devised. Of course, if the instrument were to be used
as a secondary apparatus this difficulty would be avoided.

The main disadvantage of this type of viscometer lies in the
inexactness of the theory describing radial flow between plates.
Gumbel (23) in his measurements used the simple creeping flow solution
which does not take into account the loss of pressure (or its recovery
for diverging flow) due to inertia effects. The author has been primarily
concerned with investigating the various solutions available that account
for inertia effects and concludes that this potential source of error
can be adequately accounted for. This is discussed more fully elsewhere
in this thesis.

In its application to high pressure viscometry, the radial flow
viscometer designed by the author uses the principles involved in a
Rankine viscometer. The flow between the plates is produced by a
mercury pellet falling under gravity down a glass tube connected to
the plates by a horizontal connecting tube. Unfortunately this design
necessitates that the apparatus be calibrated with a fluid of known
viscosity since due to the small flows involved the plate separation
is too small to be measured with any accuracy.

Other corrections that must be made in this type of viscometer
are for the small pressure losses in the connecting tubes and the loss
in head due to the drag on the mercury pellet caused by the unequal
curvatures of the ends of the pellet. An added disadvantage of adopting
the principle of a Rankine viscometer is that a semi-empirical expression

for the loss of pressure in the inlet length of the plates must be used similar to that used in capillary viscometers.

Advantages of the system are:-

(a)   the pressure drop due to inertia effects is small due to the small flow rates involved - the creeping flow solution was estimated to incur only a slight error;

(b)   the test volume is constant and relatively small so that the temperature can be maintained constant with relative ease.

It is felt that the principle of radial flow could best be utilised for high pressure viscometry by developing a flow through viscometer in which the difficulties of high pressures would be overcome with suitable control and reducing valves. The main problem which is envisaged by the author is the development of a high pressure differential manometer which although difficult to make is not impossible as has been shown by such experimenters as Jackson (22) and Schmidt and Mayinger (24) to name but a few.

The flow could be produced in various ways, the most common method being with the use of a constant speed pump. In this way the advantages listed above of a radial flow viscometer could best be used and a suitable alternative to capillary viscometers consequently found.

CHAPTER II

Review of Analyses of Radial Flow

The substance of this problem is contained within the Navier Stokes equations, which themselves incorporate various assumptions, the main one being the relationship between the stress and strain of the liquid. This relationship can only be given empirically and for liquids it is given by Stokes' law of friction which states that the forces opposing deformation of the body are proportional to the rate of strain. For water, the flow can be assumed incompressible i.e. the density is constant, and since the temperature variations in the test section are very small, the viscosity can be assumed constant.

In vector notation the Navier Stokes equations become

$$\rho \frac{Dw}{Dt} = -grad\,p + \mu \nabla^2 w \qquad \ldots\ldots(1)$$

where ∇^2 denotes the Laplace operator $\frac{\partial^2}{\partial x^2} + \frac{\partial^2}{\partial y^2} + \frac{\partial^2}{\partial z^2}$,

and $\frac{Dw}{Dt}$ denotes the substantive acceleration. For the study of steady laminar radial flow of an incompressible fluid, the Navier Stokes equations are expressed in the cylindrical coordinates r, θ, z, the corresponding velocities in these directions being u, v, and w, (see fig (2.1)).

For steady radial flow, the following terms are zero

$$v, \ \frac{\partial u}{\partial t}, \ \frac{\partial v}{\partial t}, \ \frac{\partial w}{\partial t}, \ \frac{\partial u}{\partial \theta}, \ \frac{\partial v}{\partial \theta}, \ \frac{\partial w}{\partial \theta}, \ \frac{\partial^2 u}{\partial \theta^2}, \ \frac{\partial^2 v}{\partial \theta^2}, \ \frac{\partial^2 w}{\partial \theta^2}$$

This reduces the Navier Stokes equations to

$$\rho\left(u\frac{\partial u}{\partial r} + w\frac{\partial u}{\partial z}\right) = -\frac{\partial p}{\partial r} + \mu\left[\frac{\partial\left(\frac{1}{r}\frac{\partial(ru)}{\partial r}\right)}{\partial r} + \frac{\partial^2 u}{\partial z^2}\right] \qquad \ldots\ldots(2)$$

FIG. 2.1.

DIRECTION OF FLOW.
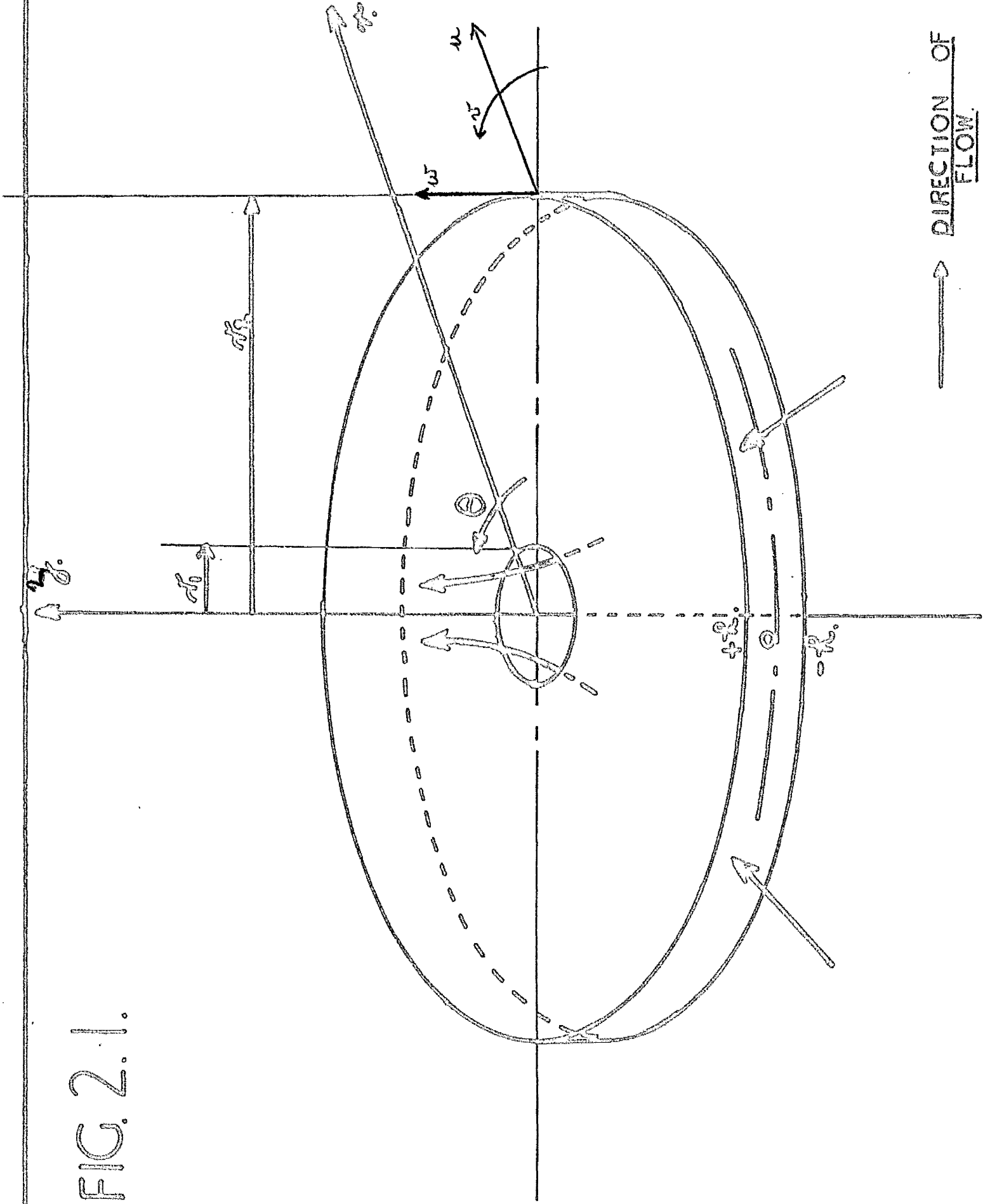
and $\rho\left(u\frac{\partial w}{\partial r} + w\frac{\partial w}{\partial z}\right) = -\frac{\partial p}{\partial z} + \mu\left[\frac{1}{r}\frac{\partial\left(r\frac{\partial w}{\partial r}\right)}{\partial r} + \frac{\partial^2 w}{\partial z^2}\right]$ .....(3)

The continuity equation becomes

$$\frac{1}{r}\frac{\partial(ru)}{\partial r} + \frac{\partial w}{\partial z} = 0 \qquad\qquad .....(4)$$

An exact solution to these equations has never been found and although it appears impossible to solve analytically a numerical approach might yield a solution. Consequently all attempts at solving the problem have embodied some approximations. Numerous authors have investigated the above equations and from a study of their solutions they have solved the problem by one of two methods.

The first method employed assumes that the axial velocity component w can be ignored and involves integration of the resulting equations of motion across the film thickness at any radius r. This is the method adopted by Karman in his momentum equation solutions to the boundary layer problem.

The other method requires the velocities and pressures to be expressed as power series and by putting these expressions into the equations of motion (2), (3) and (4) and identifying like terms (in this case terms in $\frac{1}{r}$, $\frac{1}{r^2}$, $\frac{1}{r^3}$ etc) the velocities and pressures can be evaluated.

As stated above, the first method makes the assumption that the axial velocity component is zero i.e. w = 0. This reduces equations (2), (3) and (4) to

$$\rho u\frac{\partial u}{\partial r} = -\frac{\partial p}{\partial r} + \mu\left[\frac{\partial^2 u}{\partial z^2} + \frac{\partial\left(\frac{1}{r}\frac{\partial(ur)}{\partial r}\right)}{\partial r}\right] \qquad .....(5)$$

$$O = -\frac{\partial p}{\partial z} \qquad \ldots\ldots(6)$$

and

$$\frac{1}{r}\frac{\partial(ur)}{\partial r} = 0 \qquad \ldots\ldots(7)$$

Combining equations (5) and (7)

$$\rho u \frac{\partial u}{\partial r} = -\frac{dp}{dr} + \mu \frac{\partial^2 u}{\partial z^2} \qquad \ldots\ldots(8)$$

The simplest solution to equation (8) is the "creeping flow" solution which assumes the inertia term to be negligible. Equation (8) then reduces to

$$\frac{dp}{dr} = \mu \frac{d^2 u}{dz^2} \qquad \ldots\ldots(9)$$

If equation (9) is integrated twice w.r.t. z and with the boundary conditions $u = 0$ at $z = \pm h$, the velocity profile is obtained

$$u = -\frac{1}{2\mu}\frac{dp}{dr}\left(h^2 - z^2\right) \qquad \ldots\ldots(10)$$

For converging flow the overall continuity equation is

$$Q = -2\int_0^h 2\pi r u\, dz \qquad \ldots\ldots(11)$$

Substituting for u in equation (11) and integrating w.r.t. r gives the pressure drop for the well known "creeping flow" solution.

$$(p_2 - p_1) = \frac{3\mu Q}{4\pi h^3}\ln\frac{r_2}{r_1} \qquad \ldots\ldots(12)$$

From equations (10) and (11) the velocity can be expressed as

$$u = -\frac{3Q}{8\pi r h}\left(1 - \left(\frac{z}{h}\right)^2\right) \qquad \ldots\ldots(13)$$

Equation (8) has been solved by such authors as Comolet (27), Livesey (28), Moller (29), and Jackson and Symmons (30). However to do so they had to assume u, the radial velocity, could be expressed in a certain form.

Comolet assumed a parabolic distribution of the form

$$\frac{u}{U} = \left[1 - \left(\frac{3}{k} \right)^2 \right]$$

.....(14)

where U is the velocity midway between the plates.

Livesey assumed the parabolic velocity distribution of the "creeping flow" solution given by equation (13).

These expressions for u are put into equation (8) which is then integrated across the film thickness to obtain an expression for the pressure drop between the radii r_2 and r_1 ($r_2 > r_1$). For converging flow this is

$$(p_2 - p_1) = \frac{3\mu Q}{4\pi k^3} \ln \frac{r_2}{r_1} + \frac{3\rho Q^2}{80\pi^2 k^2} \left(\frac{1}{r_1^2} - \frac{1}{r_2^2} \right)$$

.....(15)

Comolet's expression for the radial velocity (eq'n (14) is identical to the expression given by equation (13).

The above authors have obtained radial pressure distributions for diverging flow. Since the author has been concerned with the study of converging flow, the various solutions have been altered to express the pressure distribution for converging flow. To obtain pressure and velocity distributions for diverging flow equation (11) is changed in sign. This results in the pressure drop for diverging flow being expressed as

$$(p_1 - p_2) = \frac{3\mu Q}{4\pi k^3} \ln \frac{r_2}{r_1} - \frac{3\rho Q^2}{80\pi^2 k^2} \left(\frac{1}{r_1^2} - \frac{1}{r_2^2} \right)$$

.....(16)

Moller also solved the problem by the momentum integral method. He stated that a general expression, for the radial velocity was

$$u = F(r) f(3)$$

.....(17)

This could be put into equation (4), the continuity equation for two dimensional flow, to give the axial velocity

$$w = \frac{1}{r} \frac{\partial [r \, F(r)]}{\partial r} \int_0^{\mathfrak{z}} f(\mathfrak{z}) \, d\mathfrak{z} \qquad \dots (18)$$

From the boundary conditions that $v = 0$ at $z = \pm h$ it follows that $rF(r)$ is constant. Thus from equation (17)

$$u = \frac{f(\mathfrak{z})}{r} \qquad \text{and} \quad w = 0 \quad \text{everywhere.}$$

However, that this cannot be so, can be explained from the statement that equation (17) is a general expression for the radial velocity. In fact, it is a particular solution of u.

The velocity profile that Moller uses in his solution makes allowances for the profile being not quite parabolic.

Taking the bottom plate as the r-axis and the plate separation as h, the radial velocity profile for half the plate separation is assumed to be

$$\frac{u}{U_0} = 4 \frac{\mathfrak{z}}{h} \left(1 - \frac{\mathfrak{z}}{h}\right) + \xi \frac{\mathfrak{z}}{h} \left(1 - 2 \frac{\mathfrak{z}}{h}\right)^3 \qquad \dots (19)$$

where Uo is the velocity at the centre of the channel and ξ is a function of r.

This expression only represents the velocity profile between the bottom plate $z = 0$ and $z = {}^h/2$ the centre line between the plates. The profile between $z = {}^h/2$ and the top plate $z = h$ is taken to be a mirror image of the profile between $z = 0$ and $z = {}^h/2$.

That equation (19) does not represent the velocity profile from $z = {}^h/2$ to $z = h$ can be seen from the fact that at $z = h$ $\frac{u}{U_0} = -\xi$ whereas the boundary conditions at the wall (at least for no slip) state that $\frac{u}{U_0}$ should equal zero. Although equation (19) satisfies

the conditions of u = 0 at z = 0 and $\frac{du}{dz} = 0$ at z = $^h/2$, it is not a very satisfactory expression for the velocity profile.

Moller proceeds in his analysis with the overall continuity equation to obtain an expression for Uo for diverging flow

$$U_0 = \frac{\varphi}{2\pi r h \left[\frac{2}{3} + \zeta/_{40}\right]} \qquad \ldots\ldots(20)$$

Using the compatibility condition at the wall that

$$\frac{dp}{dr} = \left[\mu \frac{\partial^2 u}{\partial \zeta^2}\right]_0 \qquad \ldots\ldots(21)$$

and equation (19) then

$$\zeta = -\frac{2}{3}\left[1 + \frac{dp}{dr} \frac{h^2}{8\mu U_0}\right] \qquad \ldots\ldots(22)$$

Moller ignores the $\zeta/_{40}$ term in equation (20) since it must be small for viscous flow so that

$$U_0 = \frac{3\varphi}{4\pi r h} \qquad \ldots\ldots(23)$$

He further assumes that the ζ term can be ignored when dealing with the inertia term in equation (8).

With these approximations the equation of motion is now integrated across the film thickness and replacing Uo and ζ by the above values then for a gap of 2h (so as to compare with equations (12), (15) etc.)

$$\frac{dp}{dr} = -\frac{3\mu\varphi}{4\pi r h^3} + \frac{9\rho\varphi^2}{100\pi^2 h^2 r^3} \qquad \ldots\ldots(24)$$

Integrating w.r.t. r between r_1 and r_2 then for diverging flow

$$(p_1 - p_2) = \frac{3\mu\varphi}{4\pi h^3} \ln \frac{r_2}{r_1} - \frac{9\rho\varphi^2}{200\pi^2 h^2}\left(\frac{1}{r_1^2} - \frac{1}{r_2^2}\right) \qquad \ldots\ldots(25)$$

The author has attempted to ascertain the effect of Moller's approximations in the calculation of the latter's solution. The

following analysis for converging flow incorporates several minor

approximations to simplify the algebra. Using the values of u and ζ

given in equation (19) and (22) the equation of motion becomes

$$\frac{4091\,h\,r^2U_0^2}{11340} - \frac{1858\,U_0\,r^2h^3}{11340\,\mu}\frac{dp}{dr} - \frac{1759\,h^5r^2}{45360}\left(\frac{dp}{dr}\right)^2 = \frac{5h\,r^3}{6\rho}\frac{dp}{dr} + \frac{5\nu\,r^3U_0}{3h} \quad \ldots\ldots(26)$$

The $\left(\frac{dp}{dr}\right)^2$ term is only about 1% of the other terms and is ignored.

From equations (20) and (22) an expression for Uo is obtained

that does not contain ζ

$$U_0 = \left[\frac{h^2}{312\,\mu}\frac{dp}{dr} - \frac{10\,\varphi}{13\pi\,r\,h}\right] \quad \ldots\ldots(27)$$

Substituting for Uo in equation (26) and ignoring terms in $\left(\frac{dp}{dr}\right)^2$

which are again small

$$\frac{dp}{dr} = \left[\frac{3\mu\varphi}{4\pi h^3 r} + \frac{1171\,\rho\,\varphi^2}{13104\,\pi^2 h^2 r^3}\right]\left[1 + \frac{2189\,\rho\,\varphi\,h}{98280\,\pi\,\mu\,r^2}\right]^{-1} \quad \ldots\ldots(28)$$

Integrating w.r.t. r between r_1 and r_2 $(r_2 > r_1)$ and taking only the

first term of the binomial expansion gives the pressure drop for

converging flow

$$(p_2 - p_1) = \frac{3\mu\varphi}{4\pi h^3}\ln\frac{r_2}{r_1} + \frac{24.55\,\rho\,\varphi^2}{560\,\pi^2 h^2}\left(\frac{1}{r_1^2} - \frac{1}{r_2^2}\right) - \frac{5\times10^{-5}\rho^2\varphi^3\left(\frac{1}{r_1^4} - \frac{1}{r_2^4}\right)}{\pi^3\mu\,h} + \cdots \quad \ldots\ldots(29)$$

The last term of equation (29) can be ignored.

Comparing equations (25) and (29), Moller's solution gives the

coefficient of the pressure drop due to inertia as $\frac{25.2}{560}$ (i.e. $\frac{9}{200}$)

whereas with fewer assumptions the coefficient is reduced to $\frac{24.55}{560}$.

As stated above equation (19) only represents the velocity for

half the gap and does not appear to be a very satisfactory expression

for the velocity profile.

The author suggests a more suitable expression for the profile

using Moller's method would be

$$\frac{u}{U_0} = \left[1 - \left(\frac{3}{h} \right)^2 \right] + \zeta \left[1 - \left(\frac{3}{h} \right)^2 \right]^2 \qquad \dots \dots (30)$$

where the gap is 2h and the r-axis is taken midway between the plates. Equation (30) satisfies the boundary conditions of u = 0 at z = ± h and $\frac{du}{dz}$ = 0 at z = 0 and hence can be taken to represent the velocity profile across the whole gap. From the continuity equation for converging flow

$$U_0 = \frac{-Q}{4\pi r h \left[\frac{2}{3} + \frac{14}{15} \zeta \right]} \qquad \dots \dots (31)$$

and from the compatibility condition at the wall

$$\frac{dp}{dr} = \left[\mu \frac{\partial^2 u}{\partial 3^2} \right]_h \qquad \dots \dots (32)$$

it follows

$$\zeta = \left[\frac{1}{4} + \frac{1}{8} \frac{h^2}{\mu U_0} \frac{dp}{dr} \right] \qquad \dots \dots (33)$$

The expression for the velocity given by equation (30) is used to solve equation (8), the equation of motion, and integrating across the film thickness gives the resulting equation (no terms have been neglected so far).

$$\left[\frac{805 \, Q^2}{15552 \, \pi^2 h} + \frac{10 \nu r^2 Q}{18 \pi h^2} \right] + \frac{409 \, h^5 r^2}{87480 \, \mu^2} \left(\frac{dp}{dr} \right)^2 = \left[\frac{20 r^3 h}{27 \rho} - \frac{641 \, Q r h^2}{23328 \, \pi \mu} \right] \frac{dp}{dr}$$

$$\dots \dots (34)$$

The $\left(\frac{dp}{dr} \right)^2$ term is less than $\frac{1}{2}$% of the term $\frac{10 \nu r^2 Q}{18 \pi h^2}$, the largest term in equation (34), for water at atmospheric conditions, and is thus neglected.

Hence $\frac{dp}{dr} = \left[\frac{3 \mu Q}{4 \pi h^3 r} + \frac{161 \rho Q^2}{2304 \pi^2 h^2 r^3} \right] \left[1 - \frac{641 \rho Q h}{17280 \pi \mu r^2} \right]^{-1} \qquad \dots \dots (35)$

Taking only the first term of the binomial expansion (which for normal

test conditions is about [1]/30) and integrating w.r.t. r, the pressure drop for converging flow becomes

$$\left(p_2 - p_1\right) = \frac{3\mu\varphi}{4\pi h^3} \ln \frac{r_2}{r_1} + \frac{27.35 \rho \varphi^2}{560 \pi^2 h^2}\left(\frac{1}{r_1^2} - \frac{1}{r_2^2}\right) + \cdots \qquad \ldots(36)$$

A third term on the right hand side of equation (36) has been ignored as negligible. This expression is nearly identical to a solution obtained by Jackson and Symmons.

This method uses the velocity profile obtained by the "creeping flow" solution given by equation (13) to form the inertia term of equation (8).

$$\mu \frac{d^2 u}{dz^2} = \frac{dp}{dr} - \frac{9\rho\varphi^2\left(h^2 - z^2\right)^2}{64\pi^2 h^6 r^3} \qquad \ldots(37)$$

Since $\frac{dp}{dr}$ is independent of y for the assumption of no axial velocity component, equation (37) is integrated twice w.r.t. z using the boundary conditions u = 0 at z = $\pm$ h to obtain a further expression for u in the form

$$u = \frac{1}{2\mu}\left(z^2 - h^2\right)\frac{dp}{dr} - \frac{9\rho\varphi^2}{64\pi^2 h^6 \mu r^3}\left[\frac{z^6}{30} - \frac{h^2 z^4}{6} + \frac{h^4 z^2}{2} - \frac{11 h^6}{30}\right] \qquad \ldots(38)$$

Equation (38) is now used as a substitution for u in the continuity equation for diverging flow

$$\varphi = 4\pi r \int_0^h u\, dz \qquad \ldots(39)$$

and on integrating w.r.t. r the pressure drop between r_2 and r_1 ($r_2 > r_1$) for diverging flow is obtained

$$\left(p_1 - p_2\right) = \frac{3\mu\varphi}{4\pi h^3}\ln\frac{r_2}{r_1} - \frac{27\rho\varphi^2}{560\pi^2 h^2}\left(\frac{1}{r_1^2} - \frac{1}{r_2^2}\right) \qquad \ldots(40)$$

This is very similar to equation (36) obtained by Moller's method.

Jackson and Symmons have repeated the above process to obtain a further approximation of the velocity by eliminating $\frac{dp}{dr}$ in equation (38) with the use of equation (40). The radial velocity for diverging flow becomes

$$u = \frac{-3\varphi(z^2-h^2)}{8\pi r h^3} - \frac{9\rho\varphi^2}{64\pi^2 h^6 \mu r^3}\left[\frac{z^6}{30} - \frac{h^2 z^4}{6} + \frac{11h^4 z^2}{70} - \frac{h^6}{42}\right] \dots(41)$$

Equation (41) is now used to form the inertia term of equation (8). The resulting equation for the pressure given by Jackson and Symmons is

$$(p_1 - p_2) = \frac{3\mu\varphi}{4\pi h^3}\ln\frac{r_2}{r_1} - \frac{27\rho\varphi^2}{560\pi^2 h^2}\left(\frac{1}{r_1^2} - \frac{1}{r_2^2}\right) - \frac{0.000435\rho^2\varphi^3\left(\frac{1}{r_1^4} - \frac{1}{r_2^4}\right)}{\pi^3\mu h}$$

$$- \frac{0.00000114\rho^3\varphi^4\left(\frac{1}{r_1^6} - \frac{1}{r_2^6}\right)}{\pi^4\mu^2} \dots(42)$$

The author on checking equation (42) disagrees with the coefficient of the last two terms and found them to be 0.000181 and 0.0000528 respectively.

To find a more accurate expression for the pressure drop it has to be noted that the velocity distribution is not parabolic but is expressed as a polynomial in z. The continuity equation (7) can be rewritten as

$$\frac{\partial u}{\partial r} + \frac{u}{r} = 0 \dots(43)$$

and the fact that equation (41) is an approximate expression for the radial velocity can be demonstrated since $\frac{\partial u}{\partial r} \neq -\frac{u}{r}$.

It is claimed that if the iterative method described above were continued, the expression obtained for $\frac{dp}{dr}$ would become more accurate for decreasing r. However the author feels that, for small

r, any increased accuracy obtained by taking more terms is nullified by the fact that the approximations used in obtaining a solution become more pronounced as r decreases.

The second method used to solve equations (2), (3) and (4) is by expressing the pressure, radial and axial velocities as power series. Hunt and Torbe (31) have solved the equations by eliminating p from equations (2) and (3) to give

$$u\frac{\partial^2 u}{\partial r.\partial z} + \frac{\partial u}{\partial r}.\frac{\partial u}{\partial z} + w\frac{\partial^2 u}{\partial z^2} + \frac{\partial w}{\partial z}.\frac{\partial u}{\partial z} - u\frac{\partial^2 w}{\partial r^2} - \frac{\partial u}{\partial r}.\frac{\partial w}{\partial r} - w\frac{\partial^2 w}{\partial r.\partial z} - \frac{\partial w}{\partial r}.\frac{\partial w}{\partial z}$$

$$= \nu\left[\frac{\partial^3 u}{\partial r^2\partial z} + \frac{1}{r}\frac{\partial^2 u}{\partial r.\partial z} + \frac{\partial^3 u}{\partial z^3} - \frac{1}{r^2}\frac{\partial u}{\partial z} - \frac{\partial^3 w}{\partial r^3} - \frac{1}{r}\frac{\partial^2 w}{\partial r^2} - \frac{\partial^3 w}{\partial z^2\partial r} + \frac{1}{r^2}\frac{\partial w}{\partial r}\right]$$

$$\ldots\ldots(44)$$

The radial velocity is assumed to be of the form

$$u = u_1'(z)\frac{R}{r} + u_2'(z)\left(\frac{R}{r}\right)^2 + u_3'(z)\left(\frac{R}{r}\right)^3 + \cdots \qquad \ldots\ldots(45)$$

where u_1^1, u_2^1, u_3^1, are functions of z only and R denotes the outside radius. The separation of the plates is taken as h with the bottom and top plates being respectively z = 0 and z = h. From the continuity equation (4) an expression for w is deduced

$$w = \frac{1}{R}\left[u_2(z)\left(\frac{R}{r}\right)^3 + 2 u_3(z)\left(\frac{R}{r}\right)^4 + \cdots\right] + \phi(r) \qquad \ldots\ldots(46)$$

Substituting for u and w in equation (44) and assuming squares and products of u_2 and u_3 etc are negligible a set of equations can be compiled by comparing the coefficients of powers of r. Using the boundary conditions that u = w = 0 at z = 0 and z = h gives the following expressions

$$u_2(z) = 0$$

$$u_3(z) = -\frac{\bar{u}^2 h^3}{420\nu R}\left[\left(\frac{z}{R}\right)^2\left(1-\frac{z}{R}\right)^2\left(1-2\frac{z}{R}\right)\left(1+\frac{z}{R}-\left(\frac{z}{R}\right)^2\right)\right]$$

$$u_1'(z) = \bar{u}\left(\frac{z}{R}\right)\left(1-\frac{z}{R}\right)$$

$$u_2'(z) = 0$$

$$u_3'(z) = -\frac{\bar{u}^2 h^2}{420\nu R}\left(\frac{z}{R}\right)\left(1-\frac{z}{R}\right)\left[2-7\frac{z}{R}\left(1-\frac{z}{R}\right)-14\left(\frac{z}{R}\right)^2\left(1-\frac{z}{R}\right)^2\right]$$

$$.....(47)$$

where $\bar{u}$ has the dimensions of velocity.

As pointed out by Jackson and Symmons (32) the expression for $u_3^2(z)$ differs from that given by Hunt and Torbe. The rest of their paper examines the importance of the inertia terms and concludes that for the case of hydrostatic thrust bearings the inertia terms are negligible.

From equation (47) the expressions for the radial and axial velocities are

$$u = \bar{u}\left(\frac{z}{R}\right)\left(1-\frac{z}{R}\right)\frac{R}{r} - \frac{\bar{u}^2 h^2}{420\nu R}\left[\left(\frac{z}{R}\right)\left(1-\frac{z}{R}\right)\left(2-7\frac{z}{R}\left(1-\frac{z}{R}\right)-14\left(\frac{z}{R}\right)^2\left(1-\frac{z}{R}\right)^2\right)\right]\left(\frac{R}{r}\right)^3 \quad (48)$$

and

$$w = -\frac{\bar{u}^2 h^3}{210\nu R^2}\left[\left(\frac{z}{R}\right)^2\left(1-\frac{z}{R}\right)^2\left(1-2\frac{z}{R}\right)\left(1+\frac{z}{R}-\left(\frac{z}{R}\right)^2\right)\right]\left(\frac{R}{r}\right)^4 \qquad .....(49)$$

Using equations (48) and (49) to substitute for u and w in equation (2) the radial pressure distribution becomes

$$\frac{\partial p}{\partial r} = -\frac{2\mu\bar{u}}{h^2}\frac{R}{r} - \frac{8\rho\bar{u}^2 h^2}{420}\frac{R^2}{r^5}\left(\frac{z}{R}\right)\left(1-\frac{z}{R}\right)\left(2-7\frac{z}{R}-7\left(\frac{z}{R}\right)^2+28\left(\frac{z}{R}\right)^3-14\left(\frac{z}{R}\right)^4\right) + \rho\bar{u}^2\left(\frac{z}{R}\right)^2\left(1-\frac{z}{R}\right)^2\frac{R^2}{r^3}$$

$$+\frac{\rho\bar{u}^2}{70}\left[3-70\left(\frac{z}{R}\right)^2+140\left(\frac{z}{R}\right)^3-70\left(\frac{z}{R}\right)^4\right]\frac{R^2}{r^3} - \frac{\rho^2\bar{u}^3 h^2}{210\mu}\left(\frac{z}{R}\right)^2\left(1-\frac{z}{R}\right)^2\left[3-11\frac{z}{R}-13\left(\frac{z}{R}\right)^2+48\left(\frac{z}{R}\right)^3-24\left(\frac{z}{R}\right)^4\right]\frac{R^3}{r^5} \qquad .....(5$$

$$+\frac{\rho^3\bar{u}^4 h^4}{(420\mu R)^2}\left(\frac{z}{R}\right)^2\left(1-\frac{z}{R}\right)^2\left[8-44\frac{z}{R}+39\left(\frac{z}{R}\right)^2+234\left(\frac{z}{R}\right)^3-425\left(\frac{z}{R}\right)^4-336\left(\frac{z}{R}\right)^5+1288\left(\frac{z}{R}\right)^6-1008\left(\frac{z}{R}\right)^7+252\left(\frac{z}{R}\right)^8\right]\frac{R^6}{r^7}$$

Since the pressure is measured by static tappings the pressure

distribution at the walls need only be considered i.e. at

z = 0 or z = h. Thus equation (50) reduces to

$$\frac{dp}{dr} = -2\frac{\mu\bar{u}}{R^2}\frac{R}{r} + \frac{3R^2\rho\bar{u}^2}{70\,r^3} \qquad \ldots\ldots(51)$$

which is what Jackson and Symmons obtained. They then found an

expression for $\bar{u}$ using the overall continuity equation

$$Q = \int_0^h 2\pi r\,u\,dy \qquad \ldots\ldots(52)$$

and substituting for u from equation (48) in (52) gives

$$\bar{u} = \frac{3Q}{\pi R h} \qquad \ldots\ldots(53)$$

Putting the value of $\bar{u}$ into equation (51), integrating w.r.t. r

and making the gap 2h instead of h gives for diverging flow

$$(p_1 - p_2) = \frac{3\mu Q}{4\pi h^3}\ell n\frac{r_2}{r_1} - \frac{27\rho Q^2}{560\,\pi^2 h^2}\left(\frac{1}{r_1^2} - \frac{1}{r_2^2}\right) \qquad \ldots\ldots(54)$$

This of course is identical to equation (40) obtained by Jackson

and Symmons using a uni-directional flow analysis.

Although the series method of Hunt and Torbe attempts to

take into consideration the two dimensional nature of the problem,

the radial velocity u is limited to three terms and products and

squares of u_2 and u_3 are ignored. There also seems to be no attempt

at evaluating the term $\phi(r)$ in equation (46).

A more complete solution using the power series approach is that

given by Peube (33) and Savage (34). Although Savage did not express

the radial and axial velocities exactly as Peube (he introduced a stream function to express them), as one would expect, the final results are identical.

Taking Peube's calculation to illustrate the method the velocity and pressure terms are expressed as

$$u = \frac{f_1(\frac{z}{\ell})}{r} + \frac{f_2(\frac{z}{\ell})}{r^2} + \frac{f_3(\frac{z}{\ell})}{r^3} + \cdots \cdots + \frac{f_n(\frac{z}{\ell})}{r^n} + \cdots \qquad \ldots\ldots(55)$$

$$v = \frac{g_1(\frac{z}{\ell})}{r} + \frac{g_2(\frac{z}{\ell})}{r^2} + \frac{g_3(\frac{z}{\ell})}{r^3} + \cdots \cdots + \frac{g_n(\frac{z}{\ell})}{r^n} + \cdots \qquad \ldots\ldots(56)$$

$$p = p_0 + h_0(\frac{z}{\ell})\ln r + \frac{h_1(\frac{z}{\ell})}{r} + \frac{h_2(\frac{z}{\ell})}{r^2} + \cdots \cdots + \frac{h_n(\frac{z}{\ell})}{r^n} + \cdots \qquad \ldots\ldots(57)$$

The above expressions are now inserted into equations (2), (3) and (4). By identifying terms in r a series of equations are obtained relating f_1, f_2, f_3 etc. with g_1, g_2, g_3 etc. and h_0, h_1, h_2 etc. He proved that g_1, g_2 and h_1 are zero and showed that generally the functions f_n, h_{n-1} and g_{n+1} are zero where n is an even number. Using the boundary conditions

$$f_1(\pm 1) = f_2(\pm 1) = \quad \ldots \quad \ldots \quad = f_n(\pm 1) = 0$$

$$g_1(\pm 1) = g_2(\pm 1) = \quad \ldots \quad \ldots \quad = g_n(\pm 1) = 0 \qquad \ldots\ldots(58)$$

the radial and axial velocities and pressure are found to be for converging flow

$$u = \frac{3Q}{8\pi r \ell}\left(1-(\frac{z}{\ell})^2\right) + \frac{9\rho Q^2}{64\pi^2\mu r^3}\left[\frac{1}{30}(\frac{z}{\ell})^6 - \frac{1}{6}(\frac{z}{\ell})^4 + \frac{11}{70}(\frac{z}{\ell})^2 - \frac{1}{42}\right]$$

$$- \frac{9\rho Q^2 \ell^2}{4\pi^2\mu r^5}\left[\frac{((\frac{z}{\ell})^8-1)}{1680} - \frac{((\frac{z}{\ell})^6-1)}{180} + \frac{11((\frac{z}{\ell})^4-1)}{840} - \frac{((\frac{z}{\ell})^2-1)}{84}\right] - \frac{\rho Q^2 \ell^2 ((\frac{z}{\ell})^2-1)}{175\pi^2 r^5 \mu} \qquad \ldots\ldots(59)$$

$$+ \frac{39\rho^2 Q^3 \ell ((\frac{z}{\ell})^2-1)}{43120\pi^3\mu^2 r^5} + \frac{27\rho^2 Q^3 \ell}{128\pi^3\mu^2 r^5}\left[\frac{-[(\frac{z}{\ell})^{10}-1]}{3150} + \frac{[(\frac{z}{\ell})^8-1]}{336} - 19\frac{[(\frac{z}{\ell})^6-1]}{2100} + 11\frac{[(\frac{z}{\ell})^4-1]}{840} - \frac{[(\frac{z}{\ell})^2-1]}{84}\right]$$

$$w = \frac{q\rho\varphi^2 R}{32\pi^2\mu r^4}\left[\frac{\left(\frac{\delta}{R}\right)^7}{210} - \frac{\left(\frac{\delta}{R}\right)^5}{30} + 11\frac{\left(\frac{\delta}{R}\right)^3}{210} - \frac{\frac{207}{R}}{42}\right] - \frac{q\rho\varphi^2 R^3}{\pi^2\mu r^6}\left[\frac{\left[\left(\frac{\delta}{R}\right)^9 - 9\frac{\delta}{R}\right]}{15120} - \frac{\left[\left(\frac{\delta}{R}\right)^7 - 7\frac{\delta}{R}\right]}{1260} + 11\frac{\left[\left(\frac{\delta}{R}\right)^5 - 5\frac{\delta}{R}\right]}{4200} \right.$$

$$\left. - 59\frac{\left[\left(\frac{\delta}{R}\right)^3 - 3\frac{\delta}{R}\right]}{18900}\right]\quad\dots\dots(60)$$

$$- \frac{27\rho^2\varphi^3 R^2}{32\pi^3\mu^2 r^6}\left[\frac{\left[\left(\frac{\delta}{R}\right)^{11} - 11\left(\frac{\delta}{R}\right)\right]}{34650} - \frac{\left[\left(\frac{\delta}{R}\right)^9 - 9\frac{\delta}{R}\right]}{3024} + 11\frac{\left[\left(\frac{\delta}{R}\right)^7 - 7\frac{\delta}{R}\right]}{14700} - 11\frac{\left[\left(\frac{\delta}{R}\right)^5 - 5\frac{\delta}{R}\right]}{4200} + 739\frac{\left[\left(\frac{\delta}{R}\right)^3 - 3\frac{\delta}{R}\right]}{291060}\right]$$

and

$$(p_2 - p_1) = \frac{3\mu\varphi}{4\pi R^3}\ln\frac{r_2}{r_1} + \frac{27\rho\varphi^2}{560\pi^2 R^2}\left(\frac{1}{r_1^2} - \frac{1}{r_2^2}\right) + \rho\varphi^2\left[\frac{1}{350\pi^2} - \frac{39\rho\varphi}{86240\,\pi^3\mu R}\right]\left[\frac{1}{r_1^4} - \frac{1}{r_2^4}\right]$$

$$+ \frac{9\rho\varphi^2}{32\pi^2}\left[\frac{\delta^6}{30 R^6} - \frac{\delta^4}{6R^4} + \frac{11\delta^2}{70 R^2} - \frac{1}{42}\right]$$

$$\dots\dots(61)$$

In equations (59) and (61) the author found a slight error. The third term of (59) should have 175 and not 179 on the denominator and the last term of (61) contains the term $\frac{1}{350\pi^2}$ and not $\frac{1}{358\pi^2}$. The first two term of equation (61) are identical to the expressions for the pressure drop obtained by Jackson and Symmons. The author calculated further terms in the above expansions and found that for large gaps or very small radii they could become significant.

It is felt therefore that equation (61) is an accurate evaluation of the pressure drop for large r and fairly small values of r, but cannot be used confidently for small r since (a) as r –> 0 the series diverges instead of approaching some limiting value (b) more terms need to be known and this makes the calculation somewhat involved (c) the conditions that exist at the extraction hole (i.e. at very small r) are not accounted for. The above reasons may explain why Jackson found that for small r his experimental results agreed more favourably with equation (61) reduced to the first two terms than with equation (61) as presented above. The pressure drop given by equation (61)

is reduced to

$$(p_2-p_1) = \frac{3\mu\varphi}{4\pi h^3} \ln \frac{r_2}{r_1} + \frac{27\rho\varphi^2}{560 r^2 h^2}\left(\frac{1}{r_1^2}-\frac{1}{r_2^2}\right) + \rho\varphi^2\left(\frac{1}{350\eta^2}-\frac{39\rho\varphi}{86240\pi^3\mu h}\right)\left(\frac{1}{r_1^4}-\frac{1}{r_2^4}\right) \dots (62)$$

when calculating experimental results since the pressure is
normally measured with static pressure tappings and equation (62)
gives the pressure drops at the walls i.e. z = ± h.

The radial velocity distribution given by equation (59) shows
that for r → ∞ it reduces to a parabolic profile but for smaller
r, the profile changes from the parabolic form, the effect causing
the velocity for converging flow to be less than that obtained by the
parabolic distribution midway between the plates and greater *near to* the
walls. The opposite is the case for diverging flow.

To predict generally at what value of r the axial velocity
component starts to become significant for converging flow is
difficult since it depends on at least three variables – flow,
plate separation and kinematic viscosity. Taking only the first
terms of equations (59) and (60) to give some idea of when the
axial velocity component cannot be ignored, gives

$$\left.\begin{array}{l}\dfrac{\omega}{u} = \dfrac{9\rho\varphi^2 h}{32\pi^2\mu r^4} \dfrac{8\pi r h}{3\varphi} \dfrac{\left[\left(\frac{z}{h}\right)^7 - 7\left(\frac{z}{h}\right)^5 + 11\left(\frac{z}{h}\right)^3 - 5\frac{z}{h}\right]}{\left[1-\left(\frac{z}{h}\right)^2\right]} \\[12pt] = -\dfrac{\rho\varphi h^2}{280\eta\mu r^3}\left(\frac{z}{h}\right)\left[\left(\frac{z}{h}\right)^4 - 6\left(\frac{z}{h}\right)^2 + 5\right]\end{array}\right\} \quad \dots (63)$$

Differentiating equation (63) w.r.t. (z/h) to find the maximum
value gives $(z/h) \approx 0.55$. This reduces (63) to

$$\frac{\omega}{u} = \frac{-1.8\rho\varphi h^2}{280\eta\mu r^3} \qquad \dots (64)$$

Take, as an example, experiments with water at 20 °C, a plate
separation of 1 m.m. and a flow of 10 cm³/sec, then to limit the

axial velocity to 0.1% of the radial velocity the value of r is
approximately 1.7 cm. If these values are now used in equations
(59) and (60), the second term of the expression for the radial
velocity is some 3% of the first while the third term of equation
(60) is $\frac{2}{3}$ of the first term the second term being negligible. Thus
equation (64) is only a very approximate expression to use to determine
a value of r at which w is negligible. In conclusion, of the two
methods described above, the Karman momentum integral or power series
method, it would appear that the latter is the more elegant solution
although the improvement is only small for the majority of applications.

The power series approach uses equations (2), (3) and (4) which
describe exactly laminar radial flow, whereas the other method uses
equations (5), (6) and (7) which do not exactly describe radial flow
although, since w is quite small in most cases, the error must be
small. The fact that equations (5), (6) and (7) are not strictly
correct can be easily demonstrated.

From equation (7)

$ur = f$ where f is a function of z only

and substituting for u in equation (5) gives

$$\frac{\partial p}{\partial r} = \rho \frac{f^2}{r^3} + \frac{\mu}{r} \frac{\partial^2 f}{\partial z^2} \qquad \ldots\ldots(65)$$

p cannot be a function of z by equation (6) [for radial flow it is
of course not a function of θ either]. But by equation (65) p is a
function of z unless of course f was a constant which it cannot be
to satisfy the boundary conditions of zero velocity at $z = \pm h$.
However the error incurred is small for most practical purposes as

shown by the good agreement with the power series solutions of
Peube and Savage and the solution of Jackson and Symmons obtained
by the simpler uni-directional analysis. Thus the expression for
the pressure drop that best describes laminar radial flow would
appear to be

$$\left(p_2 - p_1\right) = \frac{3\mu Q}{4\pi h^3}\ln{r_2}/{r_1} + \frac{27\rho Q^2}{560\pi^2 h^2}\left(\frac{1}{r_1^2} - \frac{1}{r_2^2}\right) \qquad \ldots\ldots(66)$$

CHAPTER III

Analysis of Laminar Radial Flow between Parallel Plates

and Discussion of the Solution

The previous chapter reviews some of the solutions to the problem, some accounting for the two dimensional nature of the flow and others using the simpler uni-directional flow analysis.

Of the former, the power series solution of Peube gives an expression for the axial velocity component which, taking terms up to r^4, can be written

$$ w = \frac{9 \rho \varphi^2 h}{32 \pi^2 \mu r^4} \left[\frac{\left(\frac{3}{h}\right)^7}{210} - \frac{\left(\frac{3}{h}\right)^5}{30} + \frac{11\left(\frac{3}{h}\right)^3}{210} - \frac{\left(\frac{3}{h}\right)}{42} \right] \qquad \ldots..(1) $$

The maximum value of w occurs at $(z/h) = 0.446$ which reduces equation (1) to

$$ w \simeq \frac{3 \rho \varphi^2 h}{1600 \pi^2 \mu r^4} \qquad \ldots..(2) $$

The experiments which the author conducted were with water at room temperatures. The plate separation (i.e. 2h) ranged from 0.0194" to 0.0098" and the limit of the flow rate was 6 cm^3/sec to 7 cm^3/sec. Taking $r = \frac{3}{8}$", the radius on which the innermost tapping is situated, the maximum axial velocity attained during the series of experiments was calculated from equation (2) to be 0.028 cm/sec compared with a mean radial velocity at that radius of 24 cm/sec.

The average value of the axial velocity was much less and in attempting a solution to the problem from the Navier Stokes equations, the author felt

justified in ignoring the axial velocity component although this will inevitably lead to small inconsistencies from a mathematical point of view e.g. as described on the last page of Chapter II.

The author would like to indicate at this point that the following solution is not necessarily superior to the solutions presented in Chapter II, but merely an alternative solution. However, as will be demonstrated in Chapter V, it is in good agreement with Peube's series solution and also, within the limits of experimental errors, with observations.

For laminar radial flow between parallel plates, using cylindrical coordinates, the θ-component of velocity is zero. and the axial velocity component is assumed to be zero. This reduces the Navier Stokes equations to those given by equations (5), (6) and (7) in Chapter II viz:-

$$\rho u \frac{\partial u}{\partial r} = -\frac{\partial p}{\partial r} + \mu \left[\frac{\partial^2 u}{\partial z^2} + \frac{\partial \left(\frac{1}{r} \frac{\partial (ur)}{\partial r} \right)}{\partial r} \right] \qquad \ldots\ldots(3)$$

and

$$0 = -\frac{\partial p}{\partial z} \qquad \ldots\ldots(4).$$

The continuity equation is given by

$$\frac{1}{r} \frac{\partial (ur)}{\partial r} = 0 \qquad \ldots\ldots(5).$$

The solution to these equations is given at the end of the thesis on pages 2, 3 and 4 of a paper (35) presented by the author at the Thermodynamics and Fluid Mechanics Convention of the Institution of Mechanical Engineers at Liverpool. Consequently, only a discussion of the solution will be given here.

Referring to the paper, the mathematics involved in obtaining equation (28.21) from (28.20) and also equation (28.25) from (28.24) is given in Appendix (2). A few printing errors that occurred in the text have been corrected.

Owing to the complexity of the equations a computer programme was devised in Algol and is given in Appendix (3).

In the analysis, the boundary conditions at $y = \pm h$ have been used while no consideration has been given as to what happens at $r = 0$ and $r = \infty$. The solution is thus only valid between the radii r_1 and r_2.

At infinite radius equation (3) reduces to

$$\frac{dp}{dr} = \mu \frac{d^2 u}{dy^2} \qquad \ldots\ldots(6)$$

which is the equation for "creeping flow" and hence at infinity the velocity profile is parabolic.

However at finite r due to the presence of small axial velocity components the profile is not parabolic and the $\rho u \frac{\partial u}{\partial r}$ term of equation (3) is not negligible.

Thus, if an attempt to solve the problem is made with the simplified equations that the author has used, between the finite radii r_1 and r_2, there will be some loss of accuracy and inconsistencies will arise in ignoring the axial velocity component flow. In addition the solution will not necessarily describe the flow at infinite or zero radius since the initial equation of motion differs from equation (6) by the term $\rho u \frac{\partial u}{\partial r}$. However it is felt that the solution describes the motion better than the creeping flow solution.

Examining the author's solution it can be seen that as $r_2 \to \infty$ $P/q \to \infty$ where

$$\frac{p}{q} = \frac{32\pi^2 h^2 \rho \, \Delta p}{\left(\frac{1}{r_1^2} - \frac{1}{r_2^2}\right) M^2} \qquad \ldots\ldots(7)$$

For $r_2 \to \infty$
$$\frac{p}{q} = \frac{32\pi^2 k^2 \rho \, \Delta p \, r_1^2}{M^2} \qquad \dots\dots(8)$$

However the pressure drop between r_1 and $r \infty$ is itself infinite, thus $P/q \to \infty$ for $r_2 \to \infty$.

Figure 3.1 shows $\log (P/q)$ plotted against B which is the dimensionless value of the velocity midway between the plates and is given by

$$\beta = \frac{4\pi\rho \, k \, r \, u}{M} \qquad \dots\dots(9)$$

Rearranging (9) to give the radial velocity

$$u = \frac{\beta \varphi}{4\pi k r} \qquad \dots\dots(10)$$

Now the velocity of the creeping flow solution, which is valid at infinite radius, midway between the plates is

$$u = \frac{3\varphi}{8\pi r k} \qquad \dots\dots(11)$$

Comparing (10) and (11) it can be seen that, for the author's solution, at $r_2 = \infty$ B should equal 1.5.

It is interesting to note that as P/q increases, as shown in figure 3.1, the curve has a point of inflexion at B = 1.5, whereas one would expect it to approach the value of B = 1.5 asymptotically. From figure 3.1 it is seen that the curve starts to rise more quickly after the point of inflexion but due to the complexity of equation (28.27) it is difficult to investigate the relationship between P/q and B by any than a numerical method. Although it would appear that $B \to \infty$ as $P/q \to \infty$ the author can only conclude that if this is so it proceeds to infinity at a much slower rate since at $P/q = 10^{10}$ it was found that B = 1.748, this being the limit of the author's calculations.
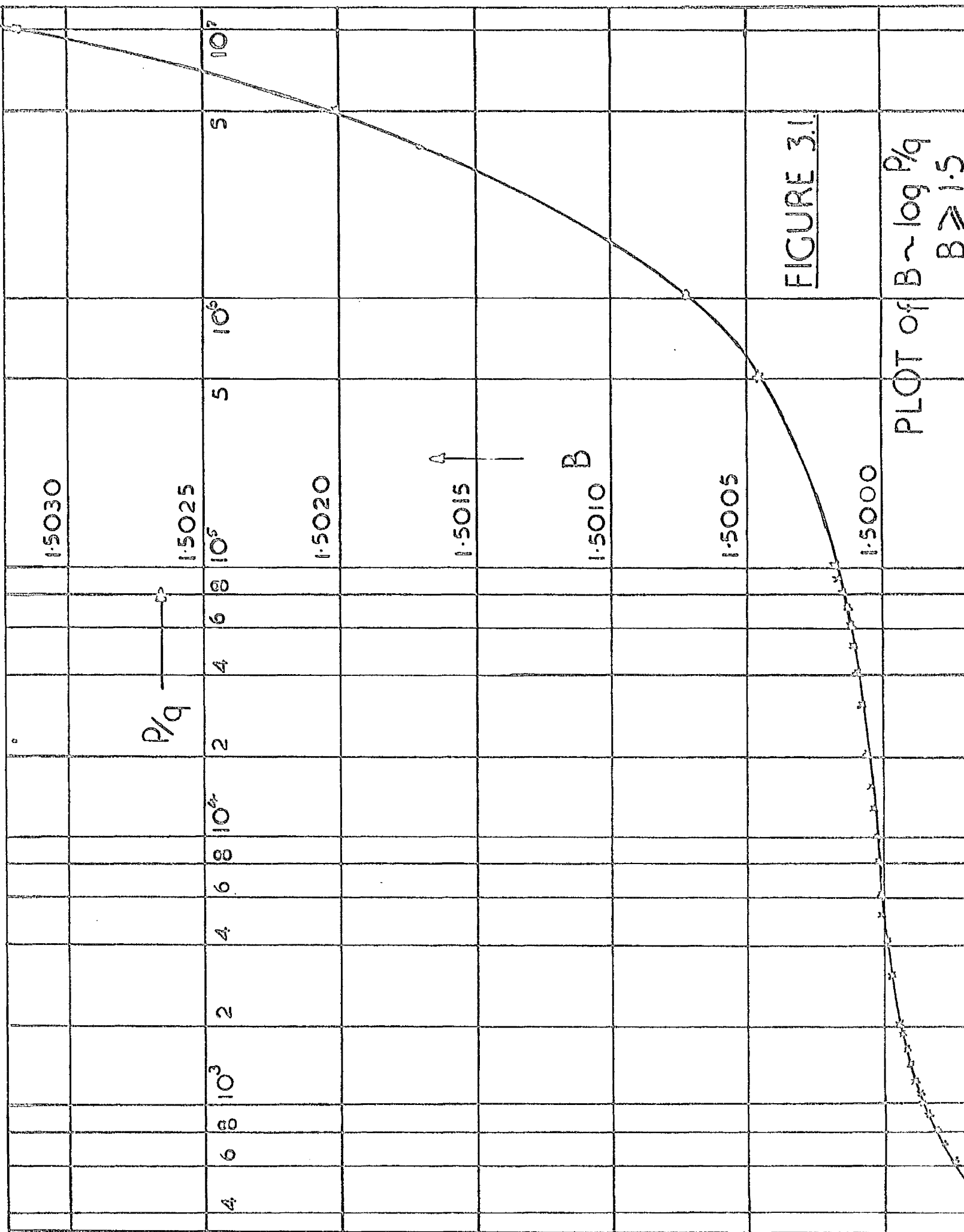
FIGURE 3.1

PLOT of $B \sim \log P/q$

$B \geqslant 1.5$

At $r_1 = 0$ $P/q = 0$ which results in equation (28.27) containing negative square roots. Thus it would appear that the solution is imaginary at $r_1 = 0$.

The condition of validity of the equation is that $P/q > B^2$. At $P/q = B^2$ equation (28.27) reduces to

$$\frac{B-1}{3B} - \left[\frac{E\left(\frac{\pi}{2},\frac{\pi}{2}\right) - E\left(\frac{\pi}{2}, 54°44'\right)}{F\left(\frac{\pi}{2},\frac{\pi}{2}\right) - F\left(\frac{\pi}{2}, 54°44'\right)}\right] = 0$$

.....(12)

Since $F\left(\frac{\pi}{2},\frac{\pi}{2}\right)$ is infinite and the other elliptic integrals finite, it can be seen that $B = 1$. Thus the limit of validity of the equation is when $P/q = 1$. This limit can help to deduce approximate design parameters for which the solution is valid since in equation (7) if Δp is substituted with the pressure drop obtained from the creeping flow solution, the resulting equation contains only the terms r_2, r_1, h, μ and M.

A sketch of P/q plotted against B (figure 3.2) shows the relationship for values of $B \leq 1.5$. It can be seen that the curve ends at $B = 1.31$ where $P/q = 1.806$ since it was found that for smaller values of P/q the time required by the computer was unduly long. The curve is shown dotted from thereon to the point $B = 1$, $P/q = 1$.

From equation (28.10) ur is independent of r and since

$$\chi = -\frac{4\pi p R(+u)}{M}$$

.....(13)

it must be independent of r.

At $x = 0$ the value of χ is B which is consequently also independent of r. The computer programme was so devised that for each experimental result it also gave a value of B, and, for a set of values, e.g. Tables 1, 2, 3, and 4 of Chapter V, at a certain mass flow temperature and plate
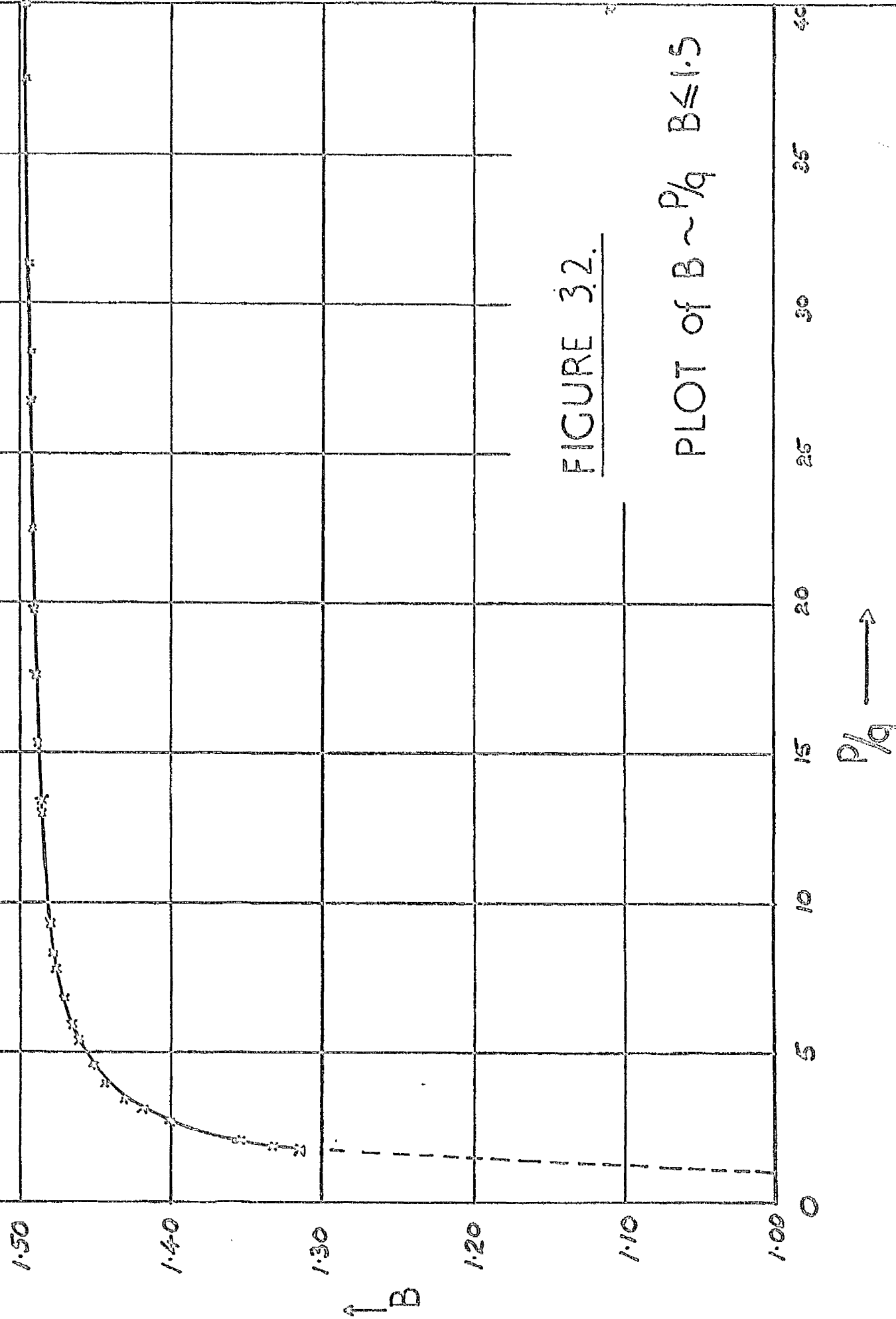
FIGURE 32.

PLOT of $B \sim P/q$ $B \leq 1.5$

separation, it can be seen that B is not independent of r. However the variation in B could be partially due to experimental error and to determine the extent of the variation it is necessary to eliminate all experimental errors by choosing the temperature and mass of water flowing through a known plate separation. This fixes the values of h, M, ρ and μ and for a certain value of r_2 (r_1 remaining constant) the value of q (equation 28.29) can be determined.

The term P/q contains the pressure drop which has not been specified -- the other unknown being B, so that it is necessary to solve equations 28.27 and 28.28 simultaneously to obtain the values of P/q and B. This was done using as an example 2h = 0.0098", Q = 1.799 cm^3/s at 5.93 ^{o}C.

In addition to obtaining the variation in B with respect to r_2, the theoretical pressure drop is obtained.

TABLE 1

Variation of B w.r.t r_2 at Q = 1.799 cm^3/s, Temperature 5.93 ^{o}C. Plate Separation 0.0098"			
r_2/r_1	P/q	B	q
$17/3$	82.27794	1.498030	0.037158
$15/3$	77.14489	1.497888	0.039681
$13/3$	71.38764	1.497714	0.042952
$11/3$	64.84034	1.497478	0.047394
$9/3$	57.27583	1.497138	0.053826
$7/3$	48.34740	1.496596	0.064092
$5/3$	37.53237	1.495583	0.083349

From the table it can be seen that although the variation is small --

the change from $r_2/r_1 = {}^{17}/3$ to $r_2/r_1 = {}^{5}/3$ being only 0.17%, B is not independent of r. This again illustrates the slight departures from exactness that exist by neglecting axial velocity components.

As stated above the theoretical pressure drops have also been obtained for the experimental values used and are tabulated below with the theoretical pressure drops obtained by Livesey's, Peube's 3 term, and Peube's 5 term solutions. A plot of the pressure drop against radius is not given here as examples of the shape of the curve are given in figures 1, 2, 3 and 4 of Chapter V.

TABLE 2

| r_2/r_1 | Theoretical Pressure Drops at $Q = 1.799$ cm^3/s, Temperature 5.93 $^{\circ}$C   Plate Separation 0.0098" | | | |
	Author	Livesey	Peube's 3 term	Peube's 5 term
${}^{17}/3$	5.9222	5.8976	5.9222	5.9220
${}^{15}/3$	5.5013	5.4775	5.5019	5.5016
${}^{13}/3$	5.0205	4.9969	5.0210	5.0207
${}^{11}/3$	4.4583	4.4353	4.4589	4.4586
${}^{9}/3$	3.7819	3.7598	3.7824	3.7821
${}^{7}/3$	2.9317	2.9113	2.9321	2.9319
${}^{5}/3$	1.7843	1.7680	1.7842	1.7839

Although the inertia term is only some 3% of the total pressure drop and consequently good agreement between the various solutions would be expected, Table 2 shows that the solutions of the author and Peube vary by less than 0.01% whereas Livesey's solution varies by 0.6% approximately.

In the paper (35) at the back of the thesis, an error has been found in figure 28.2 which shows the velocity profile for a given plate separation and flow rate. This has been revised and is shown in figure 3.3. The coordinates have been made dimensionless, χ being given by equation (13) and $x = \partial/h$, and the curve shown is for a flow of 5.187 cm^3/s, a plate separation of 0.0194" and $r = \frac{1}{2}$". In the diagram are shown the velocity profiles obtained by Peube's 3 term, the author's and the creeping flow solutions. Whereas χ will always equal 1.5 for the creeping flow solution, this will not be so for Peube's solution, which accounts for the two dimensional nature of the flow. For the author's solution χ should be independent of r, but as demonstrated above this was found to be not so.

It can be seen from figure 3.3 that only a small variation between Peube's and the author's solutions exists, this being most noticeable at the centre-line. Taking the creeping flow profile as reference, both solutions indicate that for converging flow the effect of the acceleration force is to decrease the velocity at the centre of the gap and increase it in the neighbourhood of the walls.

FIGURE 3.3.

CREEPING FLOW SOLUTION
PEUBE'S SOLUTION
AUTHOR'S SOLUTION.
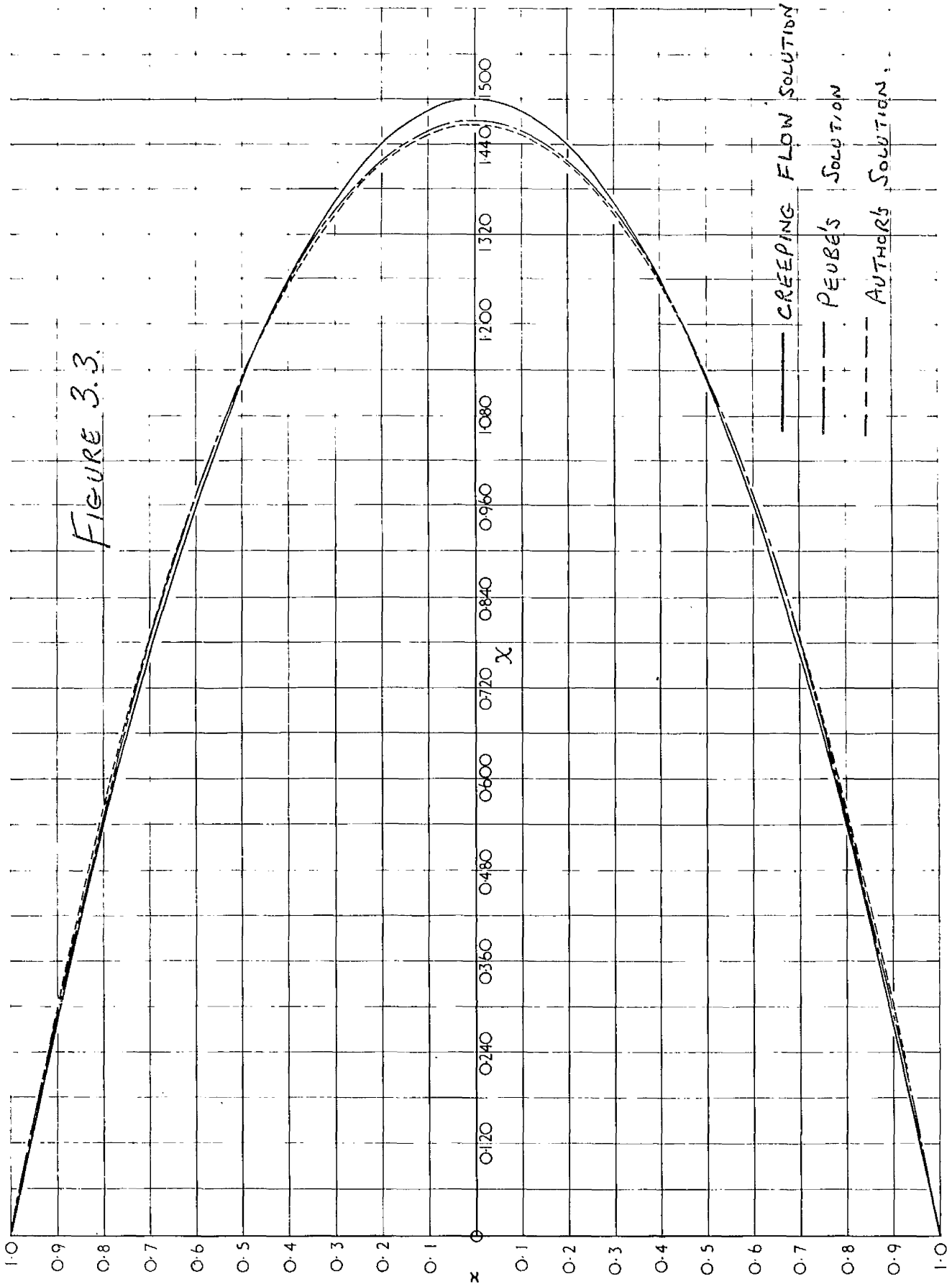
CHAPTER IV

Description of Apparatus for Preliminary

Results and Estimation of Errors

This chapter is divided into two parts - the first section describing the preliminary work and the apparatus used to investigate radial flow and the second part deals with the experimental error.

Preliminary Considerations

In view of the various solutions given in Chapter II which account for the pressure drop due to inertia effects and the need for accurate viscosity measurements it was decided to investigate experimentally laminar radial flow to ascertain which solution or solutions best suited the experimental data.

It was decided to study converging flow as opposed to diverging flow for several reasons:-

(a) It is a well known fact that due to the adverse pressure gradient caused by the retardation of the flow, diverging flow is less stable than converging flow and hence the onset of turbulence will occur at a lower Reynolds number than for the former.

(b) The inlet length - the distance over which the flow becomes almost fully developed - gets less for increasing radius and hence is smaller for converging flow. This allows pressure tappings to be positioned nearer the edge of the plates.

(c)   From a practical point of view the measurable pressure
drop is greater for the same flow with converging flow
and hence the accuracy of the experiment is improved.
This arises from the fact that the pressure drops due to
viscous and inertia effects are additive for converging
flow while the opposite is the case for diverging flow.

Stability of Radial Flow

With the plates and the casing made of Perspex, a visual study of the
flow was made possible by injecting nigrosine dye, which does not diffuse
in water, into the stream by means of a hypodermic needle situated
at the entry to the plates. The Perpex plates were 3" diameter and
the gap separations were 0.011" and 0.034". The shape of the plates
as shown in fig (4.1) was the same as that envisaged for more extensive
tests and for the final high pressure viscometer. As shown in the
drawing they were made flat with a sharp-edged entry as opposed to a
rounded entry or exit since with the high pressure viscometer no
pressure drops were to be measured directly and consequently it would
be difficult to estimate from a theoretical point of view the pressure
drop across plates with a rounded entry section.

The plate separations were effected by spacers placed on a diameter
outside the test section and were stepped to facilitate the manufacture
of the spacers since the gaps only ranged from 0.25 mm to 0.5 mm. It
was found with plates of this shape, that although turbulence was never
reached, the flow became unstable at Reynolds numbers as low as 140,
where the Reynolds number is expressed by $\frac{2\rho\bar{u}R}{\mu}$ In passing it is felt
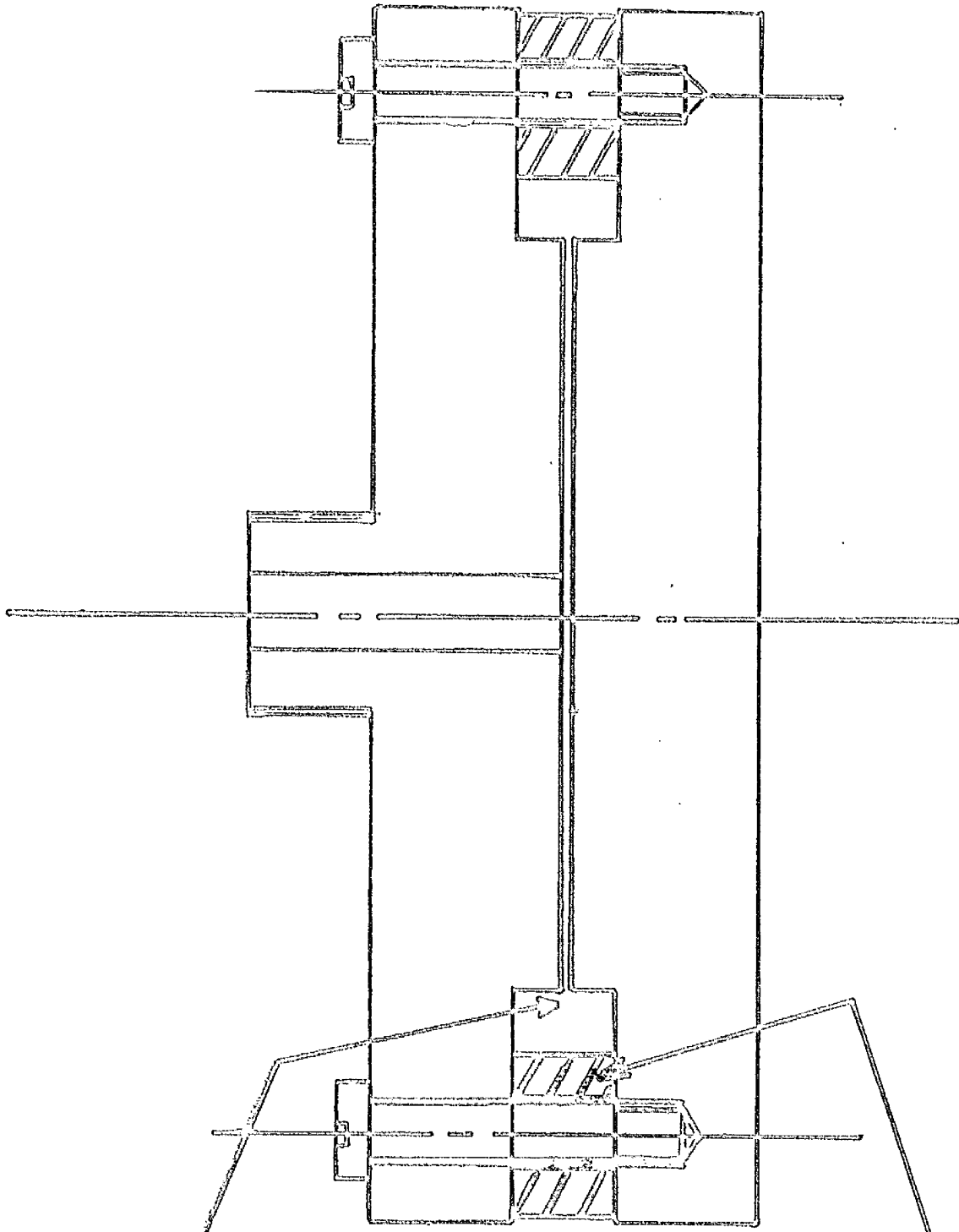
SHARP-EDGED ENTRY.

BRASS SPACERS.

BRASS PLATES. FIG 4.1

that a more suitable expression for the Reynolds number would be $\frac{4\rho\bar{u}h^2}{\mu r}$

since it is dependent on radius in addition to plate separation. However, since the separations used in the visual flow tests were similar to that used in the experiments the Reynolds number was calculated from the simpler expression.

It was noticed that about Re = 140 the dye filament, although remaining intact, began to waver and take on lateral motions as it moved radially inward which became more violent as the flow was increased. These tests were carried out with flows up to 40 cm^3/sec with no sign of turbulence appearing.

The value of the Reynolds number at which this wavering was first noticed could undoubtedly have been improved by rounding the entry but for the reason given above this was not done. For the gaps used a Re = 140 corresponded to a flow rate of 7 cm^3/sec and since these were the size of gaps used in the more extensive tests it was decided not to exceed this size of flow.

Viewing the dye filament from the side it was noticed that as the dye approached the central extraction hole, which was in the top plate, it was bent upward. This demonstrated the two dimensional nature of the flow near the exit which, although present to a very much smaller degree, could not be detected upstream of this region. For flow rates where the dye filament maintained a purely radial line, i.e. less than 7 cm^3/sec, the distance upstream of the edge of the extraction hole to which this tendency was noticed did not exceed $\frac{1}{8}$".

It was found not unsurprisingly that a blob of dye at the centre of the bottom plate, i.e. at r = 0, took a few minutes to completely

disperse showing this region to be a so-called "dead area" of water.

In addition, dye injected into the flow before it entered the plates in the vicinity of the spacers showed a line of dead water was produced across the plates which coincided with the position of the spacers. This was confirmed later when using brass plates as on examination after a series of tests six radial lines were produced on the brass coinciding with the positions of the spacers. These lines were about $^1/16"$ thick, except for one which was a bit thicker at the outer edge, and straight showing that no swirl was present in the flow. This could be demonstrated each time a new gap separation was made since, after each series of tests, it was the practice of the author to test the plates for flatness using an optical flat and invariably it was found that some lapping was required. Thus at the beginning of each test the plates were a bright yellow in colour. However after a series of tests it was found that the plates were brownish red in colour where the water had been flowing over them except for the six radial lines which were still yellow although darker in shade than they had been originally.

It was concluded that these areas of slacker water did not affect the flow and that it would be best to position the static pressure tappings midway between these radial lines.

Description of Apparatus

1) Plates   Originally a pair of brass plates 3" diameter were made with three pressure tappings. However these proved inadequate and a pair of brass plates of 4½" diameter test section were made, the thickness of the plates being $\frac{3}{4}"$ to ensure rigidity. The central

extraction hole was $\frac{1}{8}$" diameter and eight static pressure holes $\frac{1}{64}$" diameter were drilled on a radius of $2\frac{1}{8}$" to $\frac{3}{8}$" at $\frac{1}{8}$" intervals.

Since the plates were housed in a Perspex casing the pressure pipes were led out to the manometer through holes in the casing and sealed with "Devcon" - a plastic rubber solution.

The $\frac{1}{64}$" diameter holes were drilled in the $\frac{3}{4}$" thick plate to a depth of $\frac{1}{4}$" and then opened out to $\frac{1}{8}$" diameter. These holes were joined to the manometer-connecting-tubes by small adaptors which had a flange on one end with a recessed hole to house $\frac{1}{8}$" bore O-rings. The seal was effected by bolting the flange to the plate with 6 B.A. bolts. The other end of the adaptor was joined to the copper tubes connecting the manometer by rubber tubing. This is shown in fig (4.2).

2) <u>Manometer</u>   The pressure pipes from the viscometer to the manometer were made of copper tubing so that for tests at higher temperatures any heat would be conducted through the walls of the tubing instead of through the water to the manometer. Each horizontal tube was fitted with vertical pipes at each end to allow trapped air to escape.

The manometer consisted of eight limbs made of 8 mm precision bore tubing. The size of the tubing ensured that any effect due to capillarity was small although if each limb was equally clean the effect should be the same in each limb. With precision bore tubing of such size any errors caused in reading the pressure drop due to irregularities of bore such as conicality or ellipticity would be negligible.

The chamber connecting the eight limbs was fitted with a stop-cock for draining the manometer fluid and a pocket which permitted a thermometer graduated in 0.1 $^{\circ}$C to be inserted through a standard "Quickfit" seal.

FIGURE 4.2.   PRESSURE CONNECTOR

BRASS PLATES.

FLUID.

PRESSURE TAPPING HOLE.

O-RING

"DEVCON" RUBBER SOL'N.

OUTER CASING
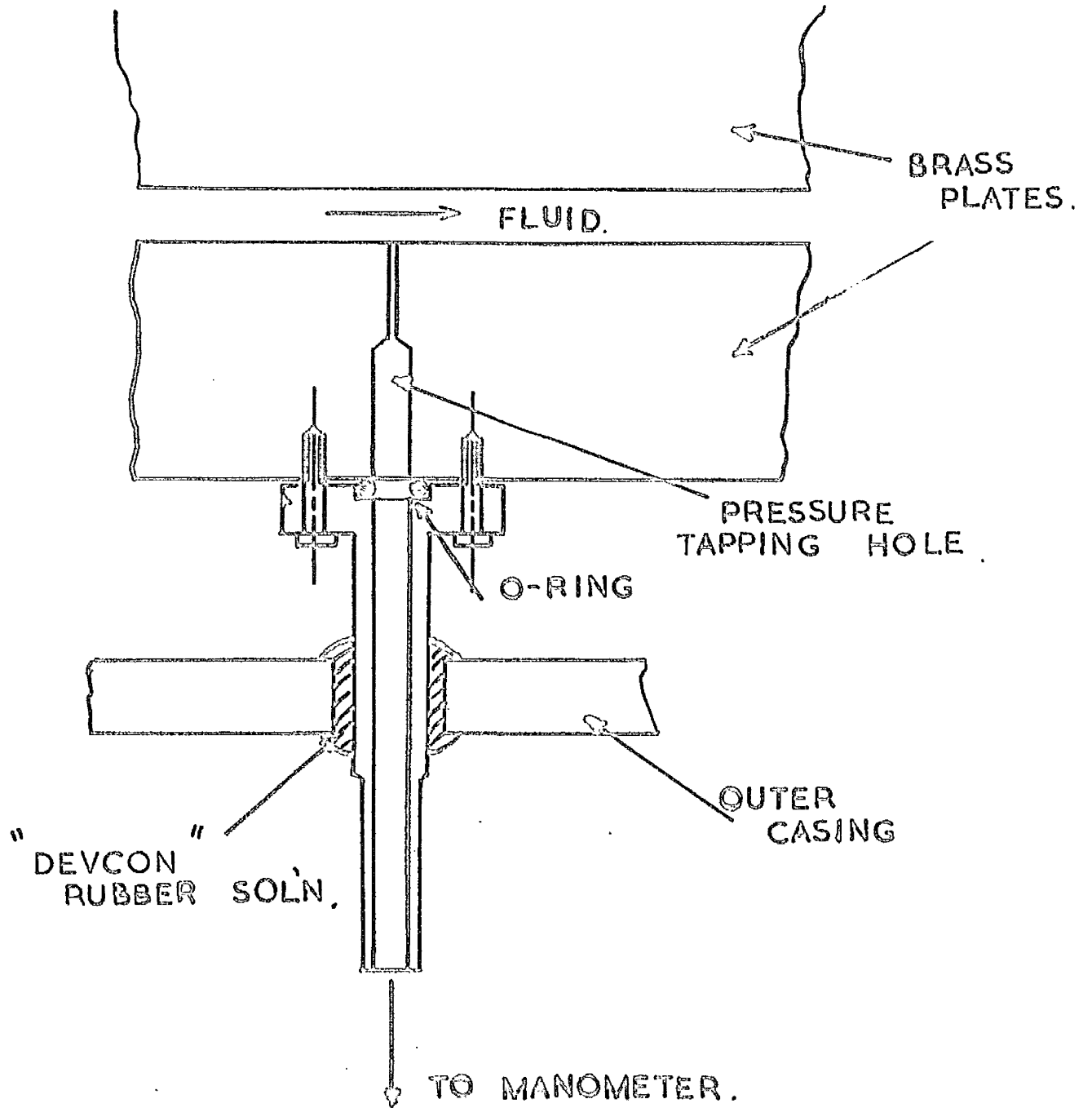
TO MANOMETER.

The manometer fluid used was "Analar" carbon tetrachloride which is considered to be immiscible in water. In addition to this necessary property for measuring pressure changes in water, it has the further advantage of a density of approximately 1.6 at room conditions. Since the pressure drops experienced were quite small, ranging from roughly 1 to 20 cm of water, the carbon tetrachloride magnified the column of fluid to be measured by the factor $\frac{5}{3}$. This is explained by taking h as the length of carbon tetrachloride, then since the density of water at room conditions is very nearly 1.0 the pressure drop in units of length of water is $h(1.6 - 1.0) = 0.6h$.

One disadvantage of carbon tetrachloride was that the manometer limbs had to be scrupulously clean. This was done with hydrofluoric acid washed through with distilled water. The manometer was only filled with this acid for about five minutes due to its strong corrosive properties.

The carbon tetrachloride was also found to rapidly attack rubber so that it was kept well clear of the rubber connections between the glass manometer limbs and the copper connecting tubes. In addition it attacked the stop-cock grease used in the drain cock and thermometer pocket. This was overcome in the case of the former by putting a slug of mercury between stop-cock and carbon tetrachloride. A similar idea was used for the thermometer pocket only, since the thermometer pocket was above the main chamber of carbon tetrachloride, water was used.

Care was taken that the manometer limbs were reasonably vertical, this being done using a plumb line.

The differences in pressure drop were measured with a Pye cathetometer which made it possible to measure the lengths of carbon tetrachloride to 0.005 cm, which is equivalent to 0.003 cm of water.

3) Temperature Measurement   Originally, the temperature was measured with a thermometer in the exit pipe. However since the water was from the tap via a constant head tank it was usually colder than the temperature of the laboratory so that on putting thermometers in the inlet and exit pipes of the apparatus, the two thermometers being previously checked that they read the same, it was found that the latter was slightly higher in temperature due to the water picking up heat as it flowed through the apparatus. This difference in temperature varied according to the flow, and although it was insignificant for 6 cm^3/sec or greater, it was decided to measure the temperature in the vicinity of the test section. This was done by inserting a thermistor through the Perspex casing.

The thermistor which had a resistance of 300 ohms at 25 $^\circ$C was calibrated with a platinum resistance thermometer up to 100 $^\circ$C in a temperature bath, a graph of resistance plotted against temperature being given in fig (4.3), and a table of the calibration values shown in Appendix (4). A recalibration was done several months later with no change in the temperature-resistance relationship being detected.

The resistance of the thermistor was measured with a simple Wheatstone-bridge circuit, the thermistor making up one arm of the circuit and a resistance box the other. The other side of the bridge circuit was made up of two 100 Ω high stability resistors embedded in a block of polysterene to ensure their temperature constancy.

THERMISTOR CALIBRATION.

FIG. 43.

TEMPERATURE °C.
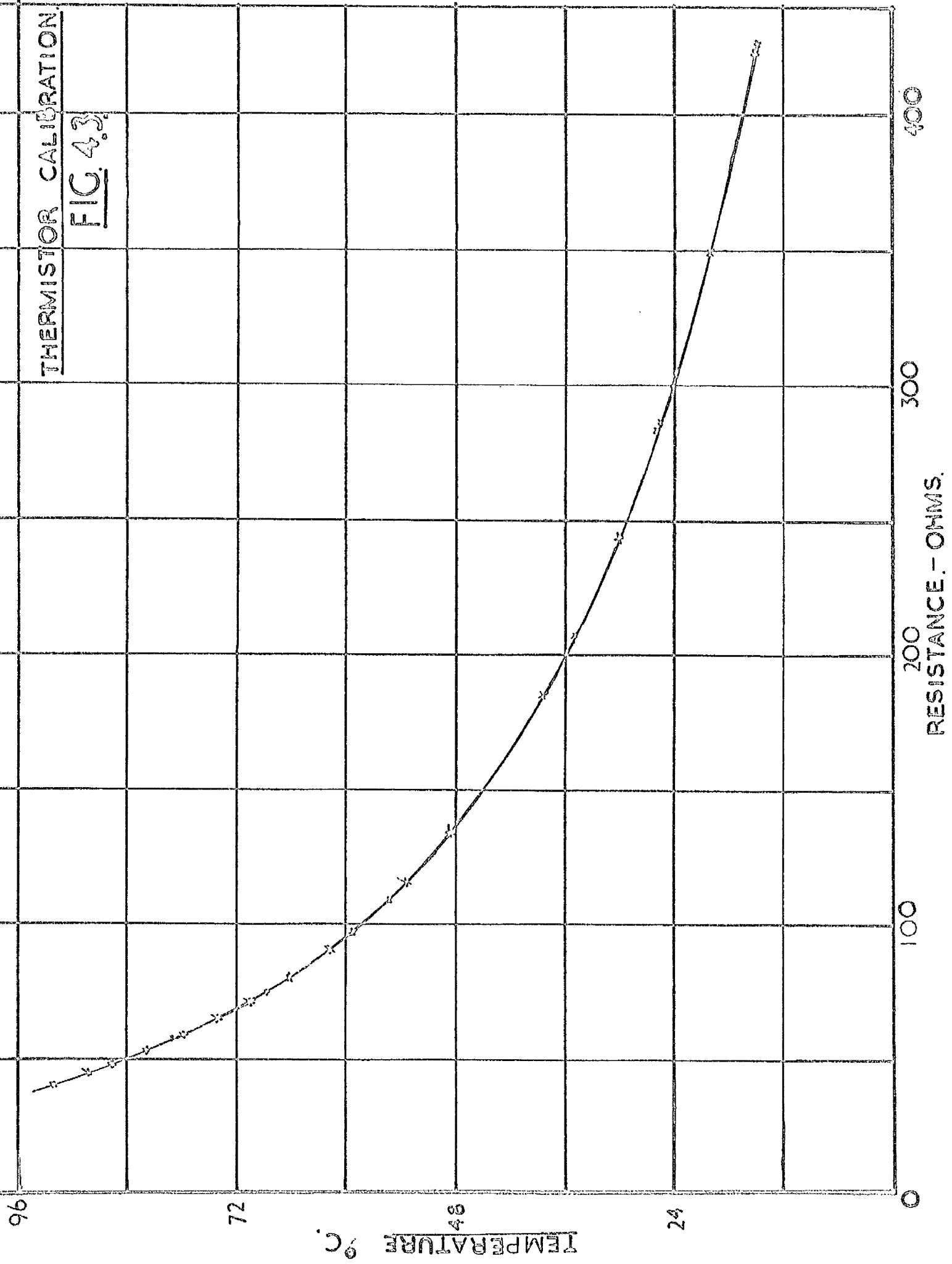
RESISTANCE - OHMS.

A galvanometer was connected across the bridge so that at zero deflection the resistance of the thermistor was the value of the resistance box.

4) Mass Flow Measurement   The flow rate was measured by simply collecting the water in measuring cylinders graduated to read correctly at 25 ^{o}C. The temperature of the water collected from the apparatus was measured and a correction made for the difference in temperature from the measuring cylinders' calibration temperature of 25 ^{o}C. However due to the small differences in temperature of the water collected from this value and the negligible change in density of the water, this correction could be safely ignored. It was ensured that before each measurement the cylinders were completely dry.

The timing of the flow was done with a 10 second stop watch and observing the bottom of the meniscus as it passed the appropriate mark on the glass.

The constant flow was produced by a constant head tank of the overflow variety, throughout the experiments it being ensured that more water entered than left the tank to the apparatus, so that the overflow pipe always had water passing through it.

5) Deaerator   Initially much trouble was experienced with air dissolved in the test water. It was found that after a short period of time, small air bubbles appeared on the Perspex casing and brass plates. Moreover, due to the small plate separations used, if air bubbles entered the gap they could not be dislodged easily since the flows were not large enough to overcome the surface tension between

the air bubbles and the brass plates.

These air bubbles clearly affected the flow regime and consequently a deaerator of the type described by Potter and Whitehead (36) was used. Briefly, this method uses established ion-exchange resins to removed the dissolved oxygen, the resin used in this case being Zeo-Karb 225 a strongly acidic cationic resin which is changed from its hydrogen form to the ferrous form by treating it with a strong solution of ferrous sulphate. The column is then washed free of ferrous sulphate with distilled water which has been deaerated by bubbling through nitrogen to reduce the partial pressure of the oxygen in solution. The resin is then activated with 0.5 N sodium hydroxide solution and ferrous hydroxide precipitated within the resin which is changed to ferric sulphate by the absorption of the oxygen dissolved in the test-water. When the column is exhausted it can be returned to its original hydrogen form by 5 N hydrochloric acid which removes the ferric hydroxide and the process is then repeated.

This deaerator proved successful as with continual use it only required to be reactivated once a fortnight. The fluctuations in flow caused by the resin bed were found to be small and rarely made themselves noticeable.

6) Measurement of Plate Separation   This undoubtedly was the most difficult measurement to make, and since the method employed required the plates to be flat to a high accuracy, as a first step it was necessary to produce plates of such a nature.

(a) Flatness of plates   After the plates had been machined on the

lathe and the pressure holes bored, they were lapped on a surface plate using paraffin as a lubricant. On checking with an optical flat, the plate with the central extraction hole was found to be high in the middle due to the boring of this hole and the other plate was found to be hollow in the centre. However, the "out-of-flatness" was only about 0.0001". Obviously rubbing one plate against the other would not improve them, although ringing them together permitted the bottom plate to be lifted by the top one due to suction.

It was thus decided to improve each plate by rubbing them in local high spots with a small quantity of "Brasso" on tissue paper and checking each against the optical flat. Although very tedious, this method improved the flatness to two fringes of light as measured by an optical flat which is equivalent to 0.00002". A further check was made on a "Taly lin" machine of Rank, Taylor, Hobson Ltd., and as can be seen by a tracing of the print-out of the machine (fig 4.4), the flatness measurement found by the optical flat was confirmed.

It is essential to have the plates perfectly flat since, in addition to producing an error in the value of the gap separation, the pressure measurement will also be affected. For example, if the bottom plate is perfectly flat and the top plate high at the centre, then there is an additional acceleration at this section, which would result in a greater pressure drop than that expected. The opposite would be the case if the top plate was higher at the outer edge.

(b) <u>Plate Separation</u>   The order of the plate separations ranged from 0.010" to 0.020". The upper limit was imposed by the size of the pressure drop for the limited flows of 7 cm^3/sec or less becoming
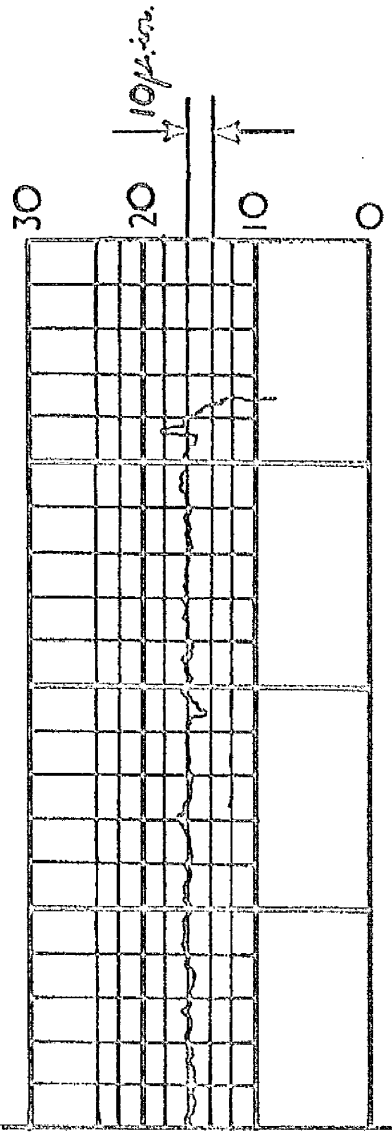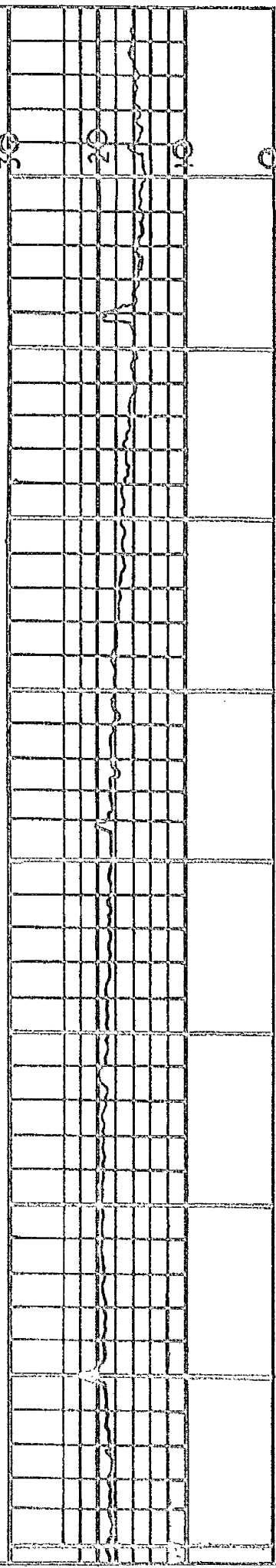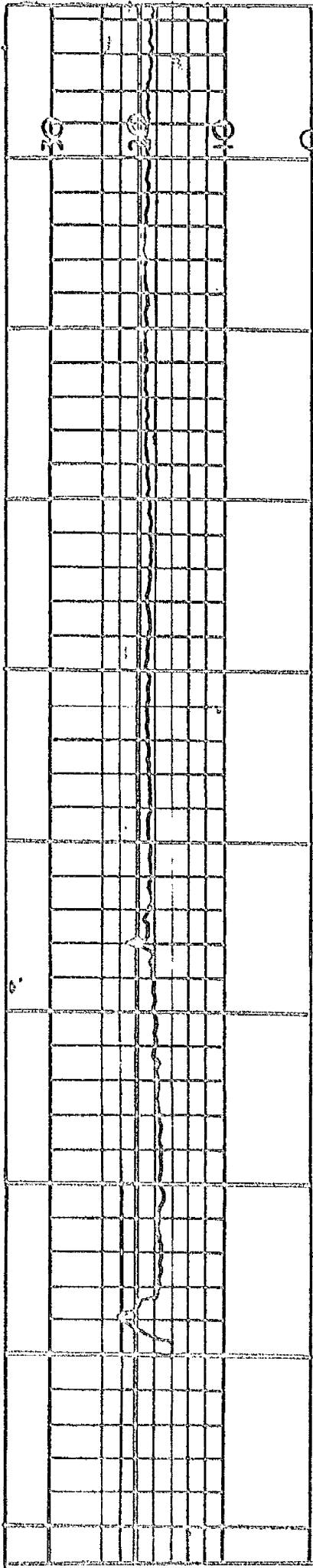
PLATE FLATNESS AS
GIVEN BY "TALYLIN" M/C.

FIGURE 44.

VERTICAL MAGNIFICATION = X10,000.

HORIZONTAL MAGNIFICATION = X5.

immeasurable, and the lower limit was due to the restriction caused by the method adopted for measuring plate separations as gaps of less than 0.010" incurred too great an error.

This measurement cannot be made directly so the following method was employed which, although the author feels could be improved, was acceptable for the measuring equipment available.

The bottom plate was clamped rigidly to the revolving table of a toolmaker's microscope and the top and bottom plates rung together. The probe of an electric comparator gauge was then brought into contact with a Johannson block placed on the upper surface of the top plate and the scale brought to zero as shown in fig (4.5). The table of the toolmaker's microscope was revolved and readings taken every 60° corresponding to the positions of the six spacers used to separate the plates. These six readings were taken as the datum values for the six spacers.

If as an example, the plate separation required was nominally 0.012", then the six datum readings were taken using a Johannson block of thickness 0.113" placed on the top surface of the top plate.

The plates were now separated and six spacers of thickness necessary to obtain a nominal gap separation of 0.012" put in position. These brass spacers were $\frac{3}{8}$" diameter with 2 B.A. clearance holes since the plates were separated with 2 B.A. bolts screwed into the bottom plate.

The six bolts were tightened as evenly as possible and using a Johannson gauge of thickness 0.101" readings of the electric comparator were again taken at the six appropriate positions. Adjustments of the screws were made until the differences of the readings between positions

COMPARATOR PROBE

JOHANNSON BLOCK

CLAMP

SLIP

BRASS PLATES

REVOLVING TABLE OF TOOLMAKER'S MICROSCOPE.
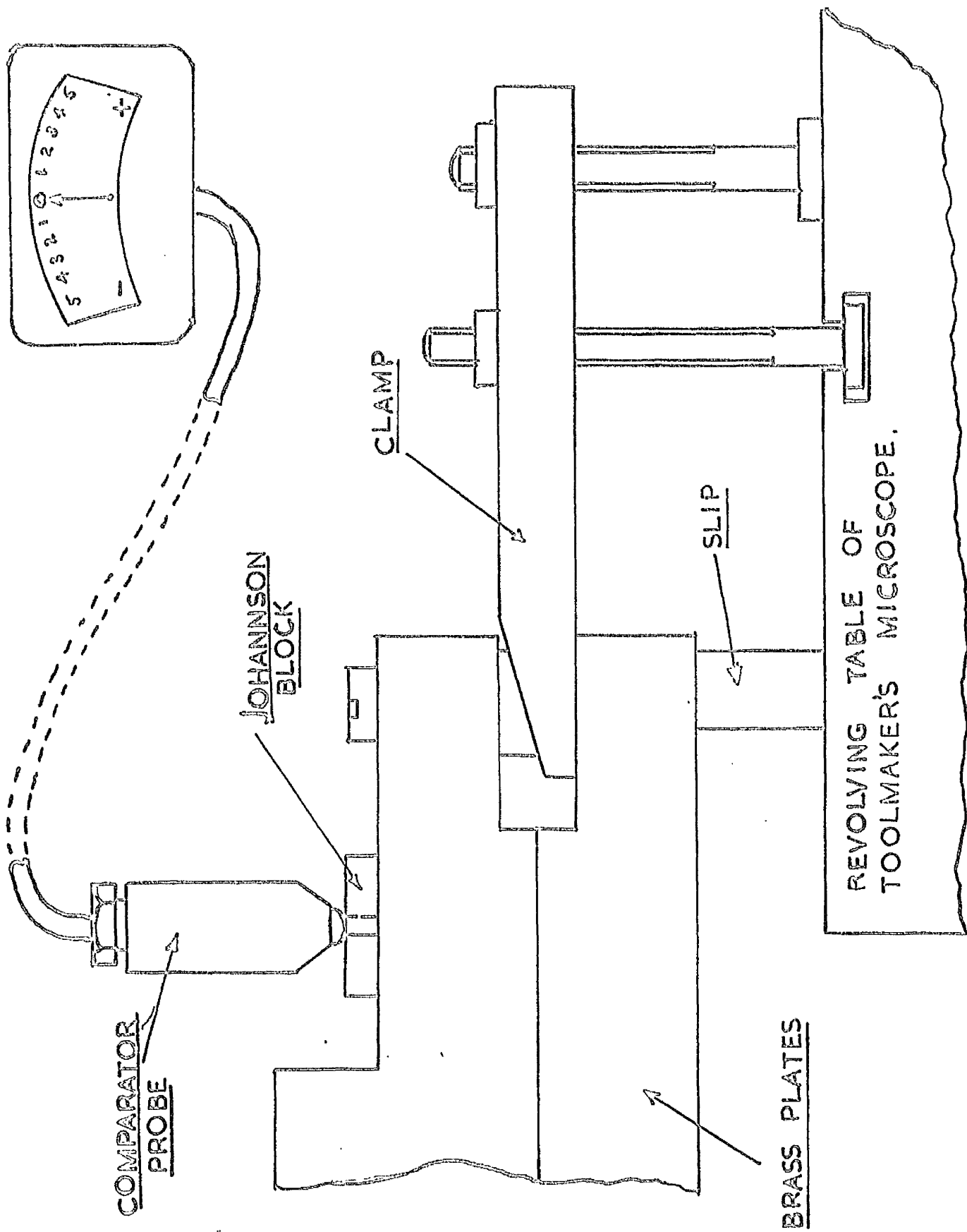
FIGURE 4.5.

1, 2, 3, 4, 5 and 6, were the same as for the readings taken at the datum position.

Thus, from the changes in the Johannson blocks and comparator gauge readings it was possible to obtain the distance the top plate had been moved from the bottom plate which remained fixed to the table of the toolmaker's microscope. The comparator head was also clamped rigid throughout the measurement.

The arrangement was left for an hour or so and the readings repeated. This was done to ensure that the plates had not "sprung" a little due to stretching of the 2 B.A. bolts holding the plates together, although no excessive tightening was ever done. As on several occasions, it was found that excessive tightening would have been necessary to bring a spacer into agreement with the other five, it was removed and rubbed on the lapping table. Thus the spacers were not interchangeable.

Given below is Table 1 a set of readings showing how a plate separation of 0.0098" was obtained, the whole numbers being 0.0001".

Table 1

Position	1	2	3	4	5	6
Datum readings using a Johannson block of 0.110"	$-2\frac{1}{2}$	$-\frac{1}{2}$	$+\frac{1}{2}$	$+1\frac{1}{2}$	0	$-2\frac{1}{2}$
Readings taken with spacers in position using a block of 0.1003"	$-1\frac{1}{2}$	0	$+1\frac{1}{2}$	$+2\frac{1}{2}$	$+1$	$-1\frac{1}{2}$

The differences in the Johannson blocks is 0.0097" and that between the readings +0.0001" (except position 2) resulting in a gap separation of 0.0098".

Part II   Estimate of Experimental Error

The six parameters that need to be measured accurately (see
equation (66) Chapter II and equation (7) Chapter III are:-

(a) r_2, the radii at which the static pressure tappings are situated
and r_1 the radius at which the innermost tapping is placed;

(b) Δp the pressure drop;   (c) 2h, the plate separation;   (d)   Q, the
volume flow rate;   (e)   the density which implies the accuracy of the
temperature measurement, and (f) the viscosity.

(a)   The Errors in r_2 and r_1

For the experiments conducted to test the various solutions to
laminar radial flow there were seven values of r_2 corresponding to
seven static pressure tappings, viz:- 2.125", 1.875", 1.625", 1.375",
1.125", 0.875", 0.625" and r_1 had the value of 0.375".

These holes were marked off on a surface table with the use of
height gauge and Johannsen blocks.   The $^1/64"$ holes were drilled with
the use of an optical chuck which permitted the drill to be centred
exactly on the required position.

A check was made on the above eight radii values.   This was done
by levelling the plate which contained the pressure tapping holes on
the surface table and with the use of a travelling microscope the pitch
between the holes and their distances from the centre were measured.
With the use of the Vernier scale the microscope could be read to 0.0004".
The actual values of the eight radii were found to be 2.129", 1.878",
1.633", 1.375", 1.125", 0.873", 0.624" and 0.3755".

The outside diameter of the plates was also measured every 60°

with a screw micrometer and the average value was found to be 4.4991",
the lowest value being 4.4988" and the largest 4.4993".

In all calculations involving experimental data, the nominal
values were used instead of the measured values of r_2 and r_1. This
resulted in a systematic error being present in the values of viscosity
and an assessment is given below of this error bearing in mind that
for all the solutions quoted except Peube's series solution which in
addition contains $(\frac{1}{r_1}^4 - \frac{1}{r_2}^4)$, the radii appear as the expressions
$(\frac{1}{r_1}^2 - \frac{1}{r_2}^2)$ and $\ln_e {}^{r_2}/r_1$.

Taking the measured values of r_2 and r_1 as reference, the error
incurred in the term $(\frac{1}{r_1}^2 - \frac{1}{r_2}^2)$ for the first five radii value was
- 0.2% and for the radii 0.875" and 0.625" - 0.4%.

Similarly for the expression $\ln {}^{r_2}/r_1$, the error incurred in the
values of ${}^{r_2}/r_1$ from ${}^{17}/3$ to ${}^{9}/3$ except the value ${}^{13}/3$ was + 0.05%.
In the latter value the error was + 0.35%, and for the radii 0.875"
and 0.625" the error incurred was - 0.4%.

In the author's solution (Chapter III equation (7)) the
expression $(\frac{1}{r_1}^2 - \frac{1}{r_2}^2)$ is used in the evaluation of P/q and also with
the expression $\ln {}^{r_2}/r_1$ in the evaluation of viscosity. Due
to the complexity of the solution, the error in the viscosity due
to the errors in r_2 and r_1 was found by taking a set of experimental
results and comparing the different values of the viscosity obtained
by varying r_2 and r_1 by a specified amount, all other parameters
remaining constant. It was found that for all values of r_2, the
variation in the viscosity was practically the same as the variation
in r_2 and r_1.

Thus, by using the nominal values of the radii instead of the measured values the author incurred a systematic error in the viscosity results of $\sim$ 0.2% for the radii $2\frac{1}{8}$", $1\frac{7}{8}$", $1\frac{5}{8}$", $1\frac{3}{8}$", and $1\frac{1}{8}$" and $\sim$ 0.4% for the radii $\frac{7}{8}$" and $\frac{5}{8}$".

From Chapter II equation (66) the viscosity can be expressed

$$\mu = \frac{4\pi R^3 \Delta p}{3Q \ln^{r_2}/_{r_1}} - \frac{q\rho Q R \left(\frac{1}{r_1^2} - \frac{1}{r_2^2}\right)}{140\pi \ln^{r_2}/_{r_1}} \qquad \ldots\ldots(4.1)$$

which is the solution of Jackson, Peube and Savage.

Since the second term on the right hand side was only some 10% of the first term, any error in the viscosity due to errors in r_2 and r_1 was principally due to the error in the term $\ln^{r_2}/r_1$. Thus for r_2 values from $2\frac{1}{8}$" to $1\frac{1}{8}$" except at $r_2 = 1\frac{5}{8}$" where an error of 0.35% was incurred the error in the viscosity is approximately 0.05% and 0.4% for the radii $\frac{7}{8}$" and $\frac{5}{8}$".

(b) Error in Pressure Drop

The use of 8 mm precision bore tubing minimised errors in the length of manometer fluid to be measured due to irregularity of bore. Measurements were made with a Pye cathetometer capable of measuring to 0.005 cm with the use of the Vernier.

However it was felt that the limitation of the pressure drop measurement was not the accuracy of the cathetometer but such things as small fluctuations in mass flow or temperature drift. The latter effect was probably the main source of error since the test water tended to increase or decrease in temperature in sympathy with the room temperature which resulted in slight changes in the manometer fluid levels. Thus

it was estimated that the probable accuracy of the measurement of length was no better than 0.010 cm which with carbon tetrachloride as the manometer fluid gives the error in the pressure drop as 0.006 cm of water.

Four plate separations were used in the experimental investigations and pressures were read for seven different r_2/r_1 ratios with flows ranging from 1 to 7 cm^3/sec.

Obviously the pressure drop can vary with plate separations, r_2/r_1 ratios, and flow, but to demonstrate how large an error can be incurred the worst conditions are taken.

In the tests carried out with water at room temperature the largest plate separation was 0.0194" and the smallest r_2/r_1 ratio $5/3$. The smallest flow used with this gap size was 2.244 cm^3/sec which gave a pressure drop of 0.222 cm of water and, using the inaccuracy in pressure drop quoted above, gives an error in the reading of $2\frac{1}{2}$%. Naturally, not much importance was attached to these results although the error was considerably reduced by taking larger flow rates and r_2/r_1 ratios.

For the smallest plate separation used of 0.00965", a r_2/r_1 ratio of $11/3$ and a flow of 1.645 cm^3/sec, the pressure drop was 3.039 cm of water which resulted in an error of 0.2%.

The above examples serve to illustrate the wide range of errors that can be incurred with the pressure measurement for different sets of experimental data and that an error must be calculated for each measurement on the basis that the limit of the accuracy is 0.006 cm of water.

(c) Errors in Plate Separation

The method by which the plate separation is measured has been described above.

The fact that the table of the toolmaker's micrsocope was probably not as accurate as the accuracy sought in this measurement was not important since the method employed involved measuring height differences. What was important was that the reproducibility of the readings was good and that no variations existed at a position for successive measurements. Such variations in the readings could be caused by a piece of grit on the sliding parts of the table as it revolved, or dust on the Johannsen blocks.

To estimate the reproducibility the six zero readings were taken for at least half a dozen times. A typical set of readings is given in Table 2 where values of the six positions are given for nine consecutive sets of readings, a whole number representing 0.0001".

Table 2

Position									
1	$-2\frac{1}{2}$	$-2\frac{1}{2}$	$-2\frac{1}{4}$	$-2\frac{1}{2}$	-3	$-2\frac{1}{2}$	-3	$-2\frac{1}{2}$	$-2\frac{1}{2}$
2	-1	-1	$-\frac{1}{2}$	$-\frac{1}{2}$	-1	-1	$-\frac{1}{2}$	$-\frac{1}{2}$	$-\frac{1}{2}$
3	$+\frac{1}{2}$	$+\frac{1}{2}$	$+\frac{1}{2}$	$+\frac{1}{2}$	$+\frac{1}{2}$	$+\frac{1}{2}$	$+\frac{1}{2}$	$+\frac{1}{2}$	$+\frac{1}{2}$
4	$+1$	$+1$	$+1$	$+1$	$+1$	$+1$	$+1\frac{1}{2}$	$+1\frac{1}{2}$	$+1\frac{1}{2}$
5	0	0	0	0	0	0	0	0	0
6	-3	-3	-3	-3	-3	$-2\frac{1}{2}$	-3	$-2\frac{1}{2}$	$-2\frac{1}{2}$

From the table it can be seen that positions 3 and 5 did not change for the nine measurements while the greatest change in other position was 0.00005".

This sort of reproducibility was attainable only if sufficient care was taken to ensure that the plates and Johannsen blocks were scrupulously clean.

The electric comparator was a product of Southern Instruments Ltd. and was capable of reading to 0.00001". The Johannsen blocks were an inspection set of gauges with an accuracy of probably better than 0.00001" and no measurements were made with a "build-up" of these blocks which can always lead to errors.

From these limits quoted above it would seem capable of measuring plate separations to 0.00001". However due to small inconsistencies it was only possible to discriminate between successive differences of 0.00005". For example, taking position 1 in Table 2 it was possible to discriminate between $-2\frac{1}{2}$ and -3 but not, say, between $-2\frac{3}{4}$ and -3. Thus the tolerance on the plate separation was put as $\pm$ 0.000025".

The smallest gap used in the experiments was 0.00965" and since the gap appears in the working equation to the third power, the error incurred was $\pm$ 0.75%. The other plate separations used were 0.0120", 0.0151", and 0.0194" which resulted in errors in the working equation of $\pm$ 0.63%, $\pm$ 0.5% and $\pm$ 0.39% respectively.

(d) Errors in the Volume Flow Rate

This error was kept to a minimum by using a range of sizes of measuring cylinders corresponding to the flow rate so that the time interval was approximately 120 seconds. A series of experiments was conducted at constant flow to estimate the reproducibility of such timings and it was felt that for the range of flows used this was of the order of 0.1% to 0.2%.

It was not known to what extent the reproducibility of the timings was due to human errors in the stopping of the stop-watch at the appropriate mark or due to small fluctuations in the flow caused by the constant head or the deaerator resin bed.

The error in the stop-watch which was used by Whitelaw is quoted by him as being 0.12%. This was checked against an electronic timer capable of an accuracy of 1 in 10^5 and the errors incurred ranged from 0.1% to 0.2%.

Thus it is felt that the greatest error that could have been incurred due to these inconsistencies is of the order of 0.25%.

(e) Errors in Temperature Measurement

The fact that the temperature of the test water was known only to the nearest Celsius degree would have little effect on the error in the density since at the conditions of the tests (14 ^{o}C to 20 ^{o}C) the variation in density is approximately 0.01% to 0.02% per Celsius degree.

However this is not the case with the viscosity, the variation being some 3% for a change of 1 C^{o}. Thus it was felt that the temperature should be known to at least $\div$ 0.01 ^{o}C.

As stated above a thermistor was used for this purpose, it being inconvenient to use thermometers or thermocouples. From the data obtained in the calibration tables of resistance against temperature were drawn up with the help of a computer programme using an equation of the form

$$\log R = A + BT + CT^2 + DT^3 \qquad \ldots\ldots(4.2)$$

Taking selected points over the range of temperature values of

A, B, C, and D were calculated, these being respectively 2.88248;
-1.79625×10^{-2}; 5.76666×10^{-5}; and -1.4846×10^{-7}. This equation
was then used to calculate intermediate values of resistance for a
certain value of temperature and the results compared with points in
the calibration other than those taken to determine A, B, C and D.

It was found that in the range 10 ^{o}C to 25 ^{o}C equation (4.2)
agreed with the calibration values to better than 0.01 C^{o} and from
25° to 65 ^{o}C it was accurate to 0.05 ^{o}C. Above 65 ^{o}C the accuracy of
the actual temperature to the equation value of the temperature for the
same resistance is only 0.1 C^{o}. However since the experiments to study
the accuracy of the solutions for radial flow were conducted at room
conditions it was concluded the calibration was sufficiently accurate.
A table comparing the calibration values and computed values is given
in Appendix (4).

The resistance box used in the Wheatstone Bridge circuit was one
manufactured by the Croydon Precision Instrument Co. Type RBB4 which is
a four dial model of total resistance 1,111 ohms in steps of 0.1 ohm,
the coils being wound non-inductively in manganin. The accuracy quoted
for this instrument is 0.5% in the 0.1 ohm decade, 0.2% in the 1 ohm
decade and 0.1% in the 100 ohm decade.

This latter error was the most serious as the resistance of the
thermistor at room temperatures was of the order of 400Ω which would
result in an uncertainty of 0.4Ω. Since the resistance coefficient of
the thermistor at these temperatures was approximately 0.15Ω per 0.01 C^{o},
it was felt that the uncertainty in the temperature measurement was

$\pm$ 0.015 C^o which in turn would give an error of 0.07% in the value

of the viscosity at these temperatures(14 ^{o}C to 20 ^{o}C).

(f) Errors in Viscosity

Since, initially, the purpose of the experiments was to investigate

the various solutions available for radial flow between parallel plates

the accuracy to which the viscosity of water in the range 14 ^{o}C to 20 ^{o}C

(the range of temperatures at which the tests were conducted) had to be

investigated.

It would appear from the literature available that the viscosity

of water in the range 5 ^{o}C to 40 ^{o}C is well defined and a summary of

the recommended values over the last fifty years is given in a paper

by Bruges, Latto, and Ray(37).

In his experiments the author has used the viscosity values given

by the correlation of Bingham and Jackson quoted in the "Handbook of

Chemistry and Physics". It was, thus, necessary to ascertain the

accuracy of this correlation by comparison with values of other authors

obtained either by correlation or experiment.

Table 3, which is not intended to be extensive, gives some of the

accepted values as a comparison with Bingham and Jackson's correlation.

Table 3   Absolute Viscosity of Water 0 ^{o}C to 40 ^{o}C in centipoise

^{o}C	1	2	3	4	5	6
0 ^{o}C	1.7921	--		1.7934	1.7920	
5 ^{o}C	1.5188	1.5230		1.5188	1.5200	
10 ^{o}C	1.3077	--		1.3097	1.3069	
15 ^{o}C	1.1404	--		1.1447	1.1383	
20 ^{o}C	1.0050	1.0050	1.0020	1.0087	1.0020	1.0025
25 ^{o}C	0.8937	--		0.8949	0.8930	
30 ^{o}C	0.8007	--		0.8004	0.7975	
35 ^{o}C	0.7225	--		0.7208	0.7193	
40 ^{o}C	0.6560	0.6551		0.6536	0.6531	

Column (1) is the values of Bingham and Jackson correlated from the data available at that time and is the set of values used by the author in his experiments (38).

Column (2) is the experimental values of Hardy and Cottington (39) obtained with a Bingham viscometer calibrated at 20 °C, the value of the viscosity at this temperature being taken as 1.005 cP. The accuracy of their determination was claimed to be 0.1%.

The absolute measurement of Swindells, Coe and Godfrey (7) is given in column (3). This value which has an accuracy of ± 0.03% is now recognised as a primary reference point.

Column (4) gives the correlated values of Dorsey (40) which are based on the observation of the experimenters listed on page 183 of his book "Properties of Ordinary Water Substance" (41). An accuracy of 0.1% to 0.2% is claimed.

One of the more recent determinations of the viscosity of water is given in column (5). This is the work of Weber (42) who used a rolling ball viscometer which was calibrated at 20 °C using the value of Swindells, Coe and Godfrey. An accuracy of ± 0.05% is claimed.

In column (6) is the value at 20 °C obtained by Roscoe and Bainbridge (43) using the oscillating vessel method for which an accuracy of ± 0.05% is claimed.

As can be seen from the table an error of between 0.1% and 0.2% is incurred in the temperature range 10 °C to 20 °C by using the correlation of Bingham and Jackson. The greatest discrepancy seems to be with Dorsey's correlation. However the fact that the value at 20 °C of 1.0087 cP seems to indicate that a slight error in his correlation

could exist since the very accurate work of Swindells, Coe and Godfrey, and Roscoe and Bainbridge seem to indicate this value is nearer 1.002 cP.

Overall Accuracy   It is difficult to put a definite value on the accuracy over the range of the experimental work due to the variation in error that can occur in the pressure measurement.

Not much importance has been attached to measurements made with small r_2/r_1 ratios at small flows as it is felt that these measurements could be in error by $2\frac{1}{2}\%$.

However at higher flow rates and smaller plate separations the error in pressure drop measurement is considerably reduced. Thus for a plate separation of 0.00965" at r_2/r_1 ratios greater than $7/3$ the estimated error is approximately 1.4%, the greatest single error being the measurement of the gap.

For plate separations of 0.0120", 0.0151", and 0.0194", the error in the plate separation is reduced but due to smaller pressure drop associated with the larger gaps this reduction in error is compensated by an increase in the error of the pressure drop measurement. Thus for r_2/r_1 ratios greater than $3/1$ and flows greater than 1.5 cm^3/sec the mean overall accuracies for plate separations of 0.0120", 0.0151" and 0.0194" are estimated to be 1.4%, 1.3% and 1.1% respectively.

X

With Δp, Q, ρ, r_2, r_1, and $2h$ all being determined experimentally, viscosity values can be calculated from the various solutions and, using Bingham and Jackson's correlation, compared with the value of viscosity corresponding to the measured temperature of the water.
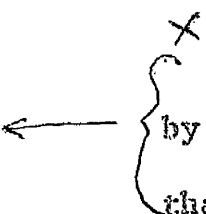
X

CHAPTER V

Results of Tests at Ambient Temperature to Investigate

Available Solutions of Laminar Radial Flow

The experimental data obtained by the author from the apparatus described in the previous chapter are given in this chapter. The experiments were carried out with plate separations of 0.00965", 0.0120", 0.0151" and 0.0194" at room temperatures for flows ranging from 1 cm^3/sec to 7 cm^3/sec. As described in the previous chapter eight pressure tappings were used resulting in seven pressure drops for seven r_2/r_1 ratios. All pressure drops were measured relative to r_1, r_1 being $\frac{3}{8}$" radius, and the respective r_2 values being $2\frac{1}{8}$", $1\frac{7}{8}$", $1\frac{5}{8}$", $1\frac{3}{8}$", $1\frac{1}{8}$", $\frac{7}{8}$", and $\frac{5}{8}$", so that seven determinations of viscosity could be obtained for each set of readings.

A comparison of the author's solution and other solutions is made by comparing the viscosities obtained from the various solutions and that obtained by measurement. This might appear an unusual method of comparison but is greatly influenced by the complexity of the author's solution whose final equation is designed to give the viscosity in terms of the other parameters. To obtain a theoretical pressure drop, say, in terms of the other measured data would be difficult.

For each plate separation only six or seven typical sets of readings over the range of flows used are tabulated along with the values obtained by Livesey's solution - equation 15 chapter II and Peube's 3 term solution - equation 66 chapter II. This latter equation is identical to the solutions of Savage and Jackson and Symmons the former being the

same as Comolet's solution. Peube's 5 term solution - equation 62 chapter II - was found to render no marked difference for the experiments conducted here and values calculated by Moller's solution are not tabulated since the difference with Peube's solution is only 0.2% to 0.4% which is less than the experimental accuracy. Thus any conclusions that are drawn concerning Peube's 3 term solution must also apply to Moller's solution.

Rearranging the solutions of Livesey and Peube to obtain expressions for the viscosity -

$$\mu = \frac{4\pi h^3 \Delta p}{3Q \ln^{r_2}/r_1} - \frac{\rho Q h \left(\frac{1}{r_1^2} - \frac{1}{r_2^2}\right)}{20\pi \ln^{r_2}/r_1} \qquad \ldots\ldots(5.1)$$

and

$$\mu = \frac{4\pi h^3 \Delta p}{3Q \ln^{r_2}/r_1} - \frac{9\rho Q h \left(\frac{1}{r_1^2} - \frac{1}{r_2^2}\right)}{140\pi \ln^{r_2}/r_1} \qquad \ldots\ldots(5.2)$$

The values of Q, the volume flow rate, Δp the pressure drop between r_2 and r_1, the r_2/r_1 ratio, and T the temperature are determined experimentally. The density values according to the measured temperature are obtained from the "Handbook of Chemistry and Physics" and in the tables μ_m is the value of viscosity in centipoise at the measured temperature as taken from the correlation of Bingham and Jackson.

The manometer fluid used was carbon tetrachloride and its density was calculated from data given in the "International Critical Tables" in vol. 111 p.28, the equation being of the form

$$\rho_T = 1.63255 - 1.911 \times 10^{-3} T - 0.69 \times 10^{-5} T^2 \qquad \ldots\ldots(5.3)$$

In tables 1, 2, 3 and 4 μ_1, μ_2, and μ_A are the viscosity values

calculated from equations (5.1), (5.2) and the author's solution given in chapter III. The dimensionless term B from the author's solution is also listed to give an indication of its variation w.r.t. r_2 although it must be remembered that this could be partially due to experimental error.

The Reynolds numbers expressed by $\dfrac{2\rho\bar{u}h}{\mu}$ where $\bar{u}$ is the mean velocity across the gap at a radius r range from 110 to 20 for the following results.

Using a Reynolds number of the form $Re = \dfrac{4\rho\bar{u}h^2}{\mu r}$ the values range from approximately 6 to 0.02. From tests carried out to estimate the limit at which stability occurred, as given in chapter IV, this expression for the Reynolds number imposed a limit of Re = 10. Thus for all the tests conducted here purely radial flow should exist.

<u>Table 1 Results for 2h = 0.00965"</u>

	Δp cm of water	r_2/r_1	μ_m	μ_1	μ_2	μ_A	$\bar{B}$
1.645 cm^3/s at 18.42 ^{o}C	4.038	17/3	1.0450	1.0492	1.0438	1.0440	1.497492
	3.753	15/3	"	1.0502	1.0442	1.0443	1.497323
	3.397	13/3	"	1.0413	1.0348	1.0350	1.497078
	3.032	11/3	"	1.0463	1.0390	1.0397	1.496791
	2.589	9/3	"	1.0538	1.0456	1.0459	1.496378
	1.946	7/3	"	1.0207	1.0110	1.0112	1.495547
	1.203	5/3	1.0450	1.0377	1.0250	1.0253	1.494303
2.943 cm^3/s at 18.39 ^{o}C	7.359	17/3	1.0458	1.0531	1.0428	1.0439	1.495526
	6.851	15/3	"	1.0553	1.0445	1.0445	1.495228
	6.218	13/3	"	1.0521	1.0405	1.0363	1.494799
	5.548	11/3	"	1.0506	1.0376	1.0387	1.494279
	4.751	9/3	"	1.0590	1.0443	1.0447	1.493550
	3.582	7/3	"	1.0247	1.0073	1.0076	1.492063
	2.238	5/3	1.0458	1.0456	1.0229	1.0235	1.489890

Table 1 (contd) 2h = 0.00965"

	Δp cm of water	r_2/r_1	μ_m	μ_1	μ_2	μ_A	B
3.748 cm³/s at 18.16 °C	9.509	17/3	1.0517	1.0591	1.0460	1.0475	1.494335
	8.858	15/3	"	1.0616	1.0479	1.0480	1.493958
	8.043	13/3	"	1.0538	1.0389	1.0392	1.493413
	7.192	11/3	"	1.0575	1.0408	1.0424	1.492764
	6.167	9/3	"	1.0664	1.0478	1.0483	1.491845
	4.665	7/3	"	1.0325	1.0203	1.0208	1.489972
	2.924	5/3	1.0517	1.0531	1.0243	1.0252	1.487224
4.520 cm³/s at 17.75 °C	11.733	17/3	1.0626	1.0754	1.0396	1.0615	1.493274
	10.844	15/3	"	1.0791	1.0626	1.0628	1.492833
	9.937	13/3	"	1.0703	1.0524	1.0529	1.492179
	8.894	11/3	"	1.0742	1.0542	1.0561	1.491412
	7.644	9/3	"	1.0846	1.0621	1.0629	1.490333
	5.791	7/3	"	1.0494	1.0227	1.0234	1.488106
	3.636	5/3	1.0626	1.0685	1.0337	1.0352	1.484827
5.252 cm³/s at 17.62 °C	13.771	17/3	1.0661	1.0774	1.0590	1.0614	1.492201
	12.836	15/3	"	1.0800	1.0608	1.0612	1.491680
	11.677	13/3	"	1.0727	1.0519	1.0525	1.490936
	10.456	11/3	"	1.0760	1.0527	1.0550	1.490042
	9.008	9/3	"	1.0850	1.0619	1.0630	1.488808
	6.832	7/3	"	1.0513	1.0203	1.0213	1.486213
	4.312	5/3	1.0661	1.0728	1.0325	1.0343	1.482455
6.241 cm³/s at 16.05 °C	16.749	17/3	1.0842	1.0925	1.0705	1.0734	1.490864
	15.626	15/3	"	1.0956	1.0727	1.0734	1.490256
	14.227	13/3	"	1.0883	1.0636	1.0642	1.489384
	12.766	11/3	"	1.0927	1.0650	1.0677	1.488352
	11.017	9/3	"	1.1057	1.0747	1.0759	1.486916
	8.397	7/3	"	1.0708	1.0339	1.0355	1.483926
	5.318	5/3	1.0842	1.0927	1.0448	1.0473	1.479540

Table 2   Results for 2h = 0.0120"

	Δp cm of water	r_2/r_1	μ_m	μ_1	μ_2	μ_A	B
$Q=0.921$ cm^3/s at 18.98 °C	1.135	17/3	1.0304	1.0176	1.0136	1.0138	1.498197
	1.052	15/3	"	1.0157	1.0115	1.0115	1.498071
	0.957	13/3	"	1.0130	1.0085	1.0086	1.497906
	0.859	11/3	"	1.0247	1.0196	1.0201	1.497716
	0.732	9/3	"	1.0303	1.0246	1.0247	1.497418
	0.554	7/3	"	1.0072	1.0005	1.0005	1.496856
	0.347	5/3	1.0304	1.0390	1.0302	1.0304	1.496036
$Q=1.412$ cm^3/s at 18.34 °C	1.791	17/3	1.0471	1.0409	1.0349	1.0350	1.497295
	1.661	15/3	"	1.0388	1.0324	1.0324	1.497106
	1.516	13/3	"	1.0385	1.0315	1.0316	1.496866
	1.347	11/3	"	1.0383	1.0305	1.0313	1.496543
	1.154	9/3	"	1.0494	1.0407	1.0408	1.496113
	0.875	7/3	"	1.0255	1.0151	1.0153	1.496264
	0.546	5/3	1.0471	1.0513	1.0378	1.0381	1.493994
$Q=2.013$ cm^3/s at 18.53 °C	2.595	17/3	1.0421	1.0490	1.0404	1.0406	1.496174
	2.409	15/3	"	1.0473	1.0382	1.0382	1.495907
	2.186	13/3	"	1.0407	1.0308	1.0309	1.495542
	1.952	11/3	"	1.0448	1.0337	1.0347	1.495103
	1.671	9/3	"	1.0535	1.0410	1.0412	1.494482
	1.268	7/3	"	1.0275	1.0127	1.0130	1.493265
	0.803	5/3	1.0421	1.0661	1.0469	1.0474	1.491562
$Q=3.016$ cm^3/s at 18.16 °C	4.022	17/3	1.0517	1.0709	1.0580	1.0585	1.494386
	3.744	15/3	"	1.0715	1.0578	1.0582	1.494008
	3.404	13/3	"	1.0651	1.0503	1.0507	1.493476
	3.037	11/3	"	1.0667	1.0500	1.0515	1.492818
	2.607	9/3	"	1.0769	1.0583	1.0590	1.491918
	1.989	7/3	"	1.0521	1.0299	1.0307	1.490152
	1.258	5/3	1.0517	1.0840	1.0552	1.0565	1.487582

Table 2 (contd) 2h = 0.0120"

	Δp cm of water	r_2/r_1	μ_m	μ_1	μ_2	μ_A	B
Q=4.440cm³/s at 17.96	6.071	17/3	1.0570	1.0782	1.0593	1.0597	1.491793
	5.665	15/3	"	1.0803	1.0601	1.0605	1.491254
	5.167	13/3	"	1.0757	1.0539	1.0544	1.490495
	4.625	11/3	"	1.0780	1.0535	1.0560	1.489552
	3.982	9/3	"	1.0892	1.0618	1.0627	1.488245
	3.066	7/3	"	1.0692	1.0365	1.0378	1.485751
	1.967	5/3	1.0570	1.1107	1.0663	1.0703	1.482186
Q=5.404cm³/s at 17.83 °C	7.578	17/3	1.0605	1.0929	1.0699	1.0706	1.490151
	7.071	15/3	"	1.0942	1.0698	1.0704	1.489496
	6.453	13/3	"	1.0890	1.0624	1.0632	1.488578
	5.784	11/3	"	1.0914	1.0615	1.0647	1.487449
	4.985	9/3	"	1.1019	1.0684	1.0700	1.485869
	3.848	7/3	"	1.0810	1.0413	1.0431	1.482863
	2.486	5/3	1.0605	1.1267	1.0751	1.0780	1.478655
Q=6.544cm³/s at 17.39 °C	9.460	17/3	1.0723	1.1123	1.0845	1.0853	1.488285
	8.839	15/3	"	1.1141	1.0844	1.0853	1.487513
	8.078	13/3	"	1.1093	1.0771	1.0782	1.486430
	7.255	11/3	"	1.1122	1.0761	1.0801	1.485100
	6.275	9/3	"	1.1258	1.0854	1.0871	1.483261
	4.857	7/3	"	1.1034	1.0553	1.0579	1.479692
	3.164	5/3	1.0723	1.1552	1.0926	1.0968	1.474828

Table 3 Results for 2h = 0.0151"

	Δp cm of water	r_2/r_1	μ_m	μ_1	μ_2	μ_A	B
$Q=1.143 cm^3/s$	0.696	17/3	0.9873	0.9938	0.9877	0.9877	1.497121
at 20.77 °C	0.643	15/3	"	0.9876	0.9811	0.9810	1.496906
	0.583	13/3	"	0.9820	0.9749	0.9750	1.496631
	0.527	11/3	"	0.9988	0.9909	0.9915	1.496344
	0.400	9/3	"	0.8897	0.8807	0.8810	1.495337
	0.343	7/3	"	0.9889	0.9784	0.9785	1.495005
	0.207	5/3	0.9873	0.9789	0.9651	0.9653	1.493436
$Q=2.334 cm^3/s$	1.674	17/3	1.1325	1.1531	1.1406	1.1408	1.494923
at 15.27 °C	1.558	15/3	"	1.1536	1.1403	1.1404	1.494580
	1.433	13/3	"	1.1609	1.1464	1.1466	1.494169
	1.286	11/3	"	1.1709	1.1547	1.1561	1.493627
	1.086	9/3	"	1.1628	1.1446	1.1450	1.492707
	0.845	7/3	"	1.1605	1.1389	1.1395	1.491301
	0.540	5/3	1.1325	1.2131	1.1850	1.1858	1.489182
$Q=3.064 cm^3/s$	2.265	17/3	1.1307	1.1760	1.1596	1.1598	1.493464
at 15.08 °C	2.107	15/3	"	1.1754	1.1578	1.1581	1.493017
	1.931	13/3	"	1.1778	1.1588	1.1590	1.492456
	1.723	11/3	"	1.1779	1.1566	1.1586	1.491687
	1.466	9/3	"	1.1776	1.1538	1.1543	1.490548
	1.133	7/3	"	1.1635	1.1351	1.1359	1.488615
	0.721	5/3	1.1307	1.2047	1.1678	1.1692	1.485714
$Q=3.967 cm^3/s$	2.956	17/3	1.1319	1.1690	1.1478	1.1481	1.491489
at 15.29 °C	2.751	15/3	"	1.1675	1.1447	1.1452	1.490901
	2.518	13/3	"	1.1669	1.1423	1.1429	1.490147
	2.265	11/3	"	1.1754	1.1478	1.1504	1.489223
	1.934	9/3	"	1.1766	1.1458	1.1467	1.487762
	1.508	7/3	"	1.1700	1.1333	1.1346	1.485356
	0.966	5/3	1.1319	1.2120	1.1643	1.1665	1.481641

Table 3 (contd) 2h = 0.0151"

	Δp cm of water	r_2/r_1	μ_m	μ_1	μ_2	μ_A	B
$Q=4.869 cm^3/s$	3.820	$^{17}/3$	1.1617	1.2174	1.1913	1.1920	1.489972
at 14.30 ^{o}C	3.560	$^{15}/3$	"	1.2173	1.1894	1.1902	1.489292
	3.257	$^{13}/3$	"	1.2147	1.1845	1.1851	1.488384
	2.935	$^{11}/3$	"	1.2241	1.1903	1.1937	1.487308
	2.509	$^{9}/3$	"	1.2249	1.1870	1.1884	1.485579
	1.949	$^{7}/3$	"	1.2093	1.1642	1.1662	1.482624
	1.248	$^{5}/3$	1.1617	1.2475	1.1889	1.1922	1.478135

Table 4   2h = 0.0194"

	Δp cm of water	x_2/x_1	μ_m	μ_1	μ_2	μ_A	B
Q=2.244cm³/s at 17.58 °C	0.725	17/3	1.0672	1.0901	1.0746	1.0749	1.493369
	0.671	15/3	"	1.0837	1.0672	1.0675	1.492877
	0.608	13/3	"	1.0728	1.0549	1.0554	1.492212
	0.539	11/3	"	1.0661	1.0460	1.0479	1.491362
	0.465	9/3	"	1.0787	1.0563	1.0569	1.490297
	0.357	7/3	"	1.0585	1.0319	1.0327	1.488232
	0.222	5/3	1.0672	1.0667	1.0320	1.0394	1.484830
Q=3.357cm³/s at 17.42 °C	1.125	17/3	1.0715	1.1050	1.0819	1.0825	1.492218
	1.047	15/3	"	1.1032	1.0785	1.0791	1.489537
	0.951	13/3	"	1.0924	1.0657	1.0664	1.488367
	0.846	11/3	"	1.0857	1.0558	1.0589	1.487331
	0.735	9/3	"	1.1061	1.0736	1.0739	1.485861
	0.558	7/3	"	1.0647	1.0248	1.0265	1.482527
	0.351	5/3	1.0715	1.0749	1.0230	1.0260	1.477539
Q=4.448cm³/s at 17.46 °C	1.511	17/3	1.0704	1.0955	1.0648	1.0659	1.486938
	1.410	15/3	"	1.0945	1.0618	1.0629	1.486041
	1.290	13/3	"	1.0903	1.0549	1.0563	1.484839
	1.155	11/3	"	1.0882	1.0465	1.0531	1.483283
	1.003	9/3	"	1.1043	1.0599	1.0621	1.481265
	0.778	7/3	"	1.0827	1.0298	1.0329	1.477282
	0.503	5/3	1.0704	1.1183	1.0495	1.0544	1.471467
Q=5.187cm³/s at 17.48 °C	1.801	17/3	1.0699	1.2037	1.0679	1.0695	1.484892
	1.684	15/3	"	1.1050	1.0669	1.0685	1.483890
	1.541	13/3	"	1.0990	1.0578	1.0596	1.482474
	1.382	11/3	"	1.0968	1.0506	1.0562	1.480684
	1.200	9/3	"	1.1111	1.0593	1.0624	1.478314
	0.936	7/3	"	1.0922	1.0305	1.0348	1.473780
	0.604	5/3	1.0699	1.1195	1.0393	1.0463	1.466850

Table 4 (contd) $2h = 0.0194''$

	Δp cm of water	r_2/r_1	μ_m	μ_1	μ_2	μ_A	B
$Q=6.300 cm^3/s$ at $17.35 ^oC$	2.252	$17/3$	1.0734	1.1135	1.0701	1.0722	1.481829
	2.109	$15/3$	"	1.1147	1.0683	1.0707	1.480624
	1.932	$13/3$	"	1.1086	1.0585	1.0612	1.478926
	1.738	$11/3$	"	1.1067	1.0505	1.0577	1.476792
	1.508	$9/3$	"	1.1172	1.0543	1.0586	1.473852
	1.265	$7/3$	"	1.1002	1.0254	1.0316	1.468469
	0.775	$5/3$	1.0734	1.1372	1.0399	1.0497	1.460503
$Q=7.534 cm^3/s$ at $17.00 ^oC$	2.787	$17/3$	1.0828	1.1279	1.0760	1.0789	1.478572
	2.616	$15/3$	"	1.1309	1.0755	1.0787	1.477191
	2.398	$13/3$	"	1.1227	1.0627	1.0665	1.475150
	2.167	$11/3$	"	1.1238	1.0567	1.0659	1.472730
	1.894	$9/3$	"	1.1419	1.0667	1.0727	1.469470
	1.496	$7/3$	"	1.1252	1.0357	1.0440	1.463226
	0.968	$5/3$	1.0828	1.1369	1.0204	1.0344	1.452979

It can be seen from equations 5.1 and 5.2 that the second term on the right hand side of the former is some 22% less than the similar term in equation 5.2. These terms account for the variations of the solution from the creeping flow solution due to inertia effects. Thus, viscosity values calculated from equation 5.1 will be greater than those obtained from equation 5.2 and since, on average, the inertia effect account for some 10% of the viscosity, the difference will be approximately 2.5%.

Disregarding for the moment the question of which solution agrees better with experiment, it can be seen from Tables 1, 2, 3 and 4 the close agreement between equation 5.2 and the author's solution. The viscosity values tabulated have been calculated using the same experimental data.

In the case of the smallest plate separation used of 0.00965" the discrepancy is greatest at the largest flow and the smallest r_2/r_1 ratio of $5/3$ and is of the order of 0.2% where the inertia term is some 20% of the viscous term. At the smallest flow rate and a r_2/r_1 ratio of $17/3$ the discrepancy in the theories is negligible, the inertia term only being about 2% of the viscous term.

For plate separations of 0.0120", 0.0151" and 0.0194" similar effects can be observed, but to a greater extent. The greatest differences between equation 5.2 and the author's solution for 2h = 0.0120", 0.0151", and 0.0194" are 0.4%, 0.5%, and 1% respectively, these values corresponding to a r_2/r_1 ratio of $5/3$ and the largest flow rate for each gap. The fraction of the pressure drop due to inertia effects in these cases are approximately 25%, 30%, and 45% respectively. As stated, these differences are for the worst conditions and on average the discrepancy is of the order of 0.2% which serves to illustrate the good theoretical agreement between equation 5.2 and the author's solution for the tests conducted here.

The extent to which the values of viscosity obtained from equations 5.1 and 5.2 vary depends, naturally enough, on how large the inertia term is in respect to the viscous term. Since the inertia term of equation 5.1 is 22% less than that of equation 5.2, the values of viscosity obtained from equation 5.1 are greater.

If equations 5.1 and 5.2 are rearranged to give expressions for the pressure drop then for converging flow

$$\Delta p = \frac{3\mu Q}{4\pi h^3} \ln \frac{r_2}{r_1} + \frac{3\rho Q^2 \left(\frac{1}{r_1^2} - \frac{1}{r_2^2}\right)}{80\pi^2 h^2} \qquad \dots\dots(5.4)$$

$$\Delta p = \frac{3\mu Q}{4\pi h^3} \ln \frac{r_2}{r_1} + \frac{27\rho Q^2 \left(\frac{1}{r_1^2} - \frac{1}{r_2^2}\right)}{560\pi^2 h^2} \qquad \dots\dots(5.5)$$

From (5.4) the percentage that the pressure drop due to inertia is of the viscous pressure drop is given by

$$\frac{\rho \varphi h \left(\frac{1}{r_1^2} - \frac{1}{r_2^2}\right) \times 100\%}{20 \pi \mu \, \ell_n \frac{r_2}{r_1}} \qquad \ldots\ldots(5.6)$$

Thus for similar flow rates, temperature, and radii, (5.6), as would be expected, shows that the inertia effect is more noticeable for larger plate separations. This can be shown by comparing the differences between μ_1 and μ_2 in Tables 1 and 4. Table 1 shows that the differences range from 0.6% to 4.0% whereas in Table 4 the range is 1.3% to 9% for essentially a similar range of values of the volume flow rate.

Poube's 5 term solution given in Chapter II by equation (62) has not been used here to calculate viscosity values from the experimental data, since, on average, the additional terms compared with equation 5.2 make a difference in the viscosity of only 0.2% approximately. However for the worst conditions of the tests recorded here a difference of some 2% can arise, if the extra terms are included in equation (5.2). A more detailed account of this discrepancy is given in Appendix (5).

From the tables it can be seen that for r_2/r_1 ratios of $7/3$ and $5/3$ the values of viscosity calculated from equation 5.2 and the author's solution were, on average, some 2% lower than values determined with greater r_2/r_1 ratios at the same mass flow rates.

It was felt that this discrepancy was partly due to the error incurred in the measurement of the pressure drop which was small for these r_2/r_1 ratios and partly due to the failure of the theories to account for the two-dimensional nature of the flow which becomes more apparent as r tends

to zero.

Equation (5.2) contains only the first two terms of a number of solutions - the uni-directional flow analysis of Jackson and Symmons, or the power series approaches of Paube, Savage, Jackson and Symmons who extended the analysis of Hunt and Torbe, and as stated above the third and fourth terms of these solutions begin to have a small but significant effect on the final answer at these small radii. It was thus concluded not to put too much emphasis on the values obtained with r_2/r_1 ratios of $^7/3$ and $^5/3$.

From Table 1 no conclusions can be drawn as to whether μ_1 or μ_2 agrees better with the experimental value μ_m since the difference between μ_1 and μ_2 is only about 1.5% which is the estimated experimental error. For the larger flow rates, however, it appears that there is a tendency for μ_1 to be greater than the measured value. Although there are exceptions probably due to experimental error, this tendency is more apparent in Tables 2, 3, and 4 where the plate separations are greater and consequently the inertia effect greater.

It would appear from Tables 2, 3, and 4, that while the results obtained by equation (5.2) and the author's solution remain on the whole within the experimental accuracy of 1.5%, equation (5.1) gives results about 2% to 3% higher than experimental values. It is thus concluded that equation (5.2) will incur less error if used with a radial flow viscometer than equation (5.1) although if the plate separation is small and suitable values of r_2 and r_1 are chosen then the pressure drop due to inertia effects can be made small enough for the difference between equations (5.1) and (5.2) to be insignificant.

A plot of pressure drop in centimetres of water relative to the innermost tapping (i.e. at $r = \frac{3}{4}''$) against radius is shown in figures 5.1, 5.2, 5.3, and 5.4, corresponding to the plate separations of 0.00965", 0.0120", 0.0151" and 0.0194". Theoretical curves of pressure drop have been calculated from equation 5.4 and 5.5 for the largest flow rates. With the exception of figure 5.1 where the results are inconclusi the curve obtained from equation 5.4 lies under the experimental curve. Equation 5.5, shown by the chain-dotted curve, seems to agree better with the experimental curve.

It should be noted that the results given in this chapter are only typical ones and that many more experimental values were actually obtaine However, to give all the results would only be to overstress the conclusi given above and thus only a selection of results covering the range of fl rates of the tests have been given.
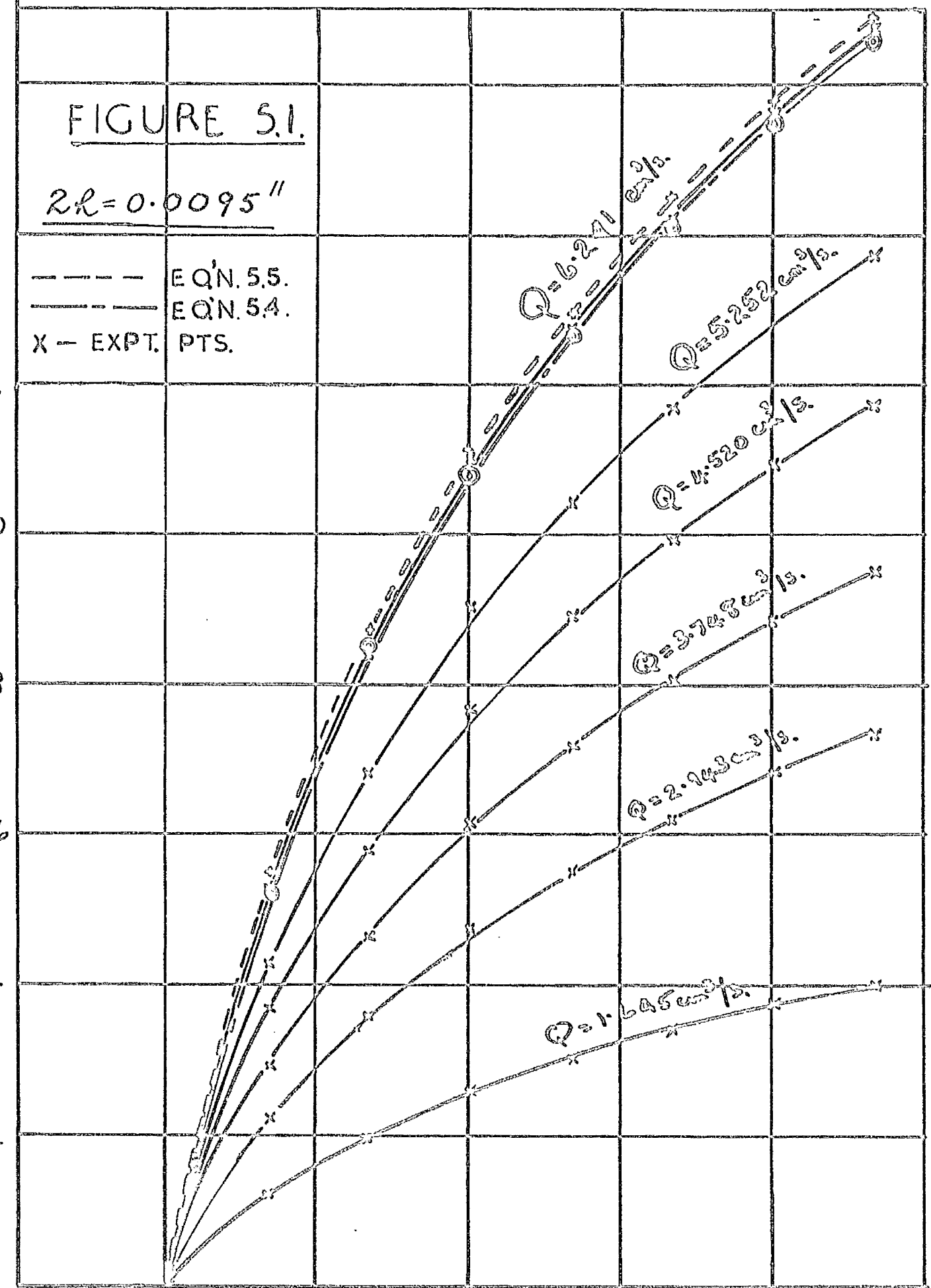
FIGURE 5.1.

$2R = 0.0095''$

- — — — EQ'N. 5.5.
- ········· EQ'N. 5.4.
- X — EXPT. PTS.

$Q = 6.241$ cm³/s.

$Q = 5.252$ cm³/s.

$Q = 4.520$ cm³/s.

$Q = 3.748$ cm³/s.

$Q = 2.943$ cm³/s.

$Q = 1.645$ cm³/s.

$\Delta p \longrightarrow$ cm. of water.

$r \longrightarrow$ INCHES.

FIGURE 5.2.

$2h = 0.0120"$

- - - - EQ'N 5.5.
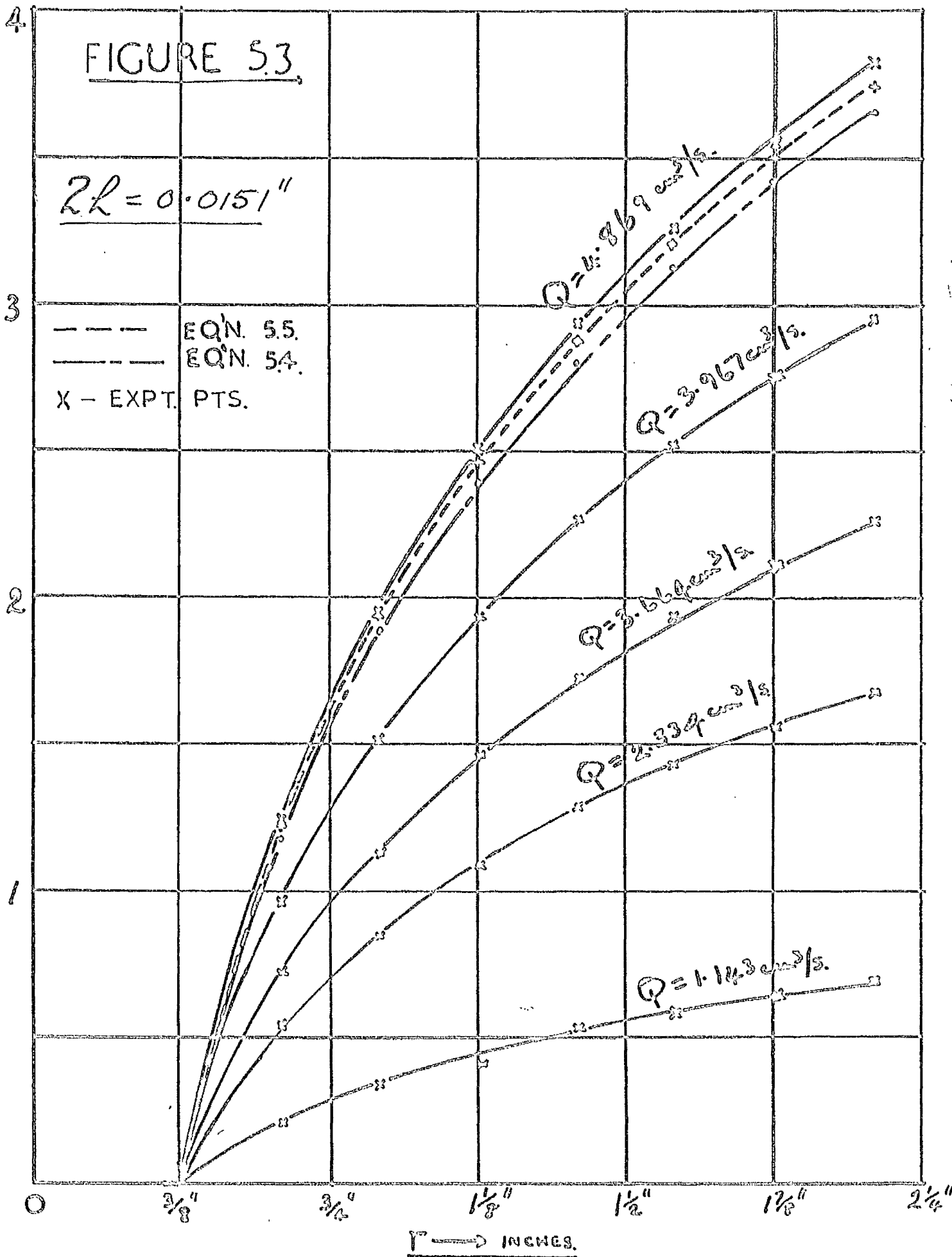— - — EQ'N 5.4.
X — EXPT PTS.

$\Delta p \rightarrow$ cm of water.

$Q = 6.54 \, cm^3/s.$

$Q = 5.404 \, cm^3/s.$

$Q = 4.440 \, cm^3/s.$

$Q = 3.016 \, cm^3/s.$

$Q = 2.013 \, cm^3/s.$

$Q = 1.412 \, cm^3/s.$

$Q = 0.921 \, cm^3/s.$

$\longrightarrow$ INCHES.

FIGURE 5.3.

$2R = 0.0151''$

- - - - EQ'N. 5.5.
———— EQ'N. 5.4.
X — EXPT. PTS.

$Q = 4.969 \, cm^3/s.$

$Q = 3.967 \, cm^3/s.$

$Q = 3.664 \, cm^3/s.$

$Q = 2.334 \, cm^3/s.$

$Q = 1.143 \, cm^3/s.$

$\Delta p \longrightarrow$ cm. of water.

$r \longrightarrow$ INCHES.

FIGURE 54.

$2\ell = 0.0194''$

EQ'N. 5.5.
EQ'N. 5.4.

X — EXPT. PTS.

$Q = 7.538 \, cm^3/s.$
$Q = 6.300 \, cm^3/s.$
$Q = 5.187 \, cm^3/s.$
$Q = 4.447 \, cm^3/s.$
$Q = 3.357 \, cm^3/s.$
$Q = 2.249 \, cm^3/s.$

$\frac{\Delta p}{\ell} \longrightarrow$ cm of water.
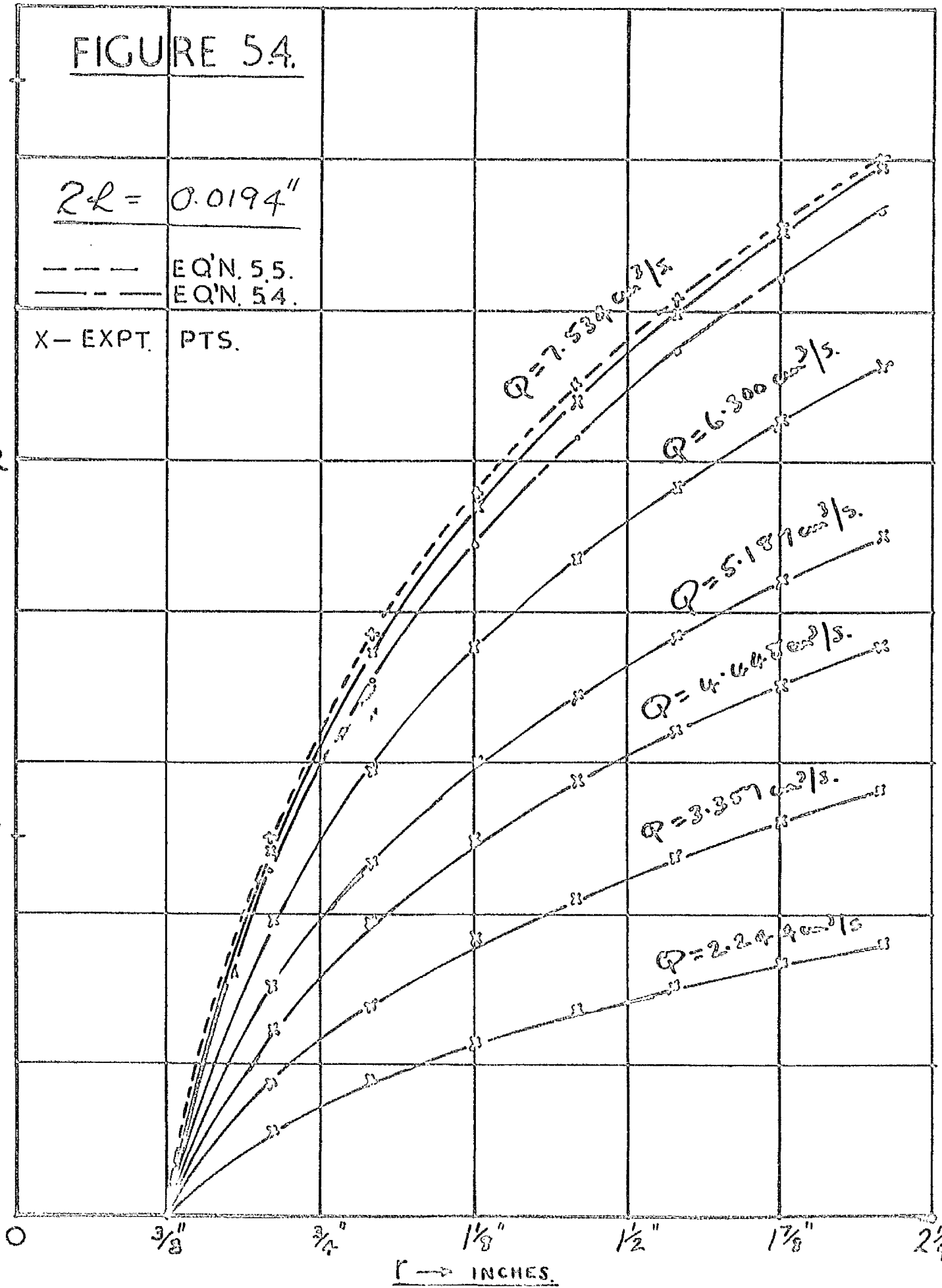
$r \longrightarrow$ INCHES.

CHAPTER VI

The viscometer described in the previous chapter was used to measure the viscosity of water in the range 0 ^{O} to 90 ^{O}C. These measurements are given below being the results of a series of tests designed to test the capabilities of the instrument over the range 0 ^{O}C to 90 ^{O}C and were thus of a preliminary nature. In view of the fact that an accuracy of, at worst, 1.5% could be attributed to the earlier results (Chapter V) it was hoped that a similar accuracy could be obtained over the range 0 ^{O}C to 90 ^{O}C.

The results from 1 ^{O}C to 10 ^{O}C were obtained with exactly the same apparatus as described previously.

However, over the range 20 ^{O}C to 90 ^{O}C the use of a deaerator was necessary to free the water of air which came out of solution and consequently disrupted the flow between the plates. Since a commercial deaerator was not available a system as shown in figure 6.1 was used. The tap water was preheated in a coil before passing to a constant head tank which regulated the flow entering the deaerator. Before entering the boiler the water was passed through a steam jacket, the deaerated water being run off from the bottom of the flask and cooled by two condensers in series.

It was hoped to use a small control valve in the line from these condensers to the viscometer but this was found to be not very satisfactory. Consequently, the pressure of the steam in the flask was kept as constant as possible by having the end of a glass tube immersed to a fixed length in water as shown in figure 6.1. This arrangement was found, not unsurprisingly, to cause fluctuations in the flow rate. This was due to

CONSTANT HEAD TANK.

OVERFLOW

STEAM BOILER

STEAM JACKET

FROM TAP

PREHEATER

PRESSURE REGULATOR

BOILER

DEAERATED WATER

GLASS SPIRAL CONDENSER
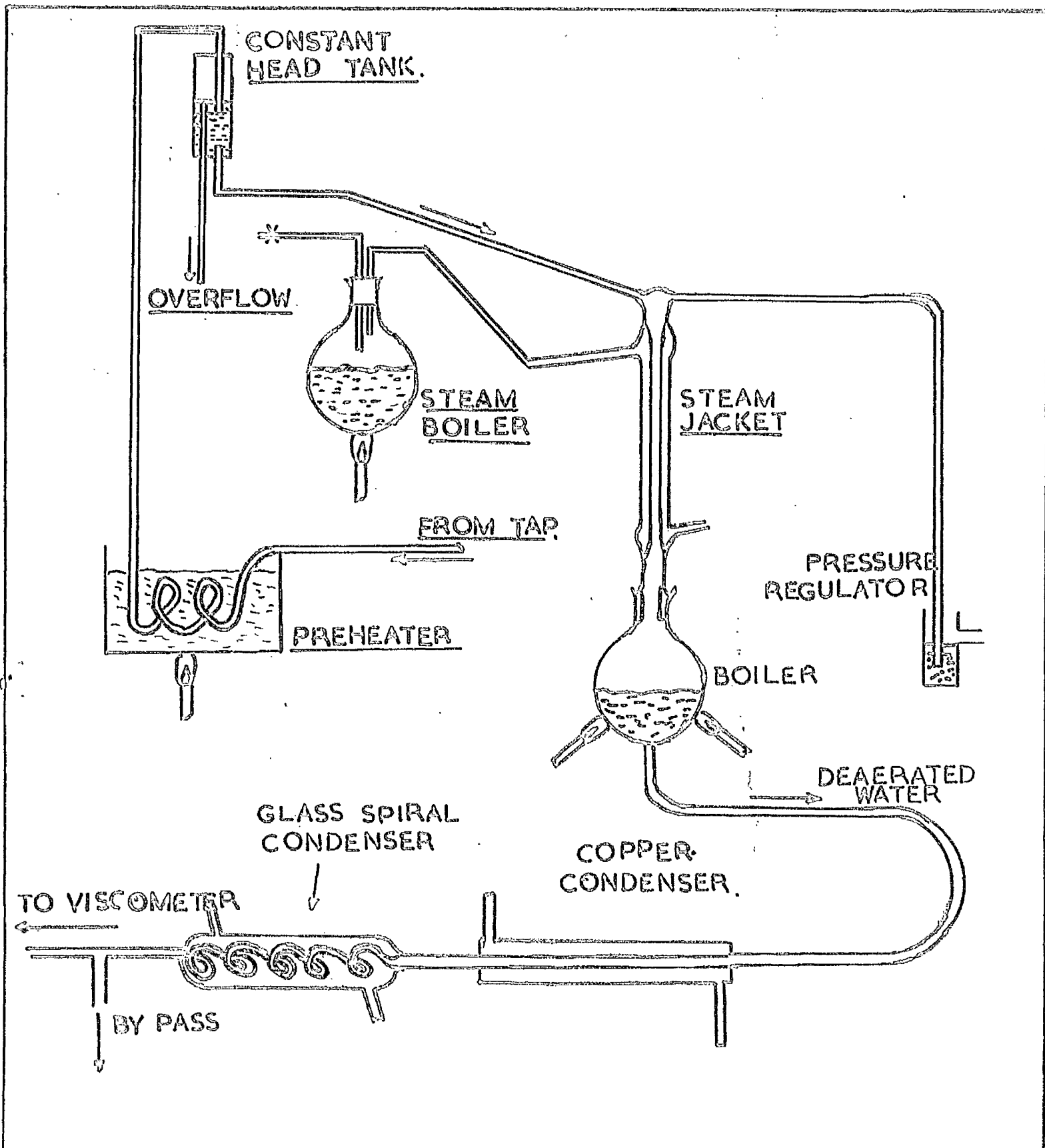
TO VISCOMETER

COPPER CONDENSER.

BY PASS

FIGURE 6.1. DEAERATOR SYSTEM

several reasons, one being the fact that if the temperature of the inlet
water dropped the pressure of the steam and hence the outflow from the
boiler decreased. This, in turn, caused the level of water in the flask
to rise. To compensate for this the gas flow to the bunsen burners had to
be increased. Equally important was the matching of the flows into and
out of the boiler. If, for example, the water flowed out more quickly
than it entered the flask, the steam pressure built up and the outflow
increased further due to the heat input being unchanged.

Thus to maintain a constant flow through the viscometer, the flows
in and out of the deaerator had to be matched, the heat input to the
boiler corresponding to a certain flow had to be found and the temperature
of the incoming water had to be constant.

The fluctuations from the deaerator, in addition to giving an error
in the flow rate, caused the manometer fluid levels to rise and fall thus
causing a random error in the pressure drop measurements. The values
found with r_2/r_1 ratios of $7/3$ and $5/3$ have been ignored since, as pointed
out in Chapter V, some doubt exists at these small radii as to the accuracy
of the available solutions.

The measurements were made in three ranges:- (a) 0 ^{o}C to 10 ^{o}C;
(b) 20 ^{o}C to 50 ^{o}C and (c) 40 ^{o}C to 90 ^{o}C.

For the first range the viscometer was immersed in a bath of ice and
an accuracy of at least 1.5% was expected since the apparatus was the same
as that described in Chapter V.

Some typical values from 1 ^{o}C to 10 ^{o}C are given in Table 1. Only
a few measurements over the temperature range have been calculated although

many more measurements were made since the reproducibility of the measurements was good and only an indication of the accuracy to which the instrument is capable need be given here.

No.	Q cm³/s	T°C	Viscosity for Different r_2/r_1 Ratios cp.				
			17/3	15/3	13/3	11/3	9/3
1	0.9151	0.99	1.7357	1.7363	1.7263	1.7259	1.7335
2	1.5737	3.01	1.6290	1.6292	1.6215	1.6235	1.6292
3	1.6334	4.44	1.5327	1.5317	1.5245	1.5226	1.5315
4	1.7991	5.93	1.4760	1.4755	1.4696	1.4705	1.4765
5	2.1327	6.60	1.4766	1.4745	1.4659	1.4603	1.4689
6	3.0587	7.39	1.4310	1.4291	1.4217	1.4190	1.4210
7	4.3369	8.02	1.3723	1.3711	1.3659	1.3650	1.3718
8	4.9534	10.26	1.2850	1.2844	1.2792	1.2794	1.2871

The plate separation for the measurements given in Table 1 was 0.0098" and as can be seen from the table the agreement between the viscosity values for different r_2/r_1 ratios at the same flow rate is good, the maximum difference being approximately 0.6% except determination No. 5 where the maximum difference is 1.1%.

Throughout the tests the flow was kept within the Reynolds number at which it was thought radial flow ceased to exist.

A deviation plot of the results is given in figure 6.2. Since insufficient points were calculated to fit a curve to the results it was felt that the best method of showing the deviation of the results from the values of other experimenters was to take a recognised set of values as a criterion. In this case, the values of Bingham and Jackson (38) found by correlation of existing data at the time havebeen used. The
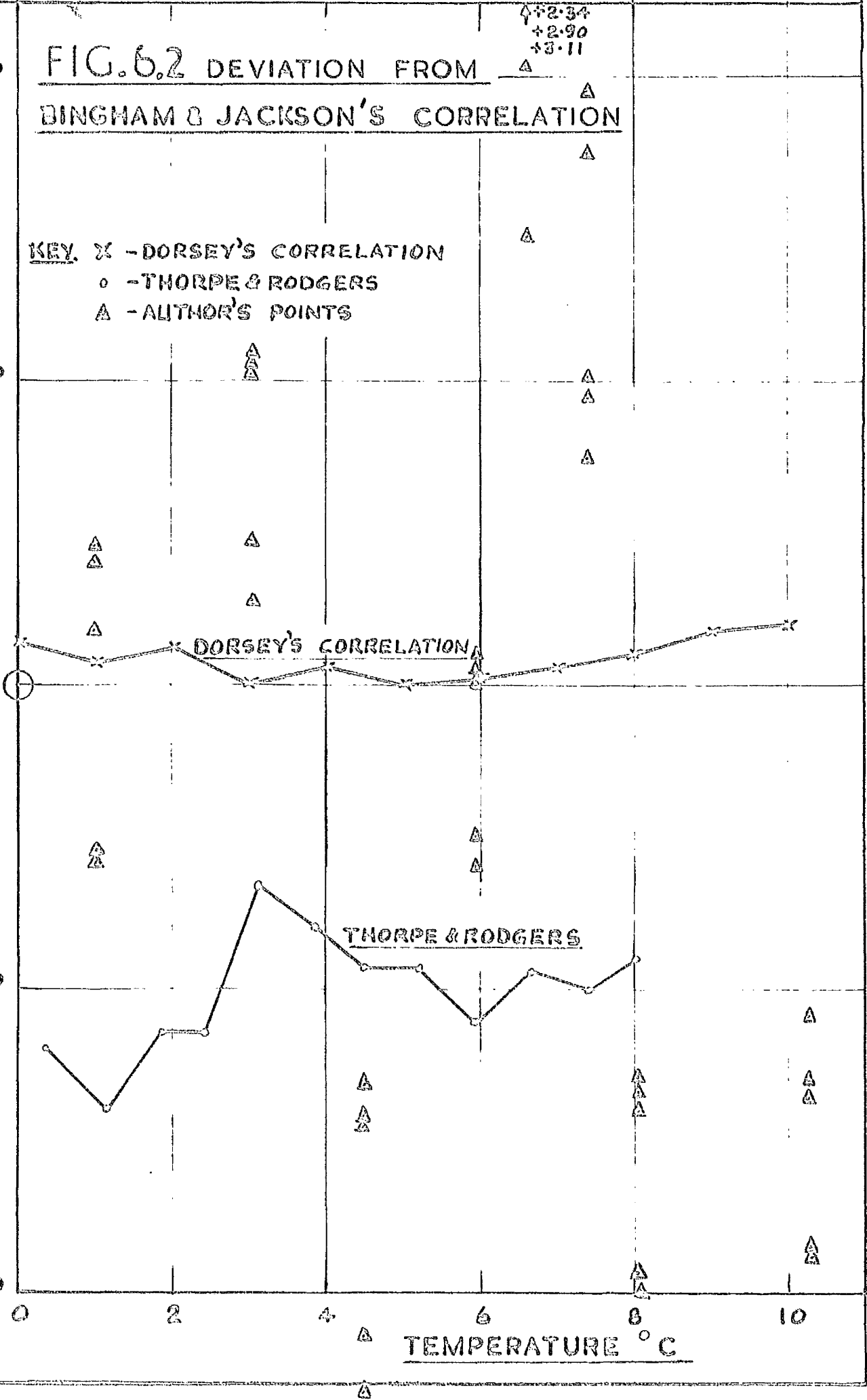
FIG.6.2 DEVIATION FROM BINGHAM & JACKSON'S CORRELATION

KEY. X — DORSEY'S CORRELATION
   o — THORPE & RODGERS
     △ — AUTHOR'S POINTS

correlation of Dorsey (40) and the experimental values of Thorpe and Rodgers (44), who used a capillary viscometer, have been added as further comparisons. The deviation plot shows the experimental values scattered uniformly about Bingham and Jackson's correlation and although individual points vary by as much as $\pm$ 1.5%, the majority of the experimental values have a variation of less than $\div$ 1%. However an accuracy of no better than $\div$ 1.5% is claimed for these results which is what was expected from the preliminary work described in the previous chapter.

As mentioned above, for measurements greater than 20 $^{\circ}$C a deaerator had to be fitted to ensure that no air bubbles were formed and lodged themselves between the plates thus disrupting the flow. Initially, much difficulty was encountered in matching the flow of water into and out of the deaerator and controlling the heat input. However when it was felt that the flow could be maintained reasonably constant a series of observations were made and experiments were conducted over the temperature range 20 $^{\circ}$C to 50 $^{\circ}$C. The plate separation was 0.0098" and the values obtained with the r_2/r_1 ratios of $7/3$ and $5/3$ were again ignored.

A plot of the actual values of viscosity against temperature has not been given as it was felt that deviation plots gave a better indication of the accuracy of the apparatus. Over the range of temperature 20 $^{\circ}$C to 50 $^{\circ}$C 550 determinations of the viscosity have been made and fitted to a curve by the method of least squares. A deviation plot of the experimental points from the computed curve is given in figure 6.3, the curve fitted to the data being of the form

$$\eta = \eta_0 + aT + bT^2 \quad \text{where T is in } ^{\circ}C$$

$$\ldots\ldots(1)$$

FIG.6.3 DEVIATION OF EXPERIMENTAL POINTS FROM COMPUTED LINE IN RANGE 20°C TO 50°C

STANDARD DEVIATION
159 μ POISE
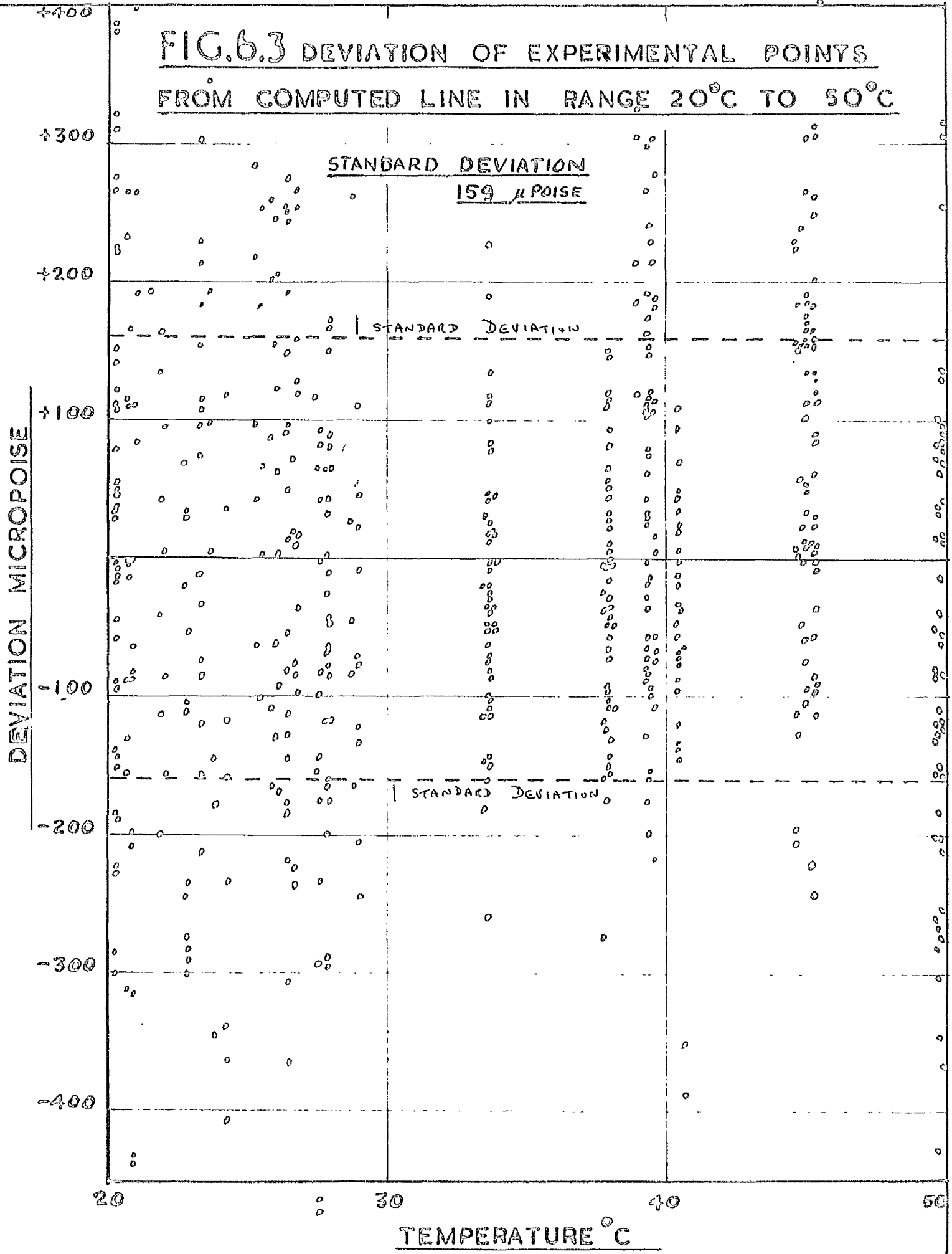
Although viscosity is usually related to temperature by an exponential in $\frac{1}{T}$, where T is the absolute temperature, the simpler power series of equation (1) was used here since only a small range in temperature was being covered.

A cubic equation was found unnecessary as it reduced the standard deviation by an insignificant amount. The computer programme was so constructed as to reject points having a deviation greater than three times the standard deviation before recalculating the constants η_o, a, and b. This is regarded, statistically, as standard practice and, of the 550 points, 10 points were eliminated in this manner. The final coefficients were η_o = 16134.99 micropoise, a = -357.3511, and b = 2.930598.
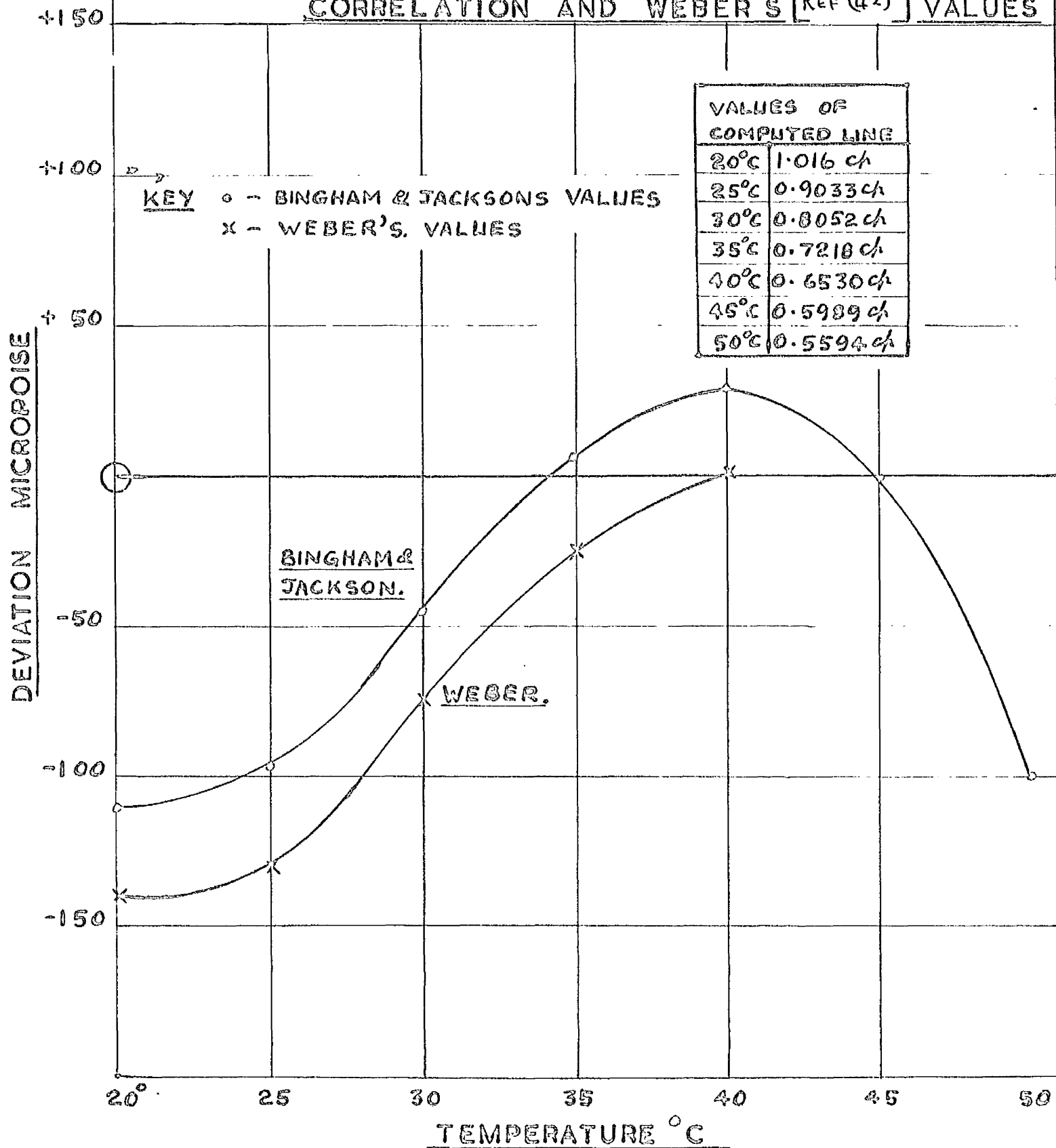
The standard deviation for this curve was 159 micropoise which resulted in a deviation of $\pm$ 1.5% at 20 ^{o}C rising to $\pm$ 3% at 50 ^{o}C. This relatively large standard deviation reflects the large scatter of the points to be expected with the fluctuations present in the flow.

A plot of the deviation of the computed curve from Bingham and Jackson's correlation and Weber's experimental values is given in Figure 6.4. It shows that at 20 ^{o}C the computed line is 1.4% higher than Weber's line and, at 50 ^{o}C, 1.8% greater than the correlation of Bingham and Jackson, whereas between 30 ^{o}C and 45 ^{o}C the discrepancy is only about 0.5%.

This suggests that while the reproducibility of the measurements is not very good due to the reasons given above, the fact that so many points have been used in the computation of the line has resulted in an equation which agrees to within at least 1.5% of recognised values.

The measurement of the viscosity of water over the range 40 ^{o}C to

FIG. 6.4 DEVIATION OF AUTHOR'S EQ'N OF VISCOSITY TEMPERATURE IN RANGE 20°C TO 50°C AGAINST BINGHAM & JACKSON'S [REF. (38)] CORRELATION AND WEBER'S [REF (42)] VALUES

KEY   o — BINGHAM & JACKSONS VALUES
       x — WEBER'S. VALUES

VALUES OF COMPUTED LINE	
20°C	1·016 ch
25°C	0·9033 ch
30°C	0·8052 ch
35°C	0·7218 ch
40°C	0·6530 ch
45°C	0·5989 ch
50°C	0·5594 ch

BINGHAM & JACKSON.

WEBER.

DEVIATION MICROPOISE

TEMPERATURE °C

90 ^{O}C was done in a similar manner as the range 20 ^{O}C to 50 ^{O}C but with the plate separation set at 0.00965". The reason for separating the plates before continuing the measurements was that no undue corrosion of the surfaces had occurred.

Consequently the data covering the 20 ^{O}C to 50 ^{O}C range and 40 ^{O}C to 90 ^{O}C range has been treated separately so that any systematic error that occurred with remeasuring the plate separation could be detected.

The curve fitted to the data was similar to equation (1), 510 measurements having been used of which 17 were rejected as being greater than three standard deviations. The values of η_{o}, a and b were respectively 11806.02 micropoise, -- 165.0686 and 0.7568252.

The standard deviation for this curve was 53 micropoise, which gives a deviation of 0.9% at 40 ^{O}C increasing to 1.8% at 90 ^{O}C. Comparing the scatter of the points with that for the range 20 ^{O}C to 50 ^{O}C it can be seen that the percentage error has been reduced almost by a factor of two, showing that the precision of the measurements had been improved over the range. This can be explained by the fact that since the measurements over the 20 ^{O}C to 50 ^{O}C temperature range were made first, the author had become more adept at controlling the flows and heat input to the deaerator when covering the 40 ^{O}C to 90 ^{O}C range, thus reducing the flow fluctuations.

A deviation plot of the experimental points from the computed curve is given in figure 6.5, and the points appear to be well distributed about the computed line.

In figure 6.6 is shown a deviation of the computed curve from the correlation of Bingham and Jackson and the experimental values of Thorpe and Rodgers. It can be seen that at 40 ^{O}C the deviation of the viscosity

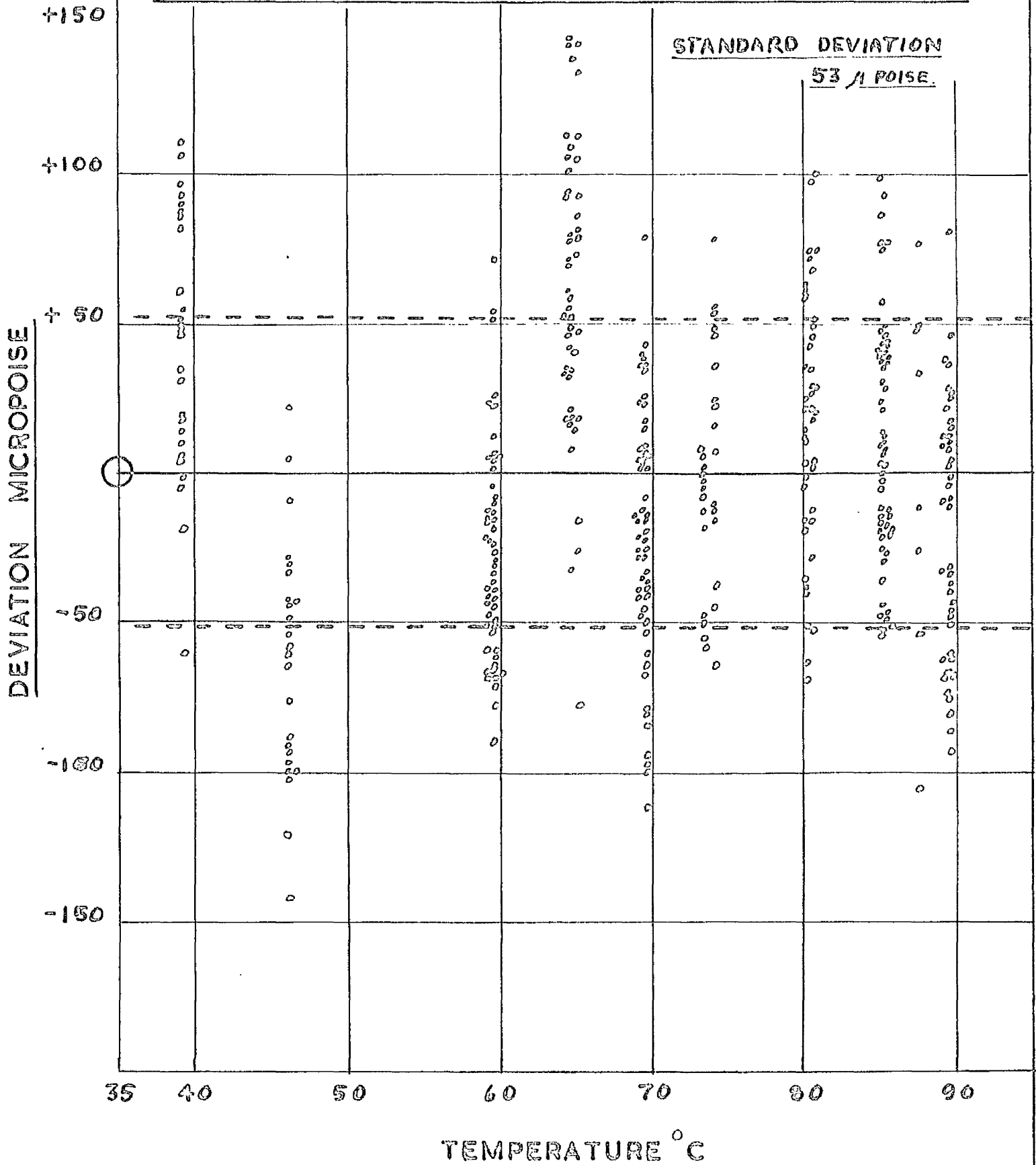FIG. 6.5 DEVIATION OF EXPERIMENTAL POINTS FROM COMPUTED LINE IN RANGE 40°C TO 90°C
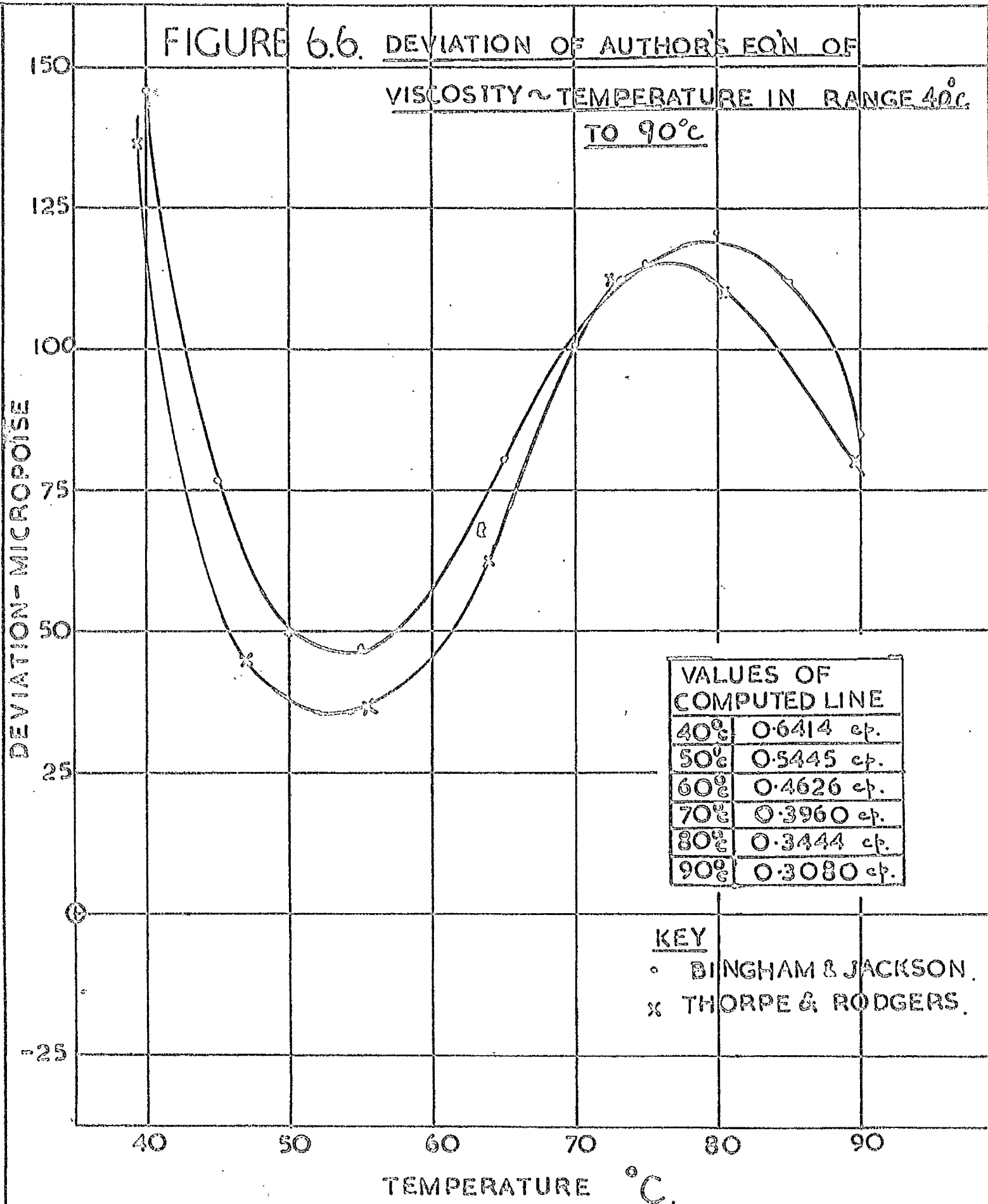
FIGURE 6.6. DEVIATION OF AUTHOR'S EQ'N OF VISCOSITY ~ TEMPERATURE IN RANGE 40°C TO 90°C

VALUES OF COMPUTED LINE	
40°C	0·6414 cp.
50°C	0·5445 cp.
60°C	0·4626 cp.
70°C	0·3960 cp.
80°C	0·3444 cp.
90°C	0·3080 cp.

KEY
∘ BINGHAM & JACKSON.
× THORPE & RODGERS.

DEVIATION~MICROPOISE

TEMPERATURE °C.

values of the computed line and Bingham and Jackson's line is - 2.2% and approximately - 3% between 70 $^{\circ}$C and 90 $^{\circ}$C. In the range 45 $^{\circ}$C to 65 $^{\circ}$C the error is approximately - 1.5%. The deviation from Thorpe and Rodger's values is slightly less. On comparing the equations of the computed lines for the ranges 20 $^{\circ}$C to 50 $^{\circ}$C and 40 $^{\circ}$C to 90 $^{\circ}$C it can be seen that the constants η_o, a and b differ. Since the equations overlap in the range 40 $^{\circ}$C to 50 $^{\circ}$C both lines should give the same values of viscosity at 40 $^{\circ}$C and 50 $^{\circ}$C. This was found to be not so. For the line covering the range 20 $^{\circ}$C to 50 $^{\circ}$C the viscosity values at 40 $^{\circ}$C and 50 $^{\circ}$C are 0.6530 cp and 0.5594 cp while the equation for the range 40 $^{\circ}$C to 90 $^{\circ}$C gives corresponding values of 0.6414 cp and 0.5445 cp, a difference of some 2.5%.

The reason for this discrepancy is probably due to the fact that between the two series of measurements the plates were separated and the gap remeasured. This could give rise to a systematic error and explain why the results over the range 40 $^{\circ}$C to 90 $^{\circ}$C are consistently lower than those of the other set of experiments.

It would appear that although the results are of a preliminary nature, a radial flow viscometer has possibilities of producing accurate measurements, and with the open type viscometer used here, the author feels that more accurate measurements could have been obtained if the control of the flow from the deaerator had been improved. Although the flow fluctuations were of the order of 1%, it was felt that the main error arose from reading the heights of the fluid in the manometer limbs.

The plate separation was of the order of 0.010" in the temperature range 20 $^{\circ}$C to 90 $^{\circ}$C in order to produce a reasonable pressure drop and

thus reduce the pressure-drop measurement error. Thus, with this small gap, to improve absolute measurements a highly accurate means of measuring the gap must be devised. Of course, the instrument could be calibrated although a secondary instrument is not as attractive as an absolute viscometer. The results over the range 0 ^{o}C to 10 ^{o}C probably give a better indication of the accuracy of the instrument as the flow could be maintained constant to better than 0.5% and, as can be seen from Table 1, the reproducibility between individual points is good while the agreement with recognised values ranges from 1% to 1.5%.

CHAPTER VII

High Pressure Radial Flow Viscometer

It has been shown that the expressions obtained for the radial flow between plates have accounted accurately enough with respect to the inertia term to warrant design of a high pressure viscometer using the method of radial flow between parallel plates. The choice of such a method has been largely influenced by the need for viscosity measurements using a method other than the conventional capillary method.

By necessity rather than choice it was decided to make the viscometer a secondary apparatus i.e. to obtain the apparatus constants c_1, c_2 and c_3 given in equations (8) and (9) of Appendix (7) using a fluid of known viscosity for calibration purposes -- the fluid in this case being water at 25 ^{o}C since its viscosity is known to at least 1 part in 500. The main reason for this step was that the method of the open-circuit flow system adopted for preliminary experiments could only be applied with difficulty at high pressures. In addition, the time required to develop such an apparatus for high pressure application would probably be too long. By far the greatest difficulty envisaged by the author would have been the development of a high pressure manometer to read differences of pressure of a few centimetres of water.

The apparatus designed to measure the viscosity of water and other fluids using the method of radial flow between parallel plates is shown in fig (7.1). The viscometer is a modified Rankine viscometer and was designed for the maximum operating conditions of 500 ^{o}C and 1000 atmospheres pressure. Many of the features are similar to the viscometers of
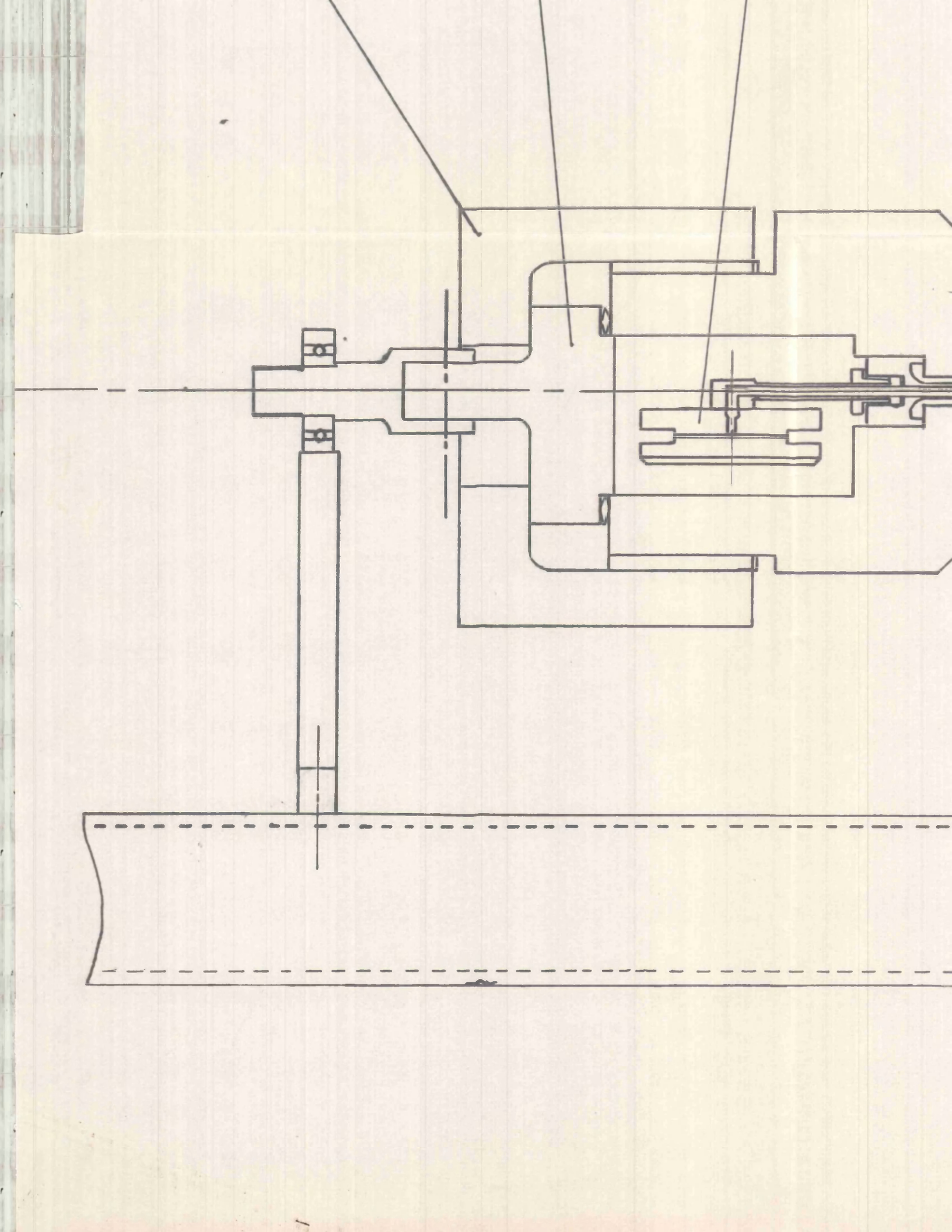
Kjelland-Fosterud (8), Whitelaw (9) and Ray (10) except that they used capillaries instead of the plates used by the author, and the method of timing the fall of the pellet is done by a light system instead of platinum contact wires.

Briefly, the viscometer operates thus:-

A mercury pellet of known mass is made to fall vertically down a glass drop tube by gravity and consequently displaces water through the connecting tubes and parallel plates. The water flows back into the drop tube from the plates through annuli formed by the horizontal connecting tube and its outer pressure tube and that formed by the glass drop-tube and its outer pressure tube. The rate of flow is found by timing the fall of the mercury pellet over a known length of the glass tube.

The adoption of the closed circuit Rankine viscometer adds further disadvantages as compared with the open-circuit viscometer, such as was used for preliminary plate tests.

A semi-empirical term has to be used in the working equation to account for excess pressure at the inlet to the plates arising from the kinetic energy and Couette corrections. In the open circuit viscometer this additional complication can be avoided by placing the pressure tappings far enough downstream. In addition a correction has to be made for the loss in pressure in the drop-tube due to the surface tension drag on the mercury pellet.

Detailed Description of the Viscometer

1) Pressure Bodies   As stated above the viscometer is designed for 1000 atmospheres pressure and 500 $^{\circ}C$. The material used is Firth-Vickers

Staybrite F.D.P. steel and the viscometer is designed with 8 tons/in^2 as a safe working stress. The first consideration was the design of a pressure vessel to house the small parallel plates. Since the whole apparatus is turned on its bearings through 180° and back again, it was decided to put the tube connecting the plates and the glass drop-tube on the axis of revolution as opposed to the flat plates. This resulted in the circular recess of the main pressure vessel being eccentric to the axis of rotation as shown in fig (7.1).

The $2\frac{3}{8}$" diameter recess that houses the plates is sealed off by a plug which transmits the load to a large nut screwed $5\frac{1}{8}$" B.S.F. This plug has on the non-pressure side a shaft which although being eccentric to the plug itself lies on the axis of rotation and is connected by a cotter pin to another shaft which runs in a roller bearing.

2) <u>Bearings</u>   The weight of the two pressure vessels and drop tube is approximately 200 lbs and this is supported by three bearings. The two outer bearings are roller bearings, the central one being a simple V-bearing. The latter takes about 50% of the total load while the load on the ball races is well within their carrying capacity. The whole is supported on a framework made of 3" x $1\frac{1}{2}$" channel.

The reason for not directly supporting the vessel that houses the parallel plates is to allow sufficient space for it to be submerged in a temperature controlled bath which will operate up to approximately 95 $^\circ$C using water.

3) <u>Seals</u>   The largest and, consequently, most difficult seal in

the viscometer is that between the plug and pressure vessel housing the plates.

Initially this seal was effected by an annealed copper ring of cross-section as shown in fig (7.2(a)). It was found to leak at approximately 100 atmospheres pressure and it was felt that this was due to scratches on the face rather than the straining of the nut holding the faces together. It was concluded that this was not a very satisfactory type of seal and was replaced by an O-ring seal strengthened by a backing ring. This seal, fig (7.2(b)), has been successfully tested to 500 atmospheres, the limit of this seal being the strength of the mild steel backing ring.

The author feels that an adequate seal would be a Ruston and Graylock type shown in fig(7.2(c)) which seals on the unsupported area principle. However, this latter method would only be used if necessary as the other methods required no machining of the pressure vessel.

Most of the other seals are the conventional lens ring type, an exception being at the flange connecting the two main vessels where there is an O-ring seal. For smaller diameters - i.e. $\frac{5}{8}$" diameter and less - the type of seal used is mainly the spherical face on conical seat and for the pressure piping, standard Ermeto couplings are used.

All the seals used in the internal system, i.e. the flat plates and connecting tubes, are either rubber or copper washers since only small differences of pressure are experienced.
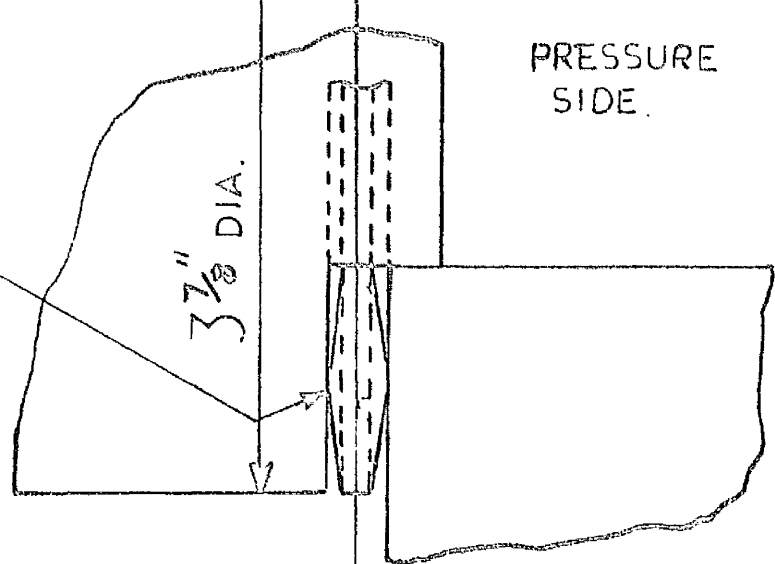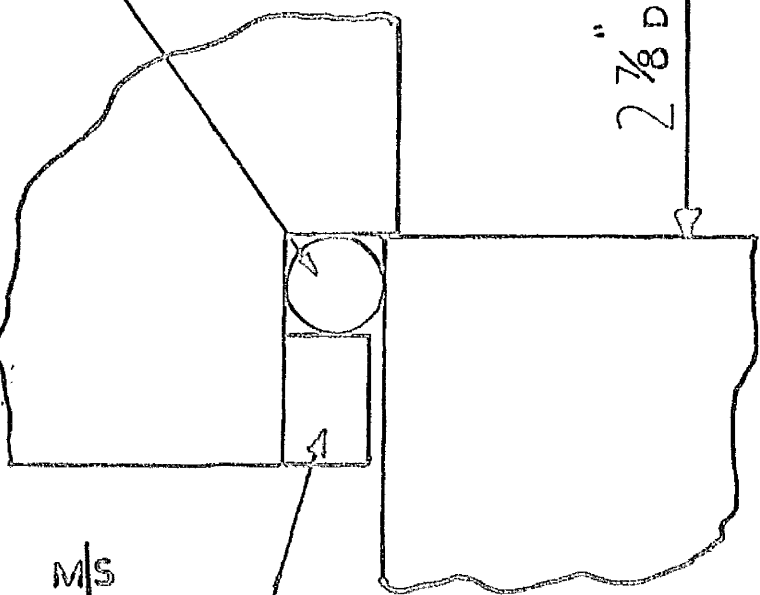
COPPER RING.

3 7/8" DIA.

PRESSURE SIDE.

FIG. 7.2.(a).

O RING

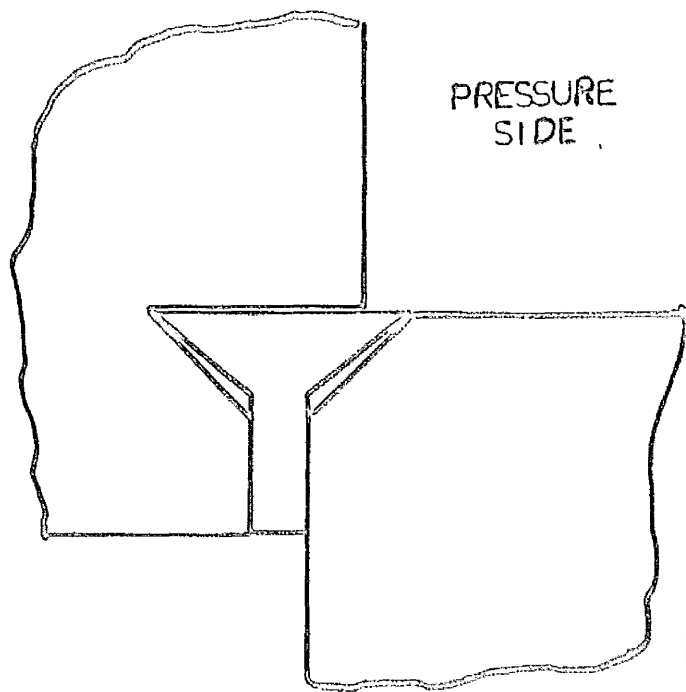2 7/8" DIA.

M/S BACKING RING.

PRESSURE SIDE.

FIG. 7.2 (b).

FIG. 7.2 (c).

108

4) <u>Plates</u>   The plates are made of stainless steel and the experimental faces are 2" diameter with a central hole of $^3/32$" diameter. These faces were lapped flat mechanically to approximately 0.00002" as checked with an optical flat. The separation of the plates required for the measurements is of the order of 0.002" to 0.004" and to obtain this separation to the necessary accuracy was beyond the limits of the measuring equipment available.

It was felt therefore, that all that could be done was to ensure that the plates were as parallel as possible and determine the plate separation by calibration. This was attempted by screwing the bottom plate 0 B.A. at three positions 120° to each other and correspondingly in the top plate screwing $\frac{1}{4}$" B.S.F. three moveable collars which could be locked to the top plate, see fig (7.3). In this way by making a bolt screwed 0 B.A. at one end and $\frac{1}{4}$" B.S.F. at the other the top plate could be "jacked" off the bottom plate with very fine adjustment since the difference of pitch between 0 B.A. and $\frac{1}{4}$" B.S.F. screws is 0.0009".

The two plates were initially wrung together and using a comparator gauge accurate to 0.00001" zero readings were taken at the three positions around the top plate. By screwing each bolt in turn and noting the change on the comparator gauge the top plate was "jacked" off the bottom plate till the required separation was obtained. It was felt that by this method the gap could be estimated at best to 0.00003", this also being the limit to which parallelism of the plates could be measured.

As stated above, a more accurate value of the plate separation could be obtained by calibration with water. However this will only
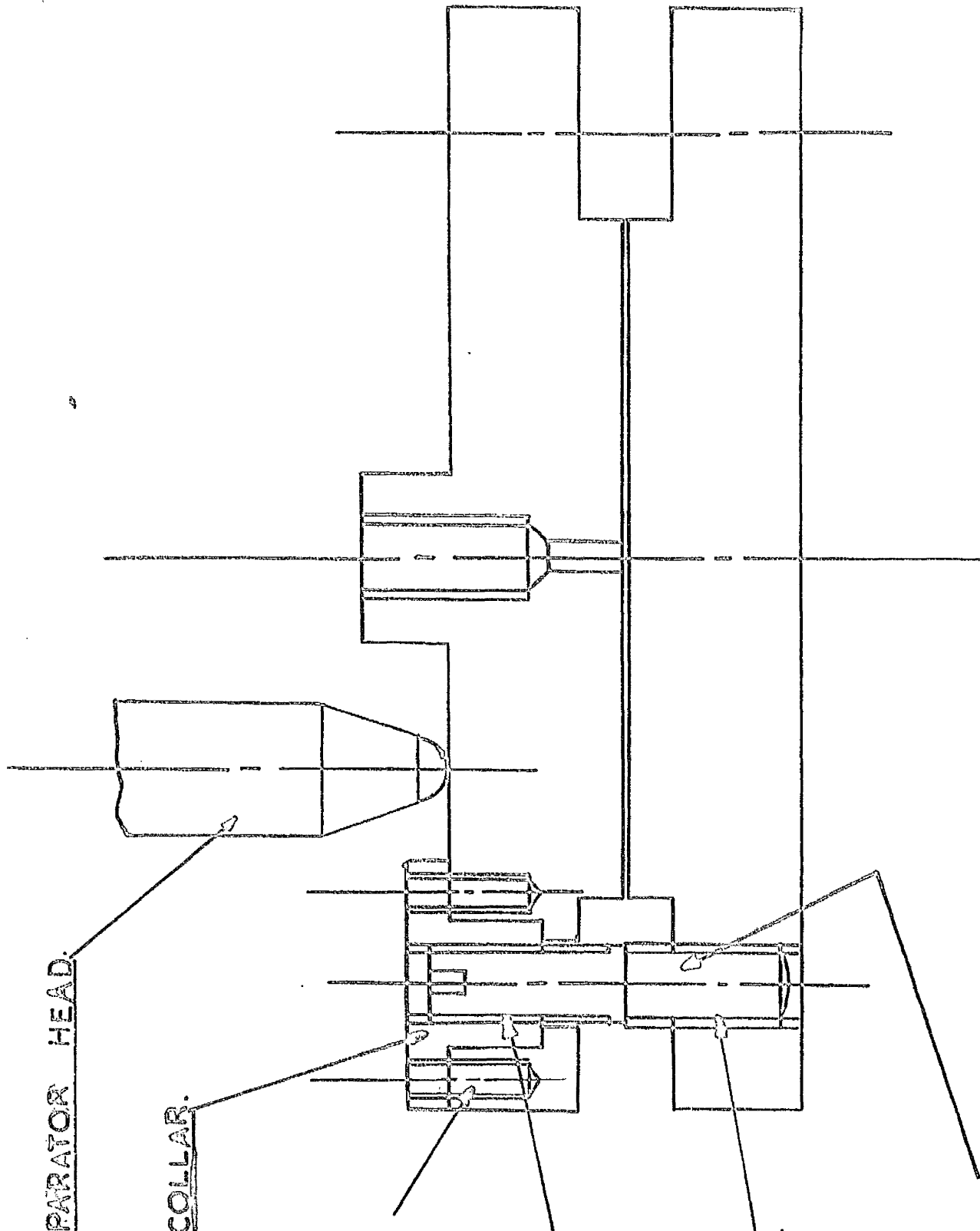
COMPARATOR HEAD.

COLLAR.

LOCKING SCREWS.

$\frac{5}{16}$ B.S.F. THREAD.

O.B.A. THREAD.

ADJUSTING SCREW.

S/S PLATES. FIG 73.

give a mean value of the separation of the plates consistent with
the accuracy to which they are set up relative to each other. This
undoubtedly could be one of the main sources of error since any mis-
alignment could cause the flow to deviate from pure radial flow.

Initially it was decided to proceed with measurements and from
an analysis of the data obtained, estimate the error incurred by the
non-parallelism of the plates and then, if necessary, develop a more
accurate method of measuring the plate separation. Any deflection
of the plates from the horizontal due to the bending of the connecting
tube was found to be negligible.

5) _Rotating Seal_   Due to the rotation of the apparatus a rotating
seal is necessary in the line connecting the pressure raising apparatus
to the viscometer. Although it is difficult to obtain commercially
such a seal to operate at such high pressures, the fact that the seal
will be used only for an occasional half-turn simplifies the problem.
A diagram of the seal used is shown in fig (7.4) which is similar in
design to that used by Whitelaw and Ray. It has been successfully
tested to 500 atmospheres pressure.

6) _Pressure Raising Equipment_   The pressure in the viscometer is
raised by a manually operated "Enerpac" oil pump, which consequently
necessitates an oil-water interface. To avoid possible contamination
of the water the interface is made with a rubber diaphragm (see fig (7.5))
with a lip which fits into the recess of a brass ring, the seal being
affected by bolting the brass ring to a face in the pressure vessel
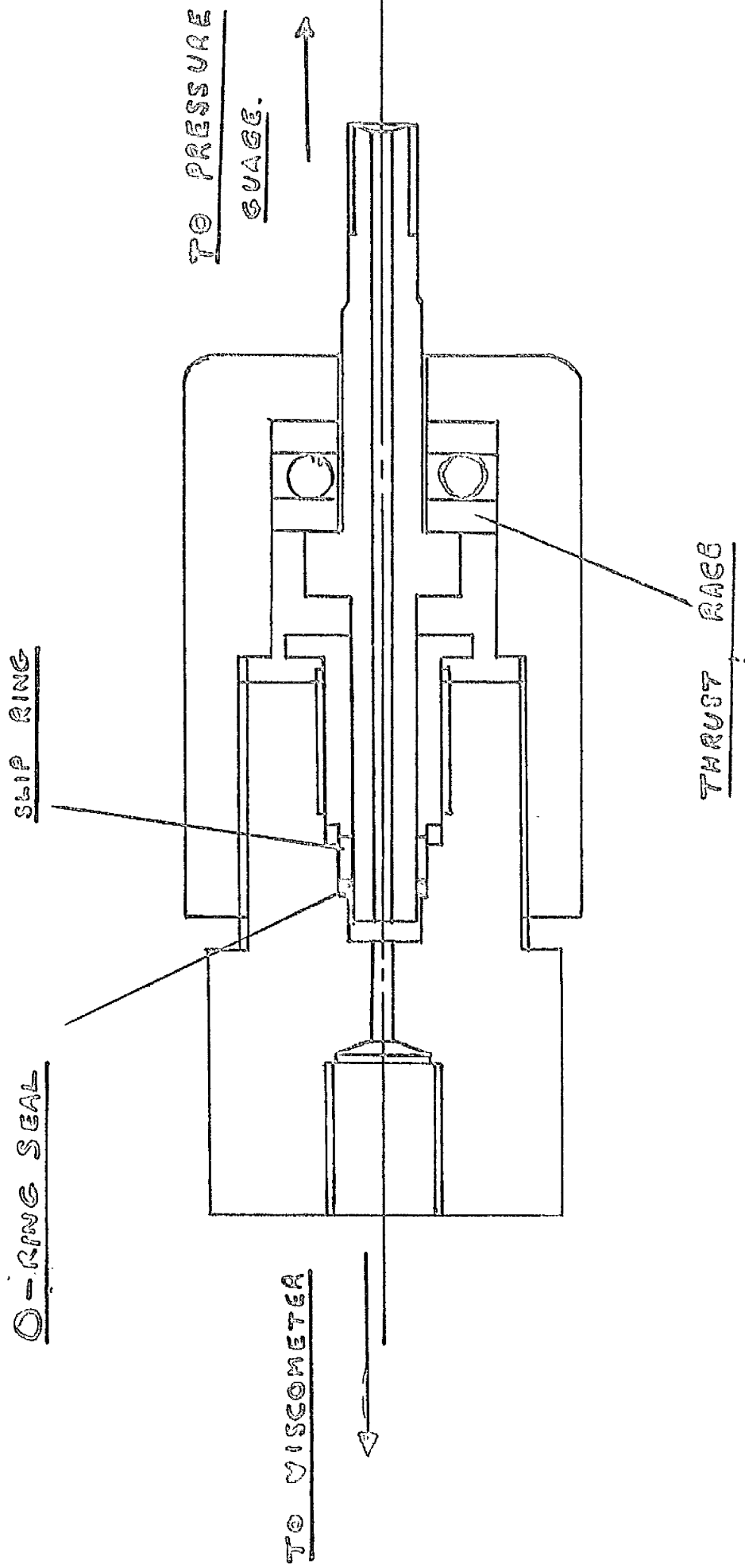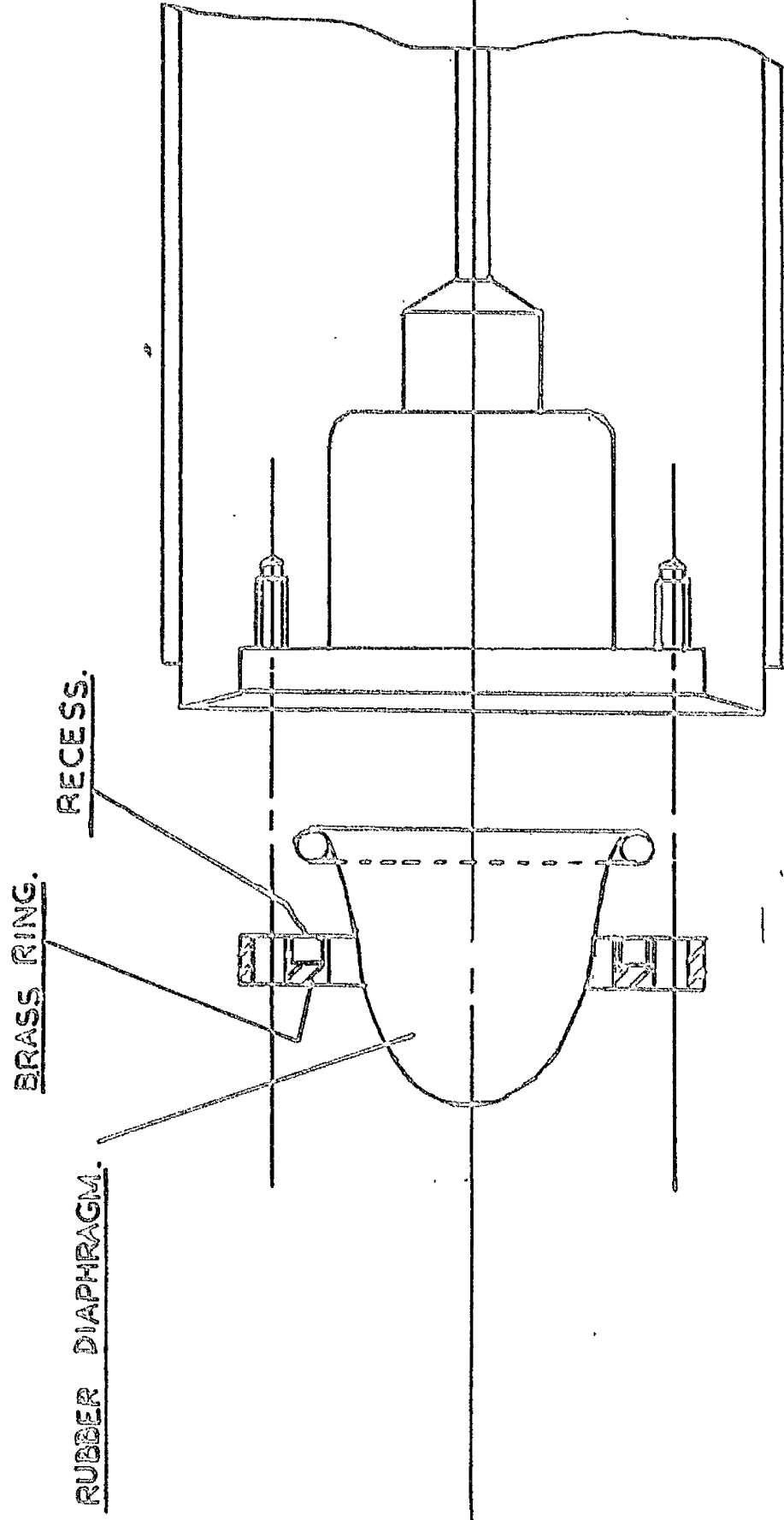and thus compressing the rubber lip which is circular in section. This

TO PRESSURE GUAGE.

SLIP RING

THRUST RACE

O-RING SEAL

TO VISCOMETER

FIG. 7.4. ROTATING SEAL.

RUBBER DIAPHRAGM.

BRASS RING.

RECESS.

SEPARATING DIAPHRAGM. FIG. 75.

interface has been tested successfully to 1500 atmospheres. Since the test fluid is water there is little fear of straining the diaphragm due to the incompressibility of water.

7) Drop-Tube   It was found by Rankine (45) that the limit of the glass drop-tube bore down which the mercury pellet falls without breaking up was approximately 3.5 mm. The bore of the drop-tube was thus limited to 2 mm and was made of precision "Veridia" bore-tubing.

The Rankine viscometers of Whitelaw and Ray used platinum contact wires threaded through small holes bored in the wall of the tube and sealed in position to time the fall of the pellet. This was done at three positions along the length of the tube, at each position there being two contact wires diametrically opposite each other but about 1 cm apart so that as the mercury pellet passed it completed the circuit and hence activated a timer.

This method had several disadvantages:-

(a)   It was found that no matter how much care was taken, the boring of the holes in the wall of the tube tended to distort the bore. In addition, the platinum contact wires, although barely protruding into the bore of the drop-tube, tended to stop the pellet so that its motion became jerky thus destroying its uniform velocity.

(b)   It was also found that, although made of platinum, the contact wire soon became dirty and thus affected the electrical contact between wires and pellet.

The method adopted by the author of timing the fall of the pellet is

an optical method which, although more difficult in setting up, dispenses with the disadvantages listed above since the pellet has an uninterrupted fall down the tube. The method is shown in fig (7.6).

The light is piped from a bulb source by $\frac{1}{8}''$ diameter Perspex rods, the other ends of which are brought up against small $45°$ angle prisms of leg size $^3/16''$ and silvered on the hypoteneuse. These prisms are cemented with Canada balsam onto flats ground on the walls of the tube so that the light from the Perspex rods is bent across the bore of the tube and by another prism and Perspex rod diametrically opposite to a photocell. Thus, as the pellet passes it cuts off the light to the photocell, the pulse so generated activating an electronic counter accurate to 1 part in 10^5.

Some difficulty arose in making the flats on the tube. However this was overcome by fixing the glass tube in a suitable jig clamped to the table of a grinding machine and by using a diamond impregnated wheel and feeding it down as the table moved backwards and forward a flat was produced. Care was taken on turning the tube to ensure the other flat was diametrically opposite. A good finish was not necessary as the Canada balsam used to cement the prisms filled in any small scratches or grooves.

The smallness of the tube – 2 mm bore x 6 mm o.d. – resulted in some of the light from the prisms being bent around instead of across the bore. This was easily overcome by masking the faces of the prisms.

The drop-tube which was approximately 75 cm long had three pairs
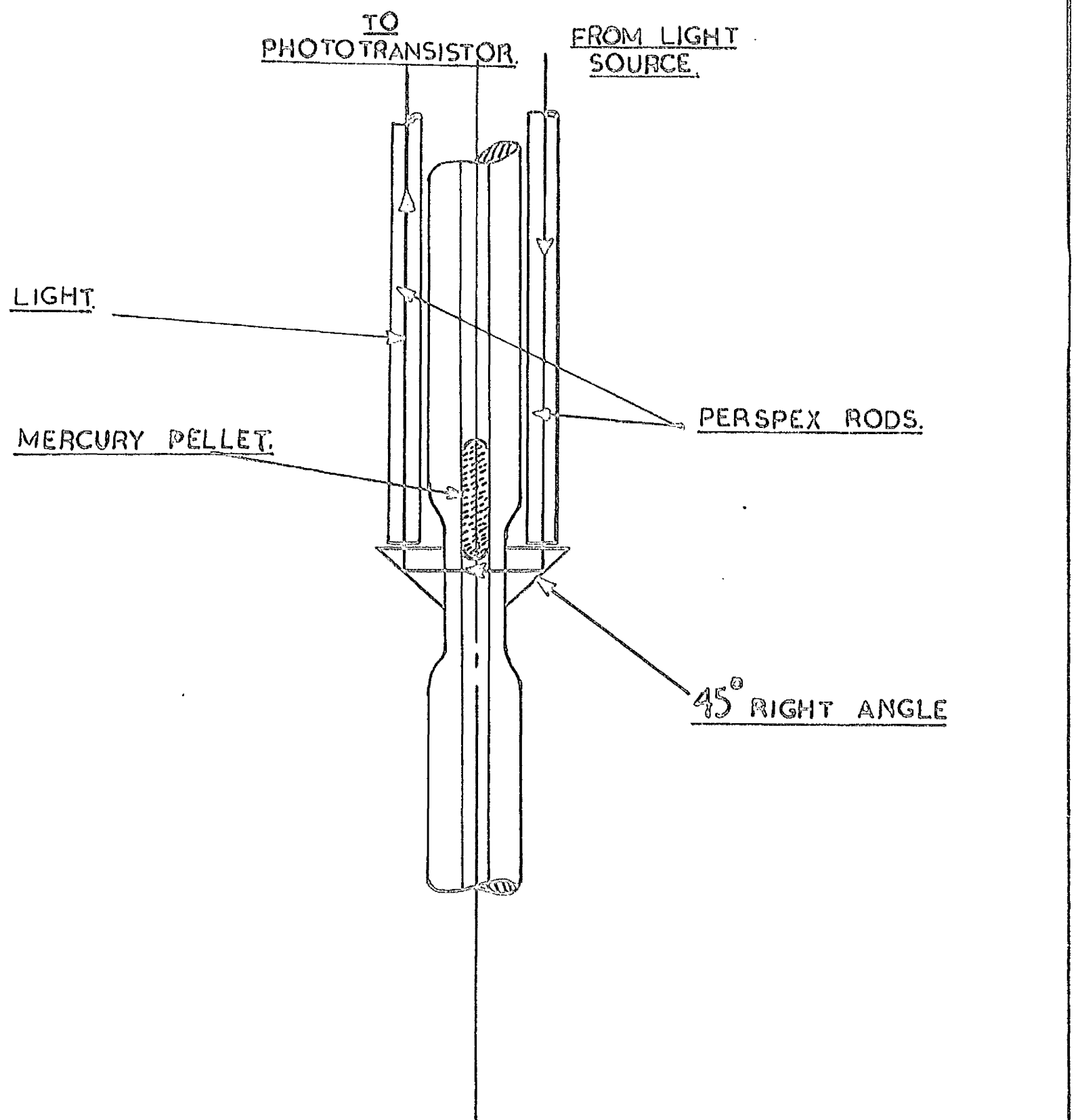
TO
PHOTOTRANSISTOR.

FROM LIGHT
SOURCE.

LIGHT.

MERCURY PELLET.

PERSPEX RODS.

45° RIGHT ANGLE

LIGHT SYSTEM. FIG. 76.

of flats, each set at 120 ° to each other to facilitate leading out the six Perspex rods, and approximately 15 cm apart. The electronic circuit was designed so that as the pellet cut off the light at the top position the pulse produced by the phototransistor did not restart the timer. This was started by the pellet passing the mid-position and stopped at the bottom position. On reversing the tube so that the pellet fell back up the tube, the pulse produced by the bottom phototransistor was ignored, the middle one started the timer and the top one stopped it.

Thus the photocell at the mid-position always started the timer while only every second pulse from the photocells at the end positions stopped the counter.

A diagram of the electronic circuit is shown in fig (7.7). The reason for giving the pellet a 15 cm length of fall prior to timing its rate of fall is to ensure that it has attained a uniform velocity.

The exact length over which the pellet is timed is not required as this is accounted for by the calibration.

A set of timings obtained in the development stages to ascertain the reproducibility of the arrangement is given in Appendix (6). For the high pressure application a method had to be devised whereby the light could be piped in and out of the pressure vessel. It was decided to make the windows of Perspex as shown in fig (7.8) a window of similar design having been successfully tested to 2000 atmospheres pressure.

The drop-tube was fitted with mercury traps at both ends. The trap at the top was simply a piece of glass tube closed at one end
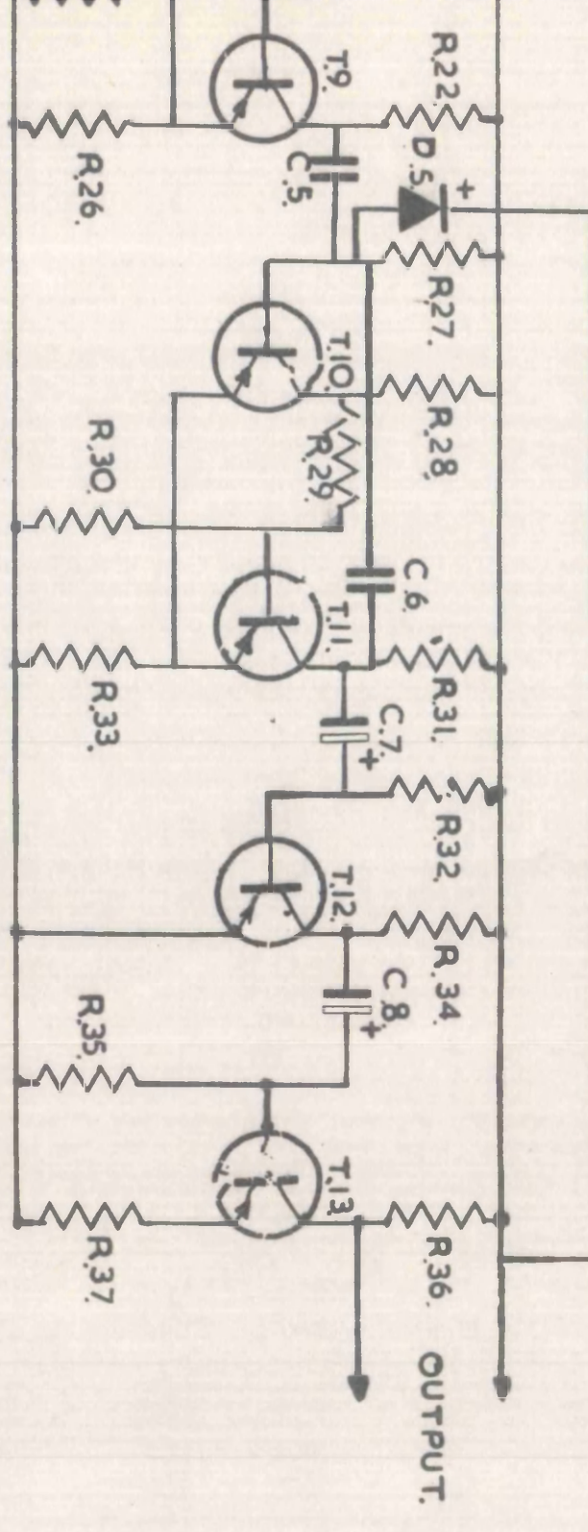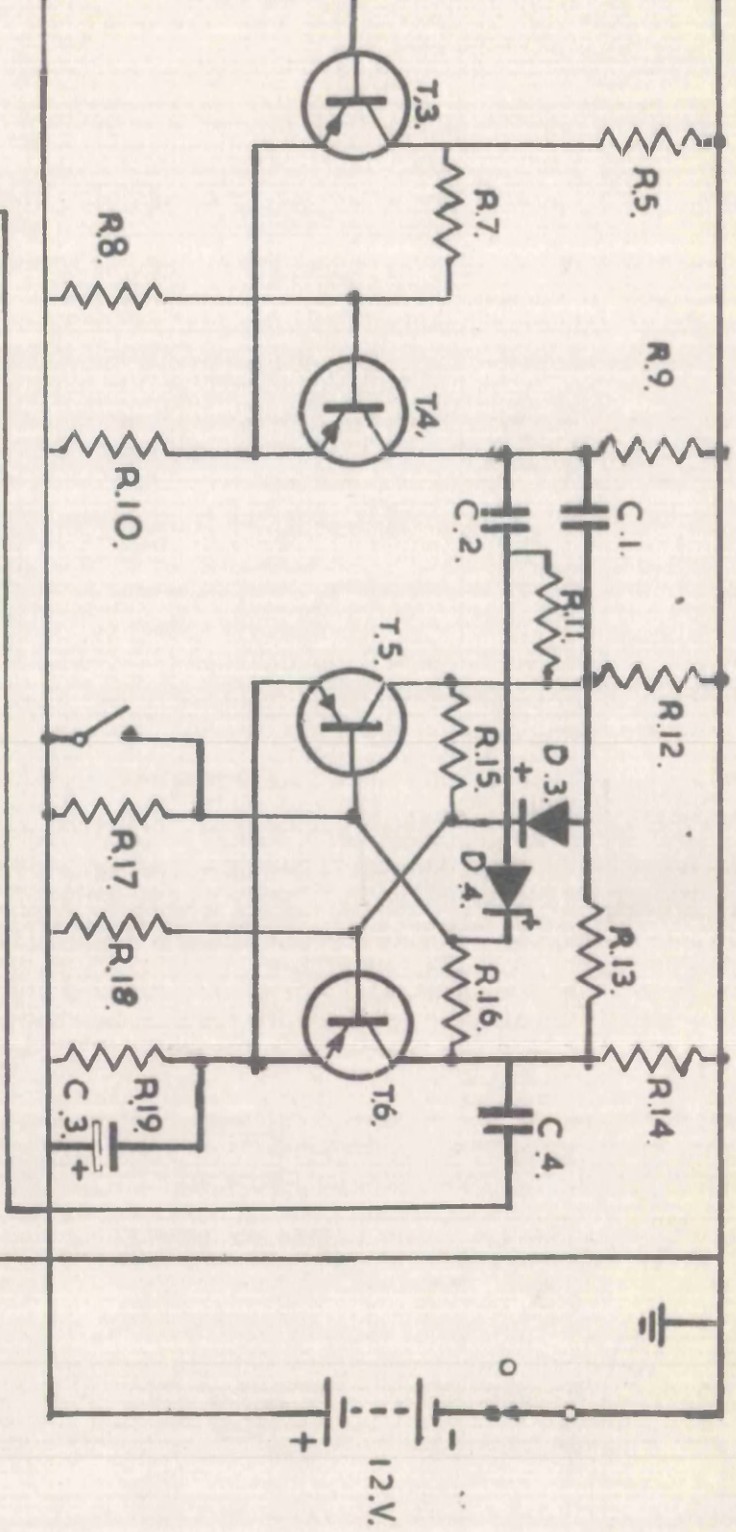
CIRCUIT FIG 7.7

RESISTORS		TRANSISTORS	
R.1.	33kΩ	T.1.	OC.71.
R.2.	1·2k	T.2.	OC.71.
R.3.	33k	T.3.	OC.71.
R.4.	100k	T.4.	OC.71.
R.5.	4·7k	T.5.	OC.71.
R.6.	1·2k	T.6.	OC.71.
R.7.	18k	T.7.	OC.71.
R.8.	6·8k	T.8.	OC.71.
R.9.	4·7k	T.9.	OC.71.
R.10.	680	T.10.	OC.202
R.11.	10k	T.11.	OC.202
R.12.	4·7k	T.12.	OC.200
R.13.	10k	T.13.	OC.200
R.14.	4·7k	**DIODES**	
R.15.	8·2k	D.1.	OA.91.
R.16.	8·2k	D.2.	OA.91.
R.17.	3·3k	D.3.	OA.91.
R.18.	3·3k	D.4.	OA.91.
R.19.	430	D.5.	OA.91.
R.20.	33k	**CAPACITORS**	
R.21.	4·7k	C.1.	4700pf
R.22.	4·7k	C.2.	4700pf
R.23.	1·2k	C.3.	50µf
R.24.	6·8k	C.4.	4700pf
R.25.	18k	C.5.	4700pf
R.26.	680	C.6.	0·1µf
R.27.	33k	C.7.	25µf
R.28.	1·5k	C.8.	2·5µf
R.29.	18k	**PHOTO-TRANSISTOR**	
R.30.	6·8k	P.1.	ORP.60.
R.31.	1·5k	P.2.	ORP.60.
R.32.	18k	P.3.	ORP.60.
R.33.	150		
R.34.	22k		
R.35.	10k		
R.36.	4·7k		
R.37.	4·7k		

KEY.

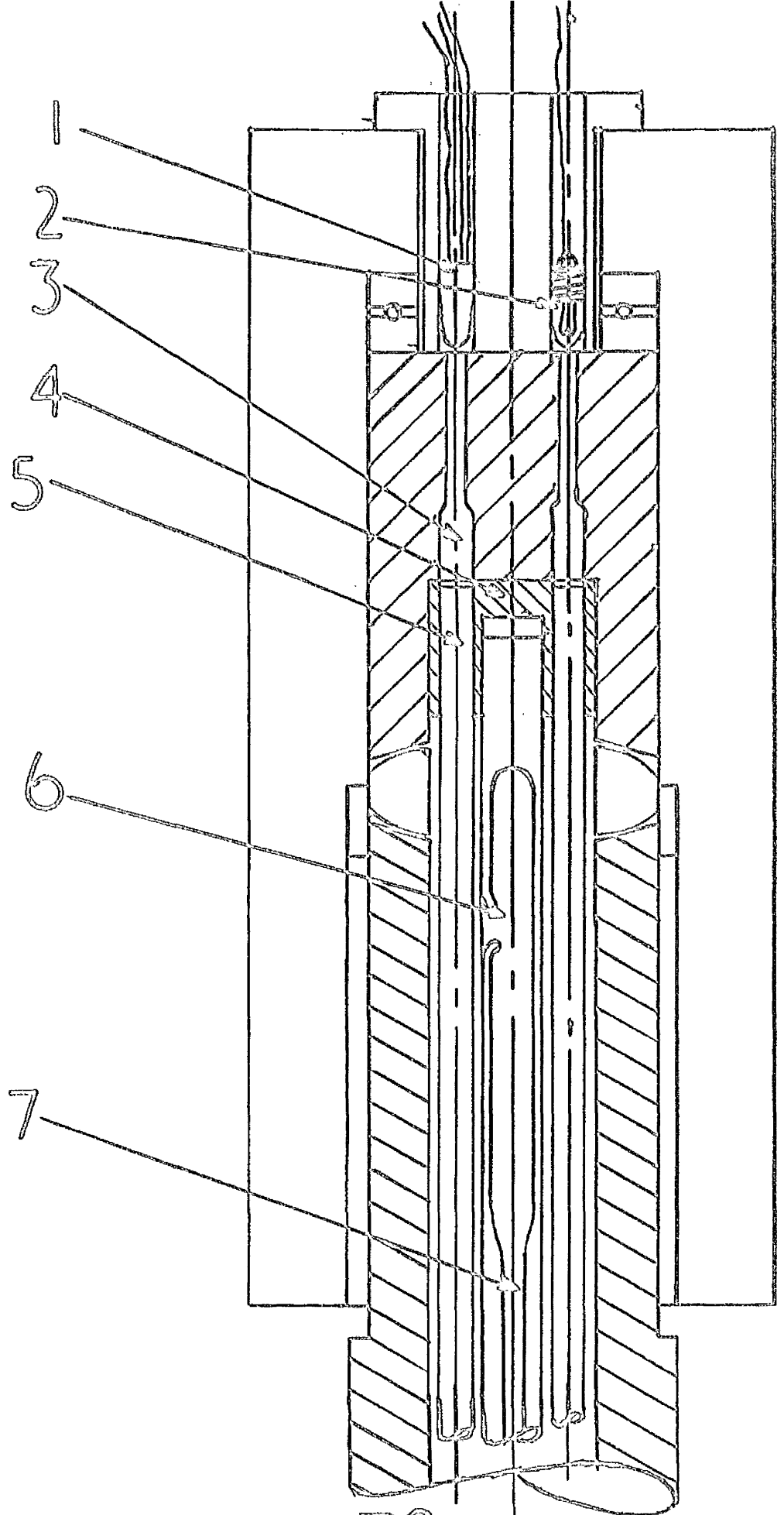PHOTOTRANSISTOR. 1.

LIGHT BULB. 2.

PERSPEX WINDOW. 3.

BRASS HOLDER. 4.

PERSPEX ROD. 5.

MERCURY TRAP. 6.

GLASS DROP TUBE. 7.

TOP-CAP ASSEMBLY. FIG. 7.8.

which was fused onto the drop-tube with a hole blown inwards in the side. The bottom trap was detachable so that it could be used for weighing the mercury pellet.

8) <u>Temperature Measurement</u>   At present no provision has been made for extensively measuring temperatures in the apparatus. However the pressure vessel housing the plates is immersed in a thermostatically controlled copper tank which will enable preliminary tests to be carried out to 95 ^{o}C. A hole has been drilled in the pressure vessel for the insertion of a thermistor which will confirm whether or not the temperature of the fluid under test is the same as the bath.

The pressure tube housing the drop-tube has been jacketed by a copper tube through which passes water pumped from a tank thermostatically controlled to 25 ^{o}C. This system has been tested successfully on the calibration apparatus which initially was unable to give reproducible timings due to its temperature drifting with the room temperature.

9) <u>Working Formula</u>   This is dealt with in Appendix (7).

ACKNOWLEDGEMENTS

BIBLIOGRAPHY

(1) Barr, G. - "Monograph of Viscometry" Oxford U.P. (1931).

(2) Dinsdale, A., and Moore, F. - "Viscosity and its Measurement" The
     Institute of Physics and the Physical Society, 1962.

(3) Kestin, J. - "On the Direct Determination of the Viscosity of Gases
     at High Pressures and Temperatures" Proceedings of the
     Second Biennial Gas Dynamic Symposium, Editors A.B.Cambel
     and J.B. Fern, Northwestern University Press (1958).

(4) Liley, P.E. - "Progress in International Research on Thermodynamic and
     Transport Properties", Academic Press, 1962.

(5) Reynolds, O. - Phil. Trans. Roy. Soc. Vol.174, Part III, p.935, 1883.

(6) Nikuradse, J. - VDI - Forschungsheft, 361, 1933.

(7) Swindells, J.F., Coe, J.R. and Godfrey, T.B. - J. Res. Natn. Bur.
     Stand. 48, R.P.B. 2279 (1952).

(8) Kjelland-Fosterud, E. J. Mech. Eng. Sci. 1, 30 (1959).

(9) Whitelaw, J.H. J. Mech. Eng. Sci. 2, 288 (1960).

(10) Ray, A.K. J. Mech Eng. Sci. 6, 137 (1964).

(11) Timrot, D.L. and Khlopkina, A.V., Teploenergetika 7, 64, 1963.

(12) Kestin, J. and Wang, H.E. - The Viscosity of Five Gases : A Re-evaluation
     Trans. ASME 1958, p.11.

(13) Kestin, J. and Moszynski, J.R. "An instrument for the measurement of the
     viscosity of steam and compressed water". Trans. ASME
     80, (1958) 1009.

(14) Kestin, J. and Wang, H.E. Corrections for the Oscillating Disc
     Viscometer, J. Appl. Mech. 1957, p.187.

(15) Kestin, J. and Richardson, P.D. ASME Paper No.62-WA 172 (1962).

(16) Kestin, J. and Leidenfrost, W. Design and operation of an oscillating body viscometer for gases at high pressures, Brown University Report AF-891/12 1960.

(17) Kearsley, E.A. "An analysis of an absolute torsional pendulum viscometer, Trans. Soc. of Rheology 3 (1959) 69.

(18) Roscoe, R. and Bainbridge, W. Proc. Phys. Soc. 72 (4) 585 (1958).

(19) Wonham, J. "A Rotating Cylinder Viscometer for Measurement at Elevated Temperature and Pressure", Proc. Inst. Mech. Engineers 1965-66, Vol.180, pt.3J.

(20) Taylor, G.I. "Stability of a Viscous Liquid Contained between Two Rotating Cylinders, Phil. Trans.A223 (1923) 289.

(21) Barnett, S.C., Jackson, T.W. and Whitesides, R.H. "An Investigation of the Viscosity of Steam at High Pressures", ASME Paper No.63-WA-240.

(22) Latto, B., Jackson, T.W. and Willbanks, C.E., Hodgson, T.W. and Yen, H.H.Y. Advances in Thermophysical Properties at Extreme Temperatures and Pressures, ASME New York 1965.

(23) Gümbel, H. Z. Techn. Physik 1920, 1, 72.

(24) Schmidt, E. and Mayinger, F. Techn. Hochschule (Munich) Report 1961.

(25) Latto, B. "Viscosity of Steam at Atmospheric Pressure", Int. J. Heat Mass Transfer, Vol.8, pp.689-720, 1965.

(26) Shifrin, A.S. Teploenergetika 6, 22, (1959).

(27) Comolet, R. "Ecoulement d'un fluide entre deux plans parallèles", Publs. scient et tech Ministr. Air 1957 (No.334).

(28) Livesey, J.L. "Inertia effects in Viscous Flows", Int.J. Mech. Sci. 1960, Vol.1, pp.84-88.

(29) Moller, P.S. "Radial Flow without Swirl between Parallel Discs", Aeronaut. Q. 1963 (May).

(30) Jackson, J.D. and Symmons, G.R. "An Investigation of Laminar Radial Flow between two Parallel Discs" - Appl. Sci. Res. Section A, Vol.15.

(31) Hunt, J.B. and Torbe, I. Int. J. Mech. Sci. 4, 503 (1962).

(32) Jackson, J.D. and Symmons, G.R. Int. J. Mech. Sci. 7, pp.239-242 (1965).

(33) Peube, J.L. J. Mécanique, Vol.2, No.4, déc.1963, pp.377-395.

(34) Savage, S.B. Trans. ASME - J. of Applied Mechanics, Dec.1964, pp.594-596.

(35) Moses, J. Ll. Proc. Instn. Mech. Engrs.1965-66, Vol.180, Pt.3J.

(36) Potter, E.C. and Whitehead, G. J. Appl. Chem., 7, Nov., 1957.

(37) Bruges, E.A., Latto, B. and Ray, A.K. Int. J. Heat Mass Transfer, Vol.9, pp.465-480 (1966).

(38) Bingham, E.C. and Jackson, R.F. Bull. Bur. Stds.14, 75 (1918).

(39) Hardy, R.C. and Cottington, R.L., J. Res. Natn. Bur. Stand. 42, 573 (1949).

(40) Dorsey, N.E. Int. Crit. Tables, III, 10, 1929.

(41) Dorsey, N.E. "Properties of Ordinary Water Substance", Reinhold, New York (1940).

(42) Weber, W. Z. Ange^{W}, Phys.7 (2) 96 (1955).

(43) Roscoe, R. and Bainbridge, W. Proc. Phys. Soc.72 (4) 585 (1958).

(44) Thorpe, T.E. and Rodgers, J.W. Phil. Trans. (A), 185, 397-710 (1894).

(45) Rankine, A.O. Proc. Roy. Soc. V83A (1910) p.265.

APPENDIX (1)

In the discussion of a paper by E.C. Bingham on the viscosity of water at 20 °C (1) a radial flow viscometer was proposed by Dr. Mooney.

He suggested this type of viscometer as a possible alternative to a capillary viscometer which has the difficulty of producing a capillary tube of uniform bore. As pointed out by Dr. Mooney glass can be made flat to within a fraction of a wave-length of light and the separation of the plates could be measured by methods of light interference. He maintained that the solution of the equations of motion for such a flow regime could be obtained and in a reply by Dr. Karrer it was pointed out that the apparent viscosity was found to be greater for liquids flowing out than with liquids flowing in.

Although no formulae are given in the reference, it would appear that this discrepancy is due to neglecting the pressure drops due to inertia effects.

REFERENCE:-

(1) Bingham, E.C. J. Rheology, pp.403-423 (1931).

APPENDIX (2)

(a)

Below are given the mathematical steps required to obtain equation (28.21) from (28.20) of the author's paper referred to in Chapter III and bound into the back of this thesis.

Equation (28.20) is written

$$\int_{x}^{\beta} \frac{dx}{\sqrt{(\beta-x)(\nu_1+x)(\nu_2-x)}} = \sqrt{\frac{2}{3}q} \; x \qquad \dots\dots(1)$$

Let
$$(\nu_1+x) = u^2 \qquad \dots\dots(2)$$

$$\therefore \quad \frac{dx}{\sqrt{\nu_1+x}} = 2\,du \qquad \dots\dots(3)$$

Substituting in (1)

$$\therefore \sqrt{\frac{2}{3}q}\; x = 2\int_{\sqrt{\nu_1+x}}^{\sqrt{\nu_1+\beta}} \frac{du}{\sqrt{(\beta+\nu_1-u^2)(\nu_1+\nu_2-u^2)}} \qquad \dots\dots(4)$$

Let
$$u = (\beta+\nu_1)^{\frac{1}{2}}\, \upsilon \qquad \dots\dots(5)$$

Substituting for u in (4)

$$\therefore \sqrt{\frac{2q}{3}}\; x = 2\int_{\sqrt{\frac{\nu_1+x}{\nu_1+\beta}}}^{1} \frac{d\upsilon}{\sqrt{(1-\upsilon^2)(\nu_1+\nu_2-(\beta+\nu_1)\upsilon^2)}} \qquad \dots\dots(6)$$

$$= \frac{2}{\sqrt{\nu_1+\nu_2}} \int_{\sqrt{\frac{\nu_1+x}{\nu_1+\beta}}}^{1} \frac{d\upsilon}{\sqrt{(1-\upsilon^2)\left(1-\left(\frac{\beta+\nu_1}{\nu_1+\nu_2}\right)\upsilon^2\right)}} \qquad \dots\dots(7)$$

$$= \frac{2}{\sqrt{\nu_1+\nu_2}}\left[\int_{0}^{1} \frac{d\upsilon}{\sqrt{(1-\upsilon^2)\left(1-\left(\frac{\beta+\nu_1}{\nu_1+\nu_2}\right)\upsilon^2\right)}} - \int_{0}^{\sqrt{\frac{\nu_1+x}{\nu_1+\beta}}} \frac{d\upsilon}{\sqrt{(1-\upsilon^2)\left(1-\left(\frac{\beta+\nu_1}{\nu_1+\nu_2}\right)\upsilon^2\right)}}\right] \qquad \dots\dots(8)$$

$$\therefore \sqrt{\frac{2q}{3}}\; x \;=\; \frac{2}{\sqrt{\nu_1+\nu_2}}\left[F\!\left(\alpha,\tfrac{\pi}{2}\right)-F(\alpha,\theta)\right] \qquad \ldots\ldots(9)$$

where $\quad \alpha = \operatorname{Sin}^{-1}\sqrt{\dfrac{B+\nu_1}{\nu_1+\nu_2}}\quad$ and $\quad \theta = \operatorname{Sin}^{-1}\sqrt{\dfrac{\nu_1+\chi}{\nu_1+B}}$

Equation (9) is equation (28.21) of the author's paper.

(b)

The following is the mathematics required to obtain equation (28.25) from (28.24).

Equation (28.24) is written

$$\sqrt{\frac{3}{2q}}\;\frac{\sqrt{2}}{\left(3\frac{p}{q}-\tfrac{3}{4}B^2\right)^{1/4}}\int_{0}^{B}\left[F\!\left(\alpha,\tfrac{\pi}{2}\right)-F(\alpha,\theta)\right]d\chi = 1 \qquad \ldots\ldots(10)$$

Now $\operatorname{Sin}\theta = \sqrt{\dfrac{\nu_1+\chi}{\nu_1+B}}\qquad\qquad \therefore\operatorname{Sin}^2\theta = \dfrac{\nu_1+\chi}{\nu_1+B}\qquad \ldots\ldots(11)$

$$\therefore\; 2\operatorname{Sin}\theta\operatorname{Cos}\theta\, d\theta = \frac{1}{\nu_1+B}\,d\chi \qquad \ldots\ldots(12)$$

Substituting for $d\chi$ in (10) and rearranging

$$\int_{\operatorname{Sin}^{-1}\sqrt{\frac{\nu_1}{\nu_1+B}}}^{\frac{\pi}{2}}\left[F\!\left(\alpha,\tfrac{\pi}{2}\right)-F(\alpha,\theta)\right]\operatorname{Sin}\theta\operatorname{Cos}\theta\, d\theta = \frac{\left(3\frac{p}{q}-\tfrac{3}{4}B^2\right)^{1/4}}{2(B+\nu_1)}\sqrt{\frac{q}{3}} \qquad \ldots\ldots(13)$$

$$\frac{1}{2}F\!\left(\alpha,\tfrac{\pi}{2}\right)\left[\operatorname{Sin}^2\theta\right]_{\operatorname{Sin}^{-1}\sqrt{\frac{\nu_1}{\nu_1+B}}}^{\frac{\pi}{2}} - \int_{\operatorname{Sin}^{-1}\sqrt{\frac{\nu_1}{\nu_1+B}}}^{\frac{\pi}{2}}F(\alpha,\theta)\operatorname{Sin}\theta\operatorname{Cos}\theta\, d\theta = \frac{\left(3\frac{p}{q}-\tfrac{3}{4}B^2\right)^{1/4}\sqrt{\frac{q}{3}}}{2(B+\nu_1)} \qquad \ldots\ldots(14)$$

$$\frac{1}{2}F\!\left(\alpha,\tfrac{\pi}{2}\right)\left(1-\frac{\nu_1}{\nu_1+B}\right) - \int_{\operatorname{Sin}^{-1}\sqrt{\frac{\nu_1}{\nu_1+B}}}^{\frac{\pi}{2}}F(\alpha,\theta)\operatorname{Sin}\theta\operatorname{Cos}\theta\, d\theta = \frac{\left(3\frac{p}{q}-\tfrac{3}{4}B^2\right)^{1/4}\sqrt{\frac{q}{3}}}{2(B+\nu_1)} \qquad \ldots\ldots(15)$$

$$\therefore \int_{\operatorname{Sin}^{-1}\sqrt{\frac{\nu_1}{\nu_1+B}}}^{\frac{\pi}{2}}F(\alpha,\theta)\operatorname{Sin}\theta\operatorname{Cos}\theta\, d\theta = \frac{1}{2(B+\nu_1)}\left[F\!\left(\alpha,\tfrac{\pi}{2}\right)B - \sqrt{\frac{q}{3}}\left(\frac{3p}{q}-\frac{3B^2}{4}\right)^{1/4}\right] \qquad \ldots\ldots(16)$$

where $F(\alpha, \theta) = \displaystyle\int_0^\theta \frac{d\psi}{\sqrt{\left(1 - \left(\frac{\nu_1 + B}{\nu_1 + \nu_2}\right) \sin^2\psi\right)}}$

and $\qquad \psi = \sin\sqrt{\dfrac{\nu_1 + x}{\nu_1 + B}}$

$$\qquad\qquad\qquad\qquad\qquad\qquad\qquad \cdots\cdots(17)$$

Taking L.H.S. of equation (16)

$$\int_{\sin^{-1}\sqrt{\frac{\nu_1}{\nu_1 + B}}}^{\pi/2} F(\alpha, \theta) \sin\theta \cos\theta \, d\theta = \int_\phi^{\pi/2} \sin\theta \cos\theta \left\{ \int_0^\theta \frac{d\psi}{\sqrt{\left(1 - \left(\frac{\nu_1 + B}{\nu_1 + \nu_2}\right)\sin^2\psi\right)}} \right\} d\theta$$

$$\qquad\qquad\qquad\qquad\qquad\qquad\qquad \cdots\cdots(18)$$

where $\sin^2\phi = \dfrac{\nu_1}{\nu_1 + B}$

Integrating by parts

$$\int_\phi^{\pi/2} \sin\theta \cos\theta \left\{ \int_0^\theta \frac{d\psi}{\sqrt{1 - \left(\frac{\nu_1 + B}{\nu_1 + \nu_2}\right)\sin^2\psi}} \right\} d\theta = \left[\frac{1}{2}\sin^2\theta \int_0^\theta \frac{d\psi}{\sqrt{1 - \left(\frac{\nu_1 + B}{\nu_1 + \nu_2}\right)\sin^2\psi}} \right]_\phi^{\pi/2}$$

$$\qquad\qquad\qquad\qquad - \frac{1}{2}\int_\phi^{\pi/2} \frac{\sin^2\theta}{\sqrt{1 - \left(\frac{\nu_1 + B}{\nu_1 + \nu_2}\right)\sin^2\theta}} \, d\theta$$

$$\qquad\qquad\qquad\qquad\qquad\qquad\qquad \cdots\cdots(19)$$

since $\sin\theta = \sin\psi = \sqrt{\dfrac{\nu_1 + x}{\nu_1 + \nu_2}}$

R.H.S. of Eq^n (19) $= \dfrac{1}{2} F\left(\alpha, \frac{\pi}{2}\right) - \dfrac{1}{2}\sin^2\phi \, F(\alpha, \phi)$

$$\qquad\qquad\qquad\qquad\qquad\qquad\qquad \cdots\cdots(20)$$

$$+ \frac{1}{2\left(\frac{\nu_1 + B}{\nu_1 + \nu_2}\right)} \int_\phi^{\pi/2} \frac{\left(1 - \left(\frac{\nu_1 + B}{\nu_1 + \nu_2}\right)\sin^2\theta\right)}{\sqrt{\left(1 - \left(\frac{\nu_1 + B}{\nu_1 + \nu_2}\right)\sin^2\theta\right)}} \, d\theta - \frac{1}{2\left(\frac{\nu_1 + B}{\nu_1 + \nu_2}\right)} \int_\phi^{\pi/2} \frac{d\theta}{\sqrt{\left(1 - \left(\frac{\nu_1 + B}{\nu_1 + \nu_2}\right)\sin^2\theta\right)}}$$

$$= \frac{1}{2} F\left(\alpha, \frac{\pi}{2}\right) - \frac{1}{2}\sin^2\phi \, F(\alpha, \phi) + \frac{1}{2\left(\frac{\nu_1 + B}{\nu_1 + \nu_2}\right)} \left[E\left(\alpha, \frac{\pi}{2}\right) - E(\alpha, \phi) \right]$$

$$\qquad\qquad\qquad\qquad\qquad\qquad\qquad \cdots\cdots(21)$$

$$- \frac{1}{2\left(\frac{\nu_1 + B}{\nu_1 + \nu_2}\right)} \left[F\left(\alpha, \frac{\pi}{2}\right) - F(\alpha, \phi) \right]$$

From equation (16)

$$\frac{1}{2} F\left(\alpha, \frac{\pi}{2}\right) - \frac{1}{2}\sin^2\phi \, F(\alpha, \phi) + \frac{1}{2\left(\frac{\nu_1 + B}{\nu_1 + \nu_2}\right)} \left[E\left(\alpha, \frac{\pi}{2}\right) - E(\alpha, \phi) \right]$$

$$- \frac{1}{2\frac{\nu_1 + B}{\nu_1 + \nu_2}} \left[F\left(\alpha, \frac{\pi}{2}\right) - F(\alpha, \phi) \right] = \frac{1}{2(B + \nu_1)} \left[B \, F\left(\alpha, \frac{\pi}{2}\right) - \sqrt{\frac{2}{L}}\left(\frac{3p}{L} - \frac{3}{4}B^2\right)\frac{1}{4} \right]$$

$$\qquad\qquad\qquad\qquad\qquad\qquad\qquad \cdots\cdots(22)$$

where $\sin^2 \phi = \dfrac{\nu_1}{\nu_1 + \beta}$

$$\therefore -\sqrt{\frac{2}{3}}\left(\frac{3p}{2} - \frac{3}{4}\beta^2\right)^{1/4} = \left(\nu_1 + \nu_2\right)\left[E\left(\alpha, \frac{\pi}{2}\right) - E(\alpha, \phi)\right] - \nu_2\left[F\left(\alpha, \frac{\pi}{2}\right) - F(\alpha, \phi)\right]$$

.....(23)

Since $\left(\nu_1 + \nu_2\right) = 2\left(\frac{3p}{2} - \frac{3}{4}\beta^2\right)^{1/2}$

$$\frac{\sqrt{\frac{2}{3}}}{2\left(\frac{3p}{2} - \frac{3}{4}\beta^2\right)^{1/4}} = \left(1 - \frac{\nu_1}{\nu_1 + \nu_2}\right)\left[F\left(\alpha, \frac{\pi}{2}\right) - F\left(\alpha, \sin^{-1}\sqrt{\frac{\nu_1}{\beta + \nu_1}}\right)\right]$$

$$- \left[E\left(\alpha, \frac{\pi}{2}\right) - E\left(\alpha, \sin^{-1}\sqrt{\frac{\nu_1}{\beta + \nu_1}}\right)\right]$$

.....(24)

which is equation (28.25) of the paper.

```
begin procedure AITKENROOT(r,x,y,eps);
    value eps;
    real array x,y;
    real eps; integer r;
    begin integer i;
        x[0]:= 1;
        if x[r]=0 then x[0]:= 0
        else if r=1 then
        begin y[2]:= y[1]+y[0];
            r:= 2
        end
        else if r=2 and sign(x[2])= sign(x[1]) then
        begin x[1]:= x[2];
            y[1]:= y[2];
            y[2]:= y[1]+y[0]
        end
        else
        begin for i:= 1 step 1 until r-1 do
            y[r]:= (y[i]×x[r]-y[r]×x[i])/(x[r]-x[i]);
            if abs(y[r]-y[r-1])<eps then x[0]:= 0
            else
            begin y[r+1]:= y[r];
                r:= r+1
            end
        end;
    end AITKENROOT;
```

```
real procedure SIN(m);

value m; real m;

begin integer i; real term,sum,mm,j;

        sum:=term:=m; mm:=m↑2;

        for i:=1,i+1 while term>10-8 do

        begin j:=2.0×i;

                term:=term×(j-1.0)↑2/(j×(j+1.0))×mm;

                sum:=sum+term;

        end;

        SIN:=sum;

end SIN;

procedure EF(a,y,E,F);

value a,y; real a,y,E,F;

begin integer j,r,h,s;

        real k,Y,f,term,KE,KF,ff,sumE,sumF,noE,noF,A,l,y1;

        k:=sin(a); Y:=sin(y); y1:=1.5707963268;

        f:=term:=KE:=KF:=1.0;

        for j:=1,j+1 while f>310-4 do

        begin r:=2×j;

                term:=(r-1)×term/r;

                f:=term×k↑j;

                ff:=f↑2;

                KE:=KE-ff/(r-1);

                KF:=KF+ff;

        end;
```

```
sumE:=sumF:=k↑2×0.25;

f:=noE:=noF:=0.5;

for j:=2,j+1 while f>₁₀-7 do

begin r:=2×j;

        noE:=noE×(r-3)/r;

        noF:=noF×(r-1)/r;

        term:=1.0/r;  A:=0.0;

        for h:=j step -1 until 2 do

        begin s:=2×h-2;

                A:=A+Y↑s×term;

                term:=term×(s+1)/s;

        end;

        A:=A+term;

        l:=k↑r;

        f:=noF×A×l;

        sumE:=sumE+noE×A×l;

        sumF:=sumF+f;

end;

Y:=Y×cos(y);

E:=KE×(y1-y)-Y×sumE;

F:=KF×(y1-y)+Y×sumF;

end EF;
```

```
integer fa,fb,fc,fd,n,i,N,j,s;

real g,pi,k,h,r1,D,ro,Q,q,ma,dro,K,dh,b,f,gg,m,p,E,F,mu;

array r,d,a,B,R[0:20];

fa:=format([d.dddddsss]);  fb:=format([ndddd.ddsss]);

fc:=format([ndd.dddddsss]);  fd:=format([nd.dddddsss]);

g:=981.6;  pi:=3.1415926536;

k:=32.0×pi↑2;

open(20);  open(70);

writetext(70,[[4s]M[10s]RO[9s]DP[10s]Q[11s]B[11s]q[11s]MU[c]]);

n:=read(20);

h:=read(20);  r1:=read(20);

for i:=1 step 1 until n do

begin D:=r[i]:=read(20);

        d[i]:=D/r1;

        a[i]:=h/D;

end;

N:=read(20);

for j:=1 step 1 until N do

begin ro:=read(20);  Q:=read(20);  dro:=read(20)×g;

        ma:=Q×ro;

        write(70,fa,ma);  write(70,fa,ro);

        K:=k×ro×dro/ma↑2;

        for i:=1 step 1 until n do

        begin dh:=read(20);

                if i≠1 then space(70,22);

                write(70,fb,dro×dh);
```

```
        ·D:=d[i]↑2-1.0;

        Q:=K×a[i]↑2×dh×r[i]↑4/D;

        write(70,fc,Q);

        B[0]:=0.05; B[1]:=1.4; s:=1;

L:      b:=B[s]×0.5;

        f:=sqrt(3.0×(Q-b↑2));

        gg:=(f-b-1.0)/(2.0×f);

        m:=sqrt((3.0×b+f)/(2.0×f));

        p:=sqrt((b+f)/(3.0×b+f));

        EF(SIN(m),SIN(p),E,F);

        R[s]:=gg-E/F;

        AITKENROOT(s,R,B,10-3);

        if R[0]≠0.0 then goto L;

END:    write(70,fd,B[s]);

        q:=3.0×F↑2/f;

        write(70,fd,q);

        mu:=D×a[i]×ma/(8.0×pi×q×r[i]×ln(d[i]));

        write(70,fd,mu);

        newline(70,1);

    end;

    newline(70,1);

end;

close(20); close(70);

end→
```

APPENDIX (4)

Calibration of Thermistor with a Nominal Resistance

of 300 ohms at 25 °C

Given below is a calibration chart for the thermistor between 10 °C and 70 °C. The values of resistance are in ohms and have been calculated from the equation given in Chapter IV.

°C	10	20	30	40	50	60	70
0	511.06	350.84	246.32	176.50	128.81	95.56	71.90
1	491.67	338.32	238.03	170.89	124.94	92.82	69.94
2	473.13	326.31	230.07	165.49	121.20	90.18	68.03
3	455.39	314.81	222.42	160.29	117.58	87.62	66.19
4	438.43	303.77	215.07	155.28	114.10	85.15	64.40
5	422.20	293.18	208.00	150.46	110.73	82.75	62.67
6	406.66	283.03	201.21	145.81	107.49	80.44	60.99
7	391.79	273.28	194.67	141.32	104.35	78.20	59.36
8	377.55	263.93	188.38	137.00	101.32	76.03	57.78
9	363.91	254.94	182.33	132.83	98.39	73.93	56.25

Table 1

Temp °C	Resistance by calibration	Resistance from equation	Temp °C	Resistance by calibration	Resistance from equation
14.87	424.55	424.27	55.46	109.23	109.23
15.20	419.20	419.04	59.24	97.80	97.67
20.22	348.05*	348.05	66.04	80.51	80.34
26.01	282.90	283.02	68.88	74.18*	74.18
30.56	241.70	241.64	74.23	64.11	64.00
35.20	206.60*	206.60	81.84	52.31	52.15
38.59	184.80	184.72	85.43	47.79	47.45
45.95	146.05	146.04	88.67	43.96	43.61
49.15	132.25*	132.25	91.86	40.59	40.18

Given in Table 1 are the values of resistance of the thermistor against temperature. The resistance of the thermistor was measured with a resistance box as described in Chapter IV and the temperature with a platinum resistance thermometer. The calibration values were fitted to an equation of the form given in Chapter IV and the four values marked with an asterisk in the table were used to obtain the constants of the equation.

For the temperatures given in the table, the resistances as obtained with the equation have been added so that the agreement between the equation and calibrated values can be judged.

The discrepancies from calibrated values by using the computed resistances amounts to 0.02 °C at 15 °C, 0.01 °C at 25 °C, 0.02 °C at 40 °C, 0.04 °C at 60 °C, 0.1 °C at 80 °C and 0.4 °C at 90 °C.

It would thus appear that the equation given in Chapter IV is in

good agreement with the calibrated values up to 50 $^{\circ}$C, and only

between 80 $^{\circ}$C and 90 $^{\circ}$C does the error become notable.

Appendix (5)

The pressure drop as given by Peube's 5 term solution (equation (61) Chapter II) for converging flow is

$$\left(p_2-p_1\right) = \frac{3\mu\varphi}{4\pi R^3}\,\ell n\,{r_2}/{r_1} + \frac{27\rho\varphi^2}{560\pi^2 R^2}\left(\frac{1}{r_1^2}-\frac{1}{r_2^2}\right) + \frac{9\rho\varphi^2}{32\pi^2}\left(\frac{1}{r_1^4}-\frac{1}{r_2^4}\right)\left[\frac{y^6}{30R^6}-\frac{y^4}{6R^4}+\frac{11y^2}{70R^2}-\frac{1}{42}\right]$$

$$+ \rho\varphi^2\left(\frac{1}{r_1^4}-\frac{1}{r_2^4}\right)\left[\frac{1}{350\pi^2}-\frac{39\rho\varphi}{86240\pi^3\mu R}\right] \quad\ldots\ldots(1)$$

For static pressure tappings the expression reduces to the pressure drop at $y = \pm\,h$ i.e.

$$\left(p_2-p_1\right) = \frac{3\mu\varphi}{4\pi R^3}\,\ell n\,{r_2}/{r_1} + \frac{27\rho\varphi^2}{560\pi^2 R^2}\left(\frac{1}{r_1^2}-\frac{1}{r_2^2}\right) + \frac{\rho\varphi^2}{350\pi^2}\left(\frac{1}{r_1^4}-\frac{1}{r_2^4}\right) - \frac{39\rho^2\varphi^3\left(\frac{1}{r_1^4}-\frac{1}{r_2^4}\right)}{86240\pi^3\mu R} \quad\ldots\ldots(2)$$

The author has extended the analysis to 7 terms and given below is the expression for the pressure drop for static pressure tappings.

$$\left(p_2-p_1\right) = \frac{3\mu\varphi\,\ell n\,{r_2}/{r_1}}{4\pi R^3} + \frac{27\rho\varphi^2}{560\pi^2 R^2}\left(\frac{1}{r_1^2}-\frac{1}{r_2^2}\right) + \frac{\rho\varphi^2\left(\frac{1}{r_1^4}-\frac{1}{r_2^4}\right)}{350\pi^2}$$

$$-\frac{39\rho^2\varphi^3\left(\frac{1}{r_1^4}-\frac{1}{r_2^4}\right)}{86240\pi^3\mu R} - \frac{0.0000107\,\rho^3\varphi^4\left(\frac{1}{r_1^6}-\frac{1}{r_2^6}\right)}{\mu^2\pi^4}$$

$$+\frac{0.014631\,\rho^2\varphi^3 R\left(\frac{1}{r_1^6}-\frac{1}{r_2^6}\right)}{\mu\pi^3} - \frac{0.021263\,\rho\varphi^2 R^2\left(\frac{1}{r_1^6}-\frac{1}{r_2^6}\right)}{\pi^2} \quad\ldots\ldots(3)$$

To estimate the difference between equation 5.2 Chapter V, and equations (2) and (3) given above, the pressure drops were calculated using the largest flow rates at each gap separation, and the smallest r_2/r_1 ratio since the variations are more noticeable at these conditions. The viscosity values are taken from tables and are the values corresponding to the temperature of the water.

Given below is a table giving the pressure drops for the various

equations in centimetres of water. In addition, the appropriate table
of Chapter V from which the data has been extracted is given, the
viscosity value used being the measured value.

Table 1

Table of Chpt. V	Vol. flow rate cm^3/s	equation (5.2)	equation (2) of Appendix	equation (3) of Appendix
1	6.241	5.485	5.456	5.454
2	6.544	3.117	3.091	3.089
3	4.869	1.229	1.221	1.2205
4	7.534	1.007	0.967	0.964

It can be seen from the table that at Q = 6.241 cm^3/s the difference
between the pressure drops obtained by equation (5.2) and equation (2) of
the Appendix is approximately 0.5% whereas at Q = 7.534 cm^3/s the difference
is some 4%. The latter example is for a plate separation of 0.0194" com-
pared with 0.00965" at Q = 6.241 cm^3/s which explains the greater divergence
from the two solutions since for the larger gap the inertia effects are much
greater and the pressure drop due to inertia a larger fraction of the viscous
pressure drop. The effect of taking more terms in the series solution is
negligible for the small plate separations but is approximately 0.3% at
Q = 7.534 cm^3/s and 2h = 0.0194".

The examples quoted above are for the worst conditions of the results
of Chapter V for each plate separation and on average the difference between
equation 5.2 and equation (2) of this Appendix was less than 0.2% and the
effect of using the extended analysis was negligible. Thus it would appear
that for the tests given in Chapter V equation (5.2) was sufficiently

accurate, although for experiments carried out at smaller radii or larger flow rates, the deviation from equation (5.2) of equations (2) and (3) of the Appendix would have to be considered.

APPENDIX (6)

To ascertain the reproducibility of the light system described in Chapter 7 for timing the fall of the mercury pellet down the drop tube a series of tests were carried out with the pellet falling vertically when the tube was filled with water. Given below are a typical set of timings, the difference between the two sets of timings being due to the top and bottom pairs of prisms not being equidistant from the central pair.

Time of fall mid to bottom position seconds	Time of fall mid to top position seconds
44.33	41.53
44.32	41.56
44.32	41.53
44.34	41.54
44.32	41.53
44.35	41.54
44.35	41.55
44.34	41.54

From the table it can be seen that the variation is of the order of $\pm$ 0.04% and it is felt that better reproducibility could be achieved if the temperature stability of the water could be improved. It is also necessary to ensure that the glass drop tube and mercury pellet are clean otherwise, as the author experienced, the timings become erratic.

APPENDIX (7)

The first consideration was to determine whether it was possible to ignore inertia effects and use the creeping flow solution, the alternative being Peube's 3 term solution which accounted for inertia effects.

For a drop tube of 2 mm bore and a fall length of 15 cm it was found that for a fall time of 25 seconds the plate separation would be 0.004".

Using these values it was calculated that at 20 $^{\circ}$C the inertia term was 0.4% of the viscous term and 1.2% at 90 $^{\circ}$C. Thus it was concluded that the term accounting for inertia effects could not be ignored.

The expression for the viscosity for Peube's 3 term solution for converging flow is

$$\mu = \frac{4\pi R^3 \Delta p}{3 \varphi \ln {}^{r_2}\!/_{r_1}} - \frac{9 \rho \varphi R \left(\frac{1}{r_1^2} - \frac{1}{r_2^2}\right)}{140 \pi \ln {}^{r_2}\!/_{r_1}} \qquad \ldots\ldots(1)$$

This can be written

$$\mu = C_1 \, Wgt \, \frac{\rho_P}{\rho_D} - C_2 \frac{\rho_D}{t} \qquad \ldots\ldots(2)$$

where t is fall time in seconds, W the weight of the pellet ρ_P and ρ_D the density of the fluid at the plates and the drop tube respectively and

$$C_1 = \frac{4\pi R^3}{3 \ln {}^{r_2}\!/_{r_1}} \frac{1}{\left({}^{\pi}\!/_{4} D^2\right)^2 L} \qquad \ldots\ldots(3)$$

and

$$C_2 = \frac{9 D^2 L R}{560 \ln {}^{r_2}\!/_{r_1}} \left(\frac{1}{r_1^2} - \frac{1}{r_2^2}\right) \qquad \ldots\ldots(4)$$

To equation (2) various corrections have to be applied:-

(a) Excess pressure loss in the inlet section

(b) Drag on the mercury pellet due to surface tension

(c) Pressure losses in connecting tubes

(d) Correction to the weight of the pellet due to buoyancy

(e) Thermal expansion

(f) Compressibility.

(a) This excess pressure drop at the inlet is due to the velocity
profile changing from an assumed uniform profile at the entry of the
plates to the fully developed shape further downstream. An additional
dissipation of energy is caused by the convergence of the streamlines as
the fluid enters.

An approximate method of obtaining the extent of this correction is
by the kinetic energy end correction (1). This method assumes that the
dissipation of energy in the inlet length is equal to the dissipation
in the same length when the velocity profile is fully developed. In
addition, there are excess pressure drops to account for the difference
in the rate of inflow and the rate of outflow of kinetic energy in the
inlet length and the kinetic energy required to start the fluid from rest.

This method was applied to radial flow and in the analysis the simple
creeping flow solution was used since the size of the inertia was small
in relation to the viscous term.

By similar reasoning to that used in ref (1) the author found that

$$(P - p_L) = \frac{3\mu \varphi \, \ell_n \frac{r_2}{r_1}}{4\pi \ell^3} + \frac{27\rho \varphi^2}{560\pi r_2^2 \ell^2} \left(\frac{r_2}{r_1}\right)^2$$

$$.....(5)$$

where P and p_L are the pressures outside the plates and at the point

where it may be considered the flow has become fully developed and r_L is the radius at which this occurs. Thus there is an additional pressure drop, given by the second term of equation (5), due to inlet effects and equation (1) can be rewritten

$$\mu = \frac{4\pi k^3 \Delta p}{3\varphi \ln \frac{r_2}{r_1}} - \frac{9\rho\varphi k \left(\frac{1}{r_1^2} - \frac{1}{r_L^2}\right)}{140\pi \ln \frac{r_2}{r_1}} - \frac{9\rho\varphi k \left(\frac{r_2}{r_L}\right)^2}{140\pi r_2^2 \ln \frac{r_2}{r_1}} \qquad \ldots\ldots(6)$$

An expression has been obtained by Wang and Longwell (2) for the inlet length for laminar flow between plates and since inertia effects are small for this particular application their expression has been used.

Thus

$$(r_2 - r_L) = \frac{0.136 \rho k^2 u_m}{\mu} \qquad \ldots\ldots(7)$$

where $u_m = \frac{\varphi}{4\pi r_2 k}$.

However Schlichting (3) found the constant of equation (7) to be 0.16. Thus the author has used the latter value. For converging flow $r_2 = 1''$ and r_L was found to be 0.9999'' for the dimensions of the apparatus and consequently $r_2 = r_L$. The last term of equation (6) was found to be negligible and could be ignored for converging flow.

However this was not the case for diverging flow with $r_2 = {}^3/64''$ the last term of equation accounting for approximately 0.5% of the viscosity.

Summarising, the equations for converging and diverging flow are respectively

$$\mu = c_1 w_g t \frac{\rho_p}{\rho_D} - c_2 \frac{\rho_D}{t} \qquad \ldots\ldots(8)$$

$$\mu = c_1 w_g t \frac{\rho_p}{\rho_D} + c_2 \frac{\rho_D}{t} - c_3 \frac{\rho_D}{t} \left(\frac{r_2}{r_L}\right)^2 \qquad \ldots\ldots(9)$$

where $c_3 = \frac{9D^2 Lh}{560 r_2^2 \ln^{r_2}/r_1}$.

(b)   Drag on the mercury pellet due to surface tension arises from the fact that the shape of the menisci at the top and bottom of the pellet are different.

The method described by Rankine (4) of splitting the pellet to determine the drag cannot be used in this application as the mercury cannot be observed and consequently no check could be made that the pellet has been split properly.

The other method requires the pellet to fall down the drop tube at a known angle to the vertical which results in the weight of the pellet being multiplied by the term

$$\left[1 - \left(\frac{\cos \theta \, t_2 - t_1}{t_2 - t_1} \right) \right] \qquad \ldots\ldots(10)$$

where θ is the angle the drop tube makes with the vertical and t_2 and t_1 are the times taken for angled and vertical runs respectively.

Below is shown how the factor given by equation (10) is derived.

For a given size of drop tube and fall length the equation of flow through the tube can be written

$$\mu = K \, Wg \, t \qquad \ldots\ldots(11)$$

If the fraction of the weight of the pellet required to overcome the drag is denoted by ε and t_1 is the time taken to fall vertically then

$$\mu = K(Wg - \varepsilon) t_1 \qquad \ldots\ldots(12)$$

For the pellet falling down the tube at an angle θ to the vertical and assuming the drag to be the same

$$\mu = K(Wg \cos \theta - \varepsilon) t_2 \qquad \ldots\ldots(13)$$

If the vertical and angled runs are done at the same temperature which in practice would be the case

$$K(Wg - \epsilon)t_1 = K(Wg \cos \theta - \epsilon)t_2 \qquad \ldots\ldots(14)$$

Thus

$$\epsilon/Wg = \frac{(\cos \theta \, t_2 - t_1)}{(t_2 - t_1)} \qquad \ldots\ldots(15)$$

and hence correction given by (10) is obtained.

It is intended to obtain this correction in a separate apparatus thus overcoming the difficulty of making a rotating seal between the drop tube and the plates which must remain in a horizontal position.

This method is not as accurate as that described by Rankine since the assumption is made that the drag is constant for vertical and angled runs.

(c) Pressure Losses in Connecting Tubes

A further loss in head arises from the flow of the fluid through the connecting tubes and mercury traps. With the small flows involved the flow could be assumed laminar for the worst conditions the Reynolds number being found not to exceed 500.

This correction although small is not negligible and accounts for about 0.2% of the viscosity.

As found by Whitelaw (5) and Ray (6) the experimental evaluation of this correction could not be found by measuring the fall time of the pellet without the plates as the resistance was too small and consequently the pellet broke up.

The resistance was found by passing water from a constant head tank through the apparatus without the plates in position and measuring the pressure drop. By plotting pressure drops against flow rates and extra-

polating the curve which was virtually a straight line the resistance at experimental conditions was obtained.

(d) Buoyancy Correction

Due to difference between the densities of water and mercury a correction has to be made for the loss of pressure due to the upthrust on the pellet. This is done by multiplying the weight of the pellet by the expression

$$\left[1 - \left(\frac{\rho_D}{\rho_m} \right) \right] \qquad \qquad \ldots\ldots(16)$$

where ρ_m is the density of mercury.

(e) Thermal Expansion

The increase in the plate separation due to temperature effects can be safely ignored.

(f) Compressibility

For water at 20 $^\circ$C $\qquad \frac{dV}{dp} = 50 \times 10^{-6}$

and the increase in head due to the length of the drop tube is approximately $^1/10$ atmosphere. Thus $dV = 5 \times 10^{-6}$ and hence the error in the density of the water due to compressibility is negligible.

REFERENCES:

(1) "Modern Developments in Fluid Dynamics" edited by S. Goldstein p.298.

(2) Wang, Y.L. and Longwell, P.A. A.I.Ch.E. Jl. Vol.10, No.3 p.323 May 1964.

(3) Schlichting, H. "Boundary Layer Theory" 4th Edition p.169.

(4) Rankine, A.O. Proc. Roy. Soc. 83A 1910 p.265.

(5) Whitelaw, J. Ph.D. Thesis, Glasgow University.

(6) Ray, A.K. Ph.D. Thesis, Glasgow University.